CHARACTERIZATION OF THE ALKALINE METAL DISSOLUTION AND SULPHUR DIOXIDE ABSORPTION OF FLY ASH SLURRIES

by

Ahmad M. Al-Haj Ali

A thesis submitted to the Faculty of Graduate Studies and
Research in partial fulfillment of the requirements
for the degree of Doctor of Philosophy

September 1989

Department of Chemical Engineering
McGill University
Montreal

ISBN 0-315-63515-0

TO THE DEAR PEOPLE WHO HAVE BEEN NEGLECTED
SO THAT THIS WORK CAN BE COMPLETED

ABSTRACT

The absorption of sulphur dioxide into aqueous slurries of two Canadian coal fly ashes (subbituminous and lignite) was studied using a semi-batch stirred tank reactor. The dissolution of alkaline metal compounds from both types of fly ash was also investigated. Only calcium and magnesium compounds were found to be important in providing soluble alkalinity for SO_2 absorption. Lignite ash provided approximately twice as high alkalinity as subbituminous ash. The concentrations of dissolved calcium and magnesium were dependent of slurry density, particle size, pH and temperature. Initial dissolution was very rapid and the initial concentration of dissolved metals was proportional to the total surface area of particles. A pH lower than 3.5 was essential for maximum dissolution. The amount of SO_2 absorbed was generally dependent of the amount of available alkalinity in the liquid. It increased with increasing slurry density, and inlet SO_2 concentration but was not affected by temperature or particle size. Limestone addition did not affect the absorption in the first 45 to 60 minutes. Initial absorption was a function of gas inlet concentration and independent of the type of absorbent. At later stages, the absorption rate was controlled by the rate of dissolution at low available alkalinity.

RESUME

On a étudié l'absorbtion de l'anhydride sulfureux dans des suspensions aqueuses de deux types de cendres du charbon canadiennes (lignite et subbitumineuses) dans un réacteur agité semi-continu. On a trouvé que seuls les composé de calcium et de magnésium avaient l'alcalinité nécessaire à l'absorbtion du SO_2. L'alcalinite des cendres de lignite était environ deux fois celle des cendres subbitumineuses. La concentration de calcium et de magnésium dépendait de la densité de la suspension, de la grosseur des particules, du pH et de la température. Initiallement, on a observé une dissolution très rapide et la concentration des métaux dissous était proportionnelle à l'aire superficielle totale des particules. Il fallait un pH de 3,5 pour obtenir une dissolution maximale. La quantité de SO_2 absorbé dépendait, en général, de l'alcalinité disponible dans le liquide. Celle-ci augmentait selon la densité de la suspension et la concentration d'arrivée du SO_2, mais indépendamment de la température et de la grosseur des particules. Pendant les 45 à 60 premières minutes de l'expérience, l'ajoût de calcaire n'affectait pas l'absorbtion. Cette dernière dépendait de la concentration d'arrivée du gaz, mais pas du type d'absorbeur. Par la suite, avec une faible alcalinité disponible, le taux de dissolution contrôlait le taux d'absorbtion.

ACKNOWLEDGEMENTS

I would like to express my sincere gratitude and appreciation to my thesis supervisor, Professor D. Berk, for his inspiration, encouragement and support throughout all the stages of this work. I also thank him for the long hours of careful reading of the thesis manuscript which provided outstanding input while the thesis was being written.

I would like to thank the technical staff at the Department of Chemical Engineering for their assistance with the equipment and, in particular, Mr. J. Dumont for helping in the provision of research materials and equipment. Thanks are due to John Sarlis for his interest in this work and for the stimulating discussions, especially during the long lab days and to all the colleages at the Department.

The financial support of the University of Jordan in the form of a scholarship is gratefully acknowledged.

Last, but definitly not least, I would like to thank my parents and all members of my family as well as my friends for so much that cannot be expressed. I am indebted to my wife for her understanding, patience and support.

TABLE OF CONTENTS

LIST OF FIGURES

LIST OF TABLES

CHAPTER 1

INTRODUCTION

1.1 The Impact of the Use of Coal on the Environment

The conversion of fossil fuels, mainly by the combustion of coal, will continue to play a major role in supplying the world's additional energy requirements in the 1990s. By the year 2000, the total steam electric capacity in Canada, for example, is expected to be evenly split between coal and nuclear energy (10). The extensive use of coal, however, is associated with serious environmental concerns. Upon combustion, most of the sulphur in coal is released to the atmosphere as sulphur dioxide (SO_2) leading to the widely-known phenomenon of acid rain.

The term "acid rain" is often used to describe the deposition of air pollutants that are acids or become acidic when they reach the earth's surface. These pollutants may be precipitated in the wet form as rain or snow, or deposited as dry gas (8). The issue of acid rain has recieved much attention at the different levels of community and government bodies.

Sulphur dioxide gas is recognized to be a major cause of this phenomenon. Scientific evidence has been accumulating over many years indicating that the release of this gas to the atmosphere in large quantities has significant adverse effects on the environment, especially the aquatic ecosystems. It has been found that in many areas of Europe and North America, the present atmospheric deposition of acidity has reached levels at which it results in detrimental changes in the water chemistry and hence a decline in the population of fish and other aquatic life (53).

Furthermore, acid precipitation has several adverse effects on the terrestrial ecosystems. It causes severe damage to crops and forests and limits plant growth by creating unfavourable root environment. Acid deposition results in corrosion of industrial equipment and construction materials causing considerable economic losses. Acid rain and SO_2 emissions may have an indirect impact on human health. This could mainly occur through the contamination of edible fish and drinking water supplies (33,53).

More than 90% of the atmospheric sulphur dioxide is attributable to man-made emissions especially from fossil fuels (53). Coal is the most common fuel for reasons of price and availability, and its SO_2 emissions dominate that of fossil fuels. Over 60% of the total SO_2 emissions is due to the combustion of coal, 90% of which comes from electric power utilities. The total SO_2 emissions in the United States, a major user of coal, in 1980 was estimated at 24 million tons, and it is projected to increase by 10% by the year 2000. The Canadian emissions comprise 20% of the U.S. figures (33). The concentrations of SO_2 in the stack gas of coal-burning power plants may range from 500 to 5000 ppm (0.05 to 0.5% by volume). The stack gas is primarily nitrogen with 10-15% CO_2, 3-10% oxygen and 5-10% water vapour (36).

The combustion of coal also results in the emissions of the fine grained particles of fly ash which are carried by the stack gas. Very small particles may escape the particulate collection system (for example, the electrostatic precipitator) and stay in the atmosphere for a period time before falling down at a large distance from their source. These tiny particles can be hazardous to human health by inhalation or external reaction with the eyes and skin (39). After collection and disposal, weathered fly ash generates leachates that contain many solubilized hazardous elements and other ions in amounts sufficient to contaminate surface and ground waters. These trace elements along with high pH can be toxic for aquatic life (54).

Coal-fired power plants in Canada produce about 3.7 million tons of ash every year with fly ash making 60-90% of the total ash production (10). In the U.S., about 70 million tons of ash produced every year with fly ash making 70-80% of the total production. Fly ash is a waste by-product and is considered a liability by most utilities. Except for a few commercial usages (mainly in cement mixtures, asphalt additives and soil modifiers) which all account for only 10-20% of the total fly ash produced, land disposal has been the common practice (24).

1.2 Pollution Control Policies and Technology

The government authorities in all industrialized countries have mandated strict regulations to control the emissions of sulphur dioxide and particulates from power plants burning fossil fuels. In the Scandinavian countries, policies for the reduction of SO_2 emissions have been in place for many years. Regulations were adopted in West Germany during the 1980s limiting SO_2 emissions to 1.3×10^{-4} mg/J (or 0.3 lb/million BTU) of heat input. The Canadian Clean Air Act issued in 1981 has limited the rate of discharge of sulphur dioxide into ambient air to 2.6×10^{-4} mg/J (or 0.6 lb/million BTU) of heat input and that of particulate matter to 4.3×10^{-5} mg/J (or 0.1 lb/million BTU). Similar standards have been in effect in the United States (8).

There are several approaches to the control of sulphur dioxide emissions. One option is to simply remove the sulphur from the coal before it is burned using an appropriate cleaning method. Unfortunately, the reduction in emissions obtained by this option is insufficient to meet the requirements of complying with environmental standards (8). Therefore, most efforts have concentrated on the removal of SO_2 from flue gas before it is released to the atmosphere. This can be achieved by reacting the gas with an alkali. The differing methods of providing this alkalinity and the nature of the final product have led to the multiplicity of commercial flue gas desulphurization (FGD) processes.

These processes can be divided into wet and dry and also into processes in which the final product is thrown away or recovered as a useful product (21,36). Dry scrubbing processes avoid cooling the stack gas, and they take the form of solid alkali injection or spray drying with a dry final product. The primary applications of dry scrubbing are at power plants burning low sulphur coal and it represents a small percent of the total FGD capacity. Some FGD processes produce a saleable product such as sulphuric acid or elemental sulphur, but these also represent less than 10% of the overall FGD capacity. However, wet scrubbing with a non-recoverable final product has been the common practice in flue gas desulphurization technology.

1.3 Wet Scrubbing FGD

The wet systems applied in this type of scrubbing technology can be either slurries as in the most common lime/limestone scrubbing or clear solutions as in the double alkali process (21,36). In the first system, sulphur dioxide is absorbed into a slurry that simultaneously provides soluble alkalinity through the dissolution of calcium oxide or calcium carbonate. Double alkali involves scrubbing in a soluble alkali (usually sodium sulphite) and regenerating this alkali with lime or limestone slurries outside the scrubber. However, both types of processes are based on the aqueous chemistry of sulphur dioxide.

1.3.1 Aqueous Absorption of SO_2

Sulphur dioxide dissolves in pure water and undergoes a hydrolysis reaction. Solubility in aqueous solutions depends on the partial pressure of the gas, the temperature of the liquid phase, the pH and the ionic strength of the solution, especially on those ions which buffer the pH (21). At 1 atm (101.3 kPa) of SO_2 pressure, the solubility of the gas decreases from 15.7% (by weight) at 10°C (283 K) to

5.8% at 40°C (23). The solution obtained by dissolving SO_2 in water is a complex system which contains physically dissolved as well as chemically associated SO_2. Depending on the conditions of the solution, the system may contain $SO_{2(aq)}$, bisulphite (HSO_3^-) ions or sulphite ($SO_3^=$) ions. Traces of disulphite ($S_2O_5^=$) ions and hydrates may also be present (23,48).

The principal reactions that describe the SO_2-water system are summarized below (48):

1. Sulphur dioxide in the gas phase comes to equilibrium with molecular (uncombined) SO_2 in solution:

$$SO_{2(g)} \equiv SO_{2(aq)} \qquad (1.1)$$

The equilibrium represented by Equation 1.1 follows Henry's law for dilute solutions:

$$C_{Ai} = H\ p_A \qquad (1.1a)$$

where C_{Ai} = concentration of molecular SO_2 at the gas-liquid interface.

H = Henry's law constant which depends on the solution temperature and composition.

and p_A = partial pressure of SO_2 in the gas phase.

2. Dissolved SO_2 undergoes hydrolysis to form the bisulphite ion:

$$SO_{2(aq)} + H_2O === HSO_3^- + H^+ \qquad (1.2)$$

which is an important reaction in the chemistry of wet scrubbing, especially at low pH. The chemical equilibria of this hydrolysis will be discussed in detail in Chapter 5.

3. Some of the bisulphite is further hydrolyzed to form sulphite ions:

$$HSO_3^- \overset{H_2O}{===} SO_3^= + H^+ \qquad (1.3)$$

This dissociation, however, has a small equilibrium constant of 6.24×10^{-8} gmol/L at 25°C (16).

The coexistence of different aqueous species depends on the pH of the solution as shown in the predominance diagram (Figure 1.1). This diagram was constructed on the basis of the equilibria of sulphur compounds in solution the pH being the only degree of freedom for a given total concentration of sulphur. $SO_{2(aq)}$ predominates at very low pH and does not exist above pH 4. Sulphite predominates in the alkaline region and cannot be found below pH 5. The main species in the moderately-acidic to neutral range (pH 2.5-6.5) is the bisulphite ion.

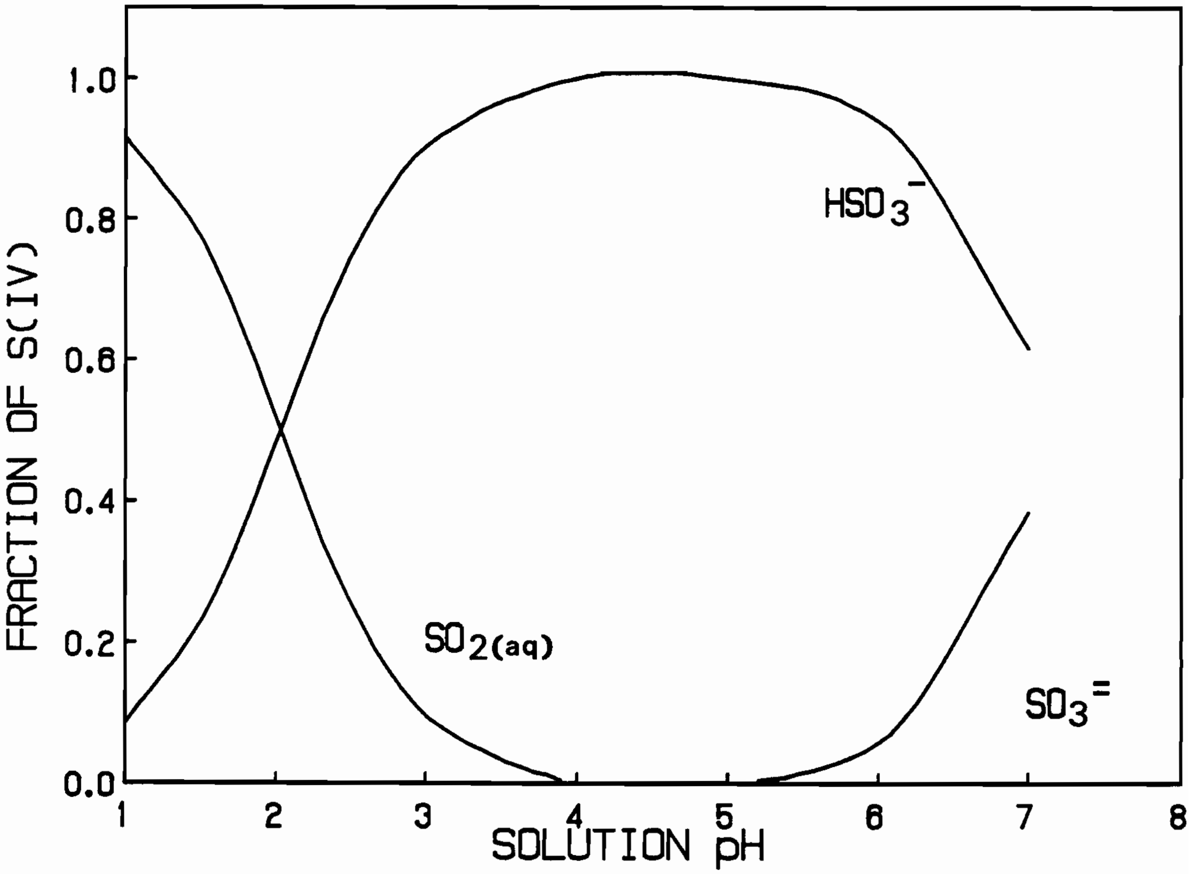

Figure 1.1 The predominance diagram of the aqueous sulphur species

All these forms of dissolved SO_2 contain sulphur in its +4 oxidation state and therefore it has become common practice to refer to them as S(IV) (35). This term will be used throughout this work to describe the total aqueous sulphur concentration.

The absorption of SO_2 in an aqueous solution can be increased by increasing the transformation of $SO_{2(aq)}$ to bisulphite and sulphite. This is possible by the addition of ions that can provide soluble alkalinity (OH^-) to neutralize the hydrogen ions produced by the hydrolysis of $SO_{2(aq)}$. Therefore, the chemical equilibria of reactions 1.2 and 1.3 will be shifted to allow for more absorption of sulphur dioxide from the gas phase.

Without the addition of alkalinity, an aqueous solution in equilibrium with a gas containing 0.2% SO_2 (by volume) will have no more than 3 mmol/L of total dissolved SO_2 while in flue gas desulphurization practice, 10-100 mmol/L of total dissolved SO_2 is required (37). This means that a sufficient alkalinity should be provided. Calcium-based reagents have been the most popular source of this alkalinity.

1.3.2 Scrubbing by Limestone Slurries

Scrubbing with limestone slurry is the most widely used process for the removal of SO_2 from power plant flue gases. Representing 80-85% of the total FGD capacity, this type of processes has proven to be more efficient and less expensive (36).

The chemistry of the process is very complex because of the limited solubility of both the reactants (mainly $CaCO_3$) and the products ($CaSO_3$ and $CaSO_4$) which has led to the presence of a large number of ionic and non-ionic components in the multi-phase system involving gases, liquids and solids. The major components include Ca^{2+}, OH^-, $SO_{2(g)}$, $CO_{2(g)}$, $O_{2(g)}$, HSO_3^-, $SO_3^=$, $SO_4^=$, HCO_3^- and $CO_3^=$. Other components which may be present in the system include Mg^{2+}, Na^+, K^+, $NO_{(g)}$, $NO_{2(g)}$ and Cl^- (1,21).

The pH of the scrubbing solution is typically 4-6 (36) and the concentrations of the dissolved species that can react with the incoming SO_2 gas are in the range of 1-2 mmol/L. This is far below the typical 10 mmol/L of SO_2 absorbed per pass through the scrubber. Therefore, the absorption rate is largely dependent upon the slow rate of limestone dissolution (38).

Research on the elucidation of the mechanisms of gas absorption, solid dissolution, chemical reactions (including oxidation) and product precipitation has been ongoing for many years. However, these are only qualitatively understood (46,51).

1.4 Wet Scrubbing by Fly Ash Alkalinity

1.4.1 Fly Ash as an Alkali Source

The basic premise underlying the use of fly ash is that the alkaline metal compounds present in the ash particles can provide soluble alkalinity upon the dissolution of these metals in an aqueous solution thus increasing its scrubbing capacity for sulphur dioxide. The metal ions react with the sulphur compounds in the liquid phase to form calcium sulphite which is then oxidized to the environmentally safe calcium sulphate for landfill disposal.

The potential of using fly ash alkalinity is established considering several factors. These factors include the percent removal of SO_2 required by environmental standards, the amount of fly ash produced by the power plant, the content of the alkaline material in the ash and the availability of this alkali (18). Environmental emission standards varies according to the rank (or the heating value) of the coal since they are based on the amount of heat released from the combustion of the coal (28). The ash content varies significantly among coals and locations of coal mines. The ratio of fly ash carried by the stack gas to the total ash produced varies depending on the coal firing method. The alkaline content of fly ash also varies considerably with the type of coal and tends to be highest in low-grade coal (or lignite) and lowest in the high-grade bituminous coal. The alkaline content of subbituminous coal is intermediate. Average alkaline metal contents of ashes from different coals are presented in Table 1.1.

As a first indication of the suitability of a coal fly ash to be used in the scrubbing of SO_2 emitted by burning that coal, the stoichiometric ratio (SR) may be used. This is defined as the molar ratio between the total alkaline metal content in a unit mass of coal (that is, the sum of CaO, MgO, K_2O and Na_2O in the ash multiplied by the ash percent in the coal) and the sulphur dioxide emitted from the same mass of coal assuming all the sulphur in the coal is converted to SO_2 after combustion (46). Only if the SR is greater than 1, the use of fly ash alkalinity is feasible and should be considered for further evaluation. The SR cannot provide information on the amount of available alkalinity for flue gas scrubbing but it serves to separate those situations where the use of fly ash alkalinity is unlikely.

Table 1.1

Alkaline Metal Contents of Ashes from

Different Coals (28)

	Bituminous	Subbituminous	Lignite
CaO	3.9-6.5	15.6-17.8	18.0-31.0
MgO	0.8-1.9	2.4-5.5	2.0-9.0
Na_2O	0.6-1.6	1.4-2.2	1.4-6.5
K_2O	0.5-0.8	0.3-0.5	0.1-1.8

1.4.2 Development of Wet Scrubbing by Fly Ash

The first fly ash wet scrubbing systems were the existing particulate control devices which were able to accomplish some SO_2 removal. The next generation of the technology was designed for combined particulate and SO_2 removals. The current design of commercial applications is based on separate particulate and SO_2 removals where a wet scrubber or an electrostatic precipitator for fly ash removal is placed upstream of a sulphur dioxide scrubber (46).

In the first arrangement of the current design, the same slurry is being used in the scrubbing of both fly ash and SO_2. In the latter arrangement, fly ash is collected dry, stored in silos and then reclaimed, slurried for use in the scrubbing of SO_2. In either case, the design is aimed at carrying out the gas absorption step in the scrubber (absorber) then reacting the resulting aqueous sulphur species (e.g. bisulphite) with the alkaline metals dissolved from fly ash in a reaction tank. The reaction tank is designed to provide adequate residence time for reactions and product precipitation to occur thus minimizing the chance of precipitation (or scaling) in the SO_2 scrubber.

The development of this technology in particular and other FGD processes in general have, of necessity, been rapid. The bulk of experimental data collected (18,19,46) aimed at answering questions of cause and effect which has the advantage of solving immediate operational problems such as scaling, plugging or disposal of solids and spent liquor. Also, works that explored the operational effects of, for example, the pH or the dissolved metal concentrations of fly ash systems on the removal of SO_2 concluded that these parameters will have an impact on the SO_2 removal efficiency. However, no quantitative relationship was available. Such a type of investigation is less helpful in understanding the basics of the system's behaviour.

The complex chemistry and transport processes of the system of SO_2 removal by fly ash alkalinity is not well understood, and therefore it is recognized that there is a need for more information and data that can be used in designing new systems and ensuring the operatability of the installed units. Therefore, the expansion of this developing technology in the flue gas desulphurization industry can only succeed a good understanding of the behaviour of fly ash slurries as a source of alkalinity in scrubbing systems either alone or combined with a conventional reagent.

1.4.3 Chemistry of SO_2 absorption into Fly Ash Slurries

When fly ash is used as the alkali source, the chemical system will be much more complicated than in the case of scrubbing with limestone. This extra complexity is mainly due to the heterogeneous nature and small solubilities of fly ash particles. The overall chemical reactions which take place in a flue gas desulphurization system using fly ash alkalinity can be represented by the following simplified equations (46):

(1) Absorption of sulphur dioxide:

$$SO_{2(g)} === SO_{2(aq)} \qquad (1.1)$$

(2) Dissolution of fly ash (assuming calcium and magnesium oxides to be the important dissolving compounds):

$$CaO + H_2O === 2\ OH^- + Ca^{2+} \qquad (1.4)$$

$$MgO + H_2O === 2\ OH^- + Mg^{2+} \qquad (1.5)$$

(3) Chemical reaction between dissolved metals and the aqueous sulphur compounds:

$$Ca^{2+} + HSO_3^- === CaSO_3 + H^+ \qquad (1.6)$$

$$Mg^{2+} + HSO_3^- === MgSO_3 + H^+ \qquad (1.7)$$

(4) Oxidation of Sulphite:

$$CaSO_3 + 1/2\ O_2 === CaSO_4 \tag{1.8}$$

$$MgSO_3 + 1/2\ O_2 === MgSO_4 \tag{1.9}$$

(5) Precipitation of Sulphite and Sulphate:

$$CaSO_3 + 1/2\ H_2O === CaSO_3.1/2\ H_2O \tag{1.10}$$

$$CaSO_4 + 1/2\ H_2O === CaSO_4.1/2\ H_2O \tag{1.11}$$

1.5 Significance and Objectives of This Study

In the foreseeable future, flue gas desulphurization industry will continue to apply wet scrubbing due to its high availability and proven experience as well as the high SO_2 removal effeciency. However, with the increased cost of emissions control dictated by tougher environmental regulations, it is important to find ways that will make the technology more cost-effective.

Reagent cost is the most significant factor effecting the operating cost of a wet scrubbing process. The average cost of lime and limestone reagents for a typical power plant were $60/ton (U.S.) and $15/ton, respectively, and the annual reagent costs could exceed $6 million for lime and $3 million for limestone (8). Fly ash has no cost as a raw material. The use of fly ash as a source of alkalinity in wet scrubbing to supplement or (if possible in some cases) eliminate the use of lime or limestone reagents has other advantages. It reduces the total amount of solids to be disposed of as waste products thus lowering the cost of the scrubbing. Also, it reduces the dangers to the aquatic environment caused by fly ash weathering which may contaminate the surface as well as the ground waters.

This study was aimed at the characterization of two types of fly ash in terms of the dissolution of metal compounds responsible for the alkalinity in their leachates and the absorption of sulphur dioxide into slurries of these fly ashes. The overall objective of this work is to obtain information that would be helpful in more understanding of the process of flue gas scrubbing by fly ash alkalinity for purposes of better design and operation.

This overall objective can be further expressed in terms of the following particular objectives:

1. To evaluate the effects of the leaching conditions on the short-term dissolution of alkaline metal compounds in fly ash.

2. To evaluate the effects of certain parameters of the gas, liquid and solid phases on the absorption of sulphur dioxide into fly ash slurries.

3. To determine the effects of the above-mentioned variables on the rates of SO_2 absorption.

4. To investigate the effect of the addition of limestone to fly ash on the absorption properties of the slurries.

This thesis consists of six chapters. This introductory chapter is followed by a literature survey (Chapter 2) which will mainly cover the characterization of fly ashes, their leaching behaviour and their use in sulphur dioxide scrubbing. Chapter 3 is devoted to the materials and methods used in this investigation. The experimental results on the dissolution of alkaline metal compounds from fly ash are discussed in Chapter 4 while the results on sulphur dioxide absorption are discussed in Chapter 5. Finally, the conclusions, original contributions and recommendations for future work are presented in Chapter 6.

CHAPTER 2

LITERATURE SERVEY

2.1 Characterization of Fly Ash Particles

The solid waste (or ash) produced by the combustion of coal is primarily derived from the inorganic material in the coal. This residue is partitioned into fly ash and bottom ash. Fly ash is the part of the coal combustion residue which is entrained in the flue gas leaving the power plant, and it comprises most of the plant's solid waste. The physical properties of fly as well as its chemical composition are dependent on the type of the parent coal, the location of the coal mine, the combustion method and the collection system (32).

2.1.1 Physical Characterization

Fly ash consists of predominantly fine-grained particles having a variable morphology and mineralogical composition. The particles range in colour from grey to reddish brown and in size from a fraction of a micrometer to 4 cm (32). The morphology of fly ash has indicated the presence of different types of particles ranging from solid spheres which predominate at small particle sizes of few micrometers to irregularly-shaped solid particles predominating above 75 μm of particle diameter. In between, other types of particles such as the cenospheres (or the hollow and thin-walled spherical particles) and the plerospheres (cenospheres filled with smaller particles) are found. Over 90 % of the particles comprising most fly ashes are solid spheres (54).

Mineralogical studies have shown that fly ash contains alpha-quartz, mullite, hematite, magnetite, calcite and sometimes gypsum and other minor crystalline phases. However, amorphous glass is the dominant component in the ash matrix (17,54). Reported specific gravities for coal fly ash range from 1.6-3.1, and it has a low bulk density in the range of 1.0-1.4 g/cm^3. Specific surface areas range between 0.2 and 0.8 m^2/g. In general, the specific area is larger when the ash is composed of smaller particles (24,39).

2.1.2 Chemical characterization

The major chemical constituents of fly ash come from the non-combustible inorganic material in the parent coal. In most fly ashes, 90% or more of the material weight is made up of the compounds of silicon, aluminium, iron, calcium and magnesium. Because of the inorganic origin of the particles, the elemental components in fly ash are commonly reported as stable oxides assuming complete oxidation of the inorganic substance during the combustion of coal (24,32). The remaining constituents include smaller amounts of potassium, sodium, sulphur, titanium, phosphorous and non-burnt carbon as well as traces of 20-50 other elements. The considerable variability in the concentrations of the major, minor and trace constituents is well documented (32,39).

The distribution of elements in fly ash may or may not depend on the size of the particles. Davidson et al. (5) reported that in fly ash particles larger than 74 μm, no dependence of elemental concentration on particle size was noticed. Below 74 μm, however, they classified the elements into three groups according to the tendency of their concentrations to increase with decreasing particle size. The first group included trace metals which showed that trend. Limited dependency on particle size was exhibited by major elements such as Si, Al and Fe and minor ones such as Mg. Other elements such as Ca and K showed no dependency on particle size. A recent study (11) has indicated that the concentrations of the principal elements in fly ash (namely, Si, Al, Fe, Ca and Mg) depend on the density but not the particle size. Hansen and Fisher (13) found that more than 70% of the calcium is associated with the an acid-soluble phase while more than 70% of the magnesium, pottasium or sodium are associated with the insoluble aluminosilicate matrix.

When fly ash solids get in contact with an aqueous phase, many of its elements dissolve in variable amounts producing leachates which have chemical characteristics determined by the composition of the solids as well as the conditions of the leaching process. The pH of these leachates may vary from 3 to 12 depending on the content of alkaline metal compounds in the particles (32).

2.2 Review of Studies on Fly Ash Leaching

2.2.1 General

The presence of large percentages of Si, Al and Fe oxides indicates that most fly ash components are water-insoluble. This has been demonstrated by experimental data (32,39). Also, the incorporation of the normally more soluble components (such as CaO, Na_2O and K_2O) inside SiO_2, Al_2O_3 and Fe_2O_3 matrices associated with the glassy interior of the particles causes these materials to be much less soluble than the corresponding pure crystalline compounds. Since the concentrations of some elements are functions of particle size, simple elemental analysis can be misleading. Hence, the conventional bulk analysis provides little information on the mobility of elements and other species upon contact with the liquid phase.

Numerous investigations have been carried out to determine the concentrations of dissolved metals and other species such as anions and also to characterize their dissolution behaviour. These investigations were provoked by different incentives. Most of the studies were concerned with the environmental impact of fly ash weathering (3,7,17,18,26,34). Few studies were conducted to determine the alkalinity available when fly ash is used in the absorption of acid gas effluents, mainly sulphur dioxide (6,49). Leaching studies were also carried out to characterize the chemical nature of the fly ash particles (5,15). An aqueous solution was the primary extractant but mineral and organic acid solutions were also employed according to the particular purpose of the study.

Leaching of fly ash can be broadly classified with respect to the duration of experiments into long-term and short-term experiments. The use of this classification, however, is relative and the long-term category includes experiments that run for several hours, weeks and may be months. Studies on the environmental and associated health impacts as well as those on soil applications belong to the first category. Short-term experiments were particularly used to characterize mass transfer from the particles to an aqueous solution (during the extraction of fly ash alkalinity) or to the aqueous environment at the disposal sites.

The overall result of these investigations indicated the extreme variability of leachates generated from fly ash (39). This variability is caused by large discrepancies in the chemical characteristics of the solid particles as well as the type of extractant used and the leaching conditions. Results reported in the literature from both long-term and short-term leaching studies relevant to the current study will be highlighted below.

2.2.2 Long-Term Leaching

The composition of fly ash leachate obtained by Dudas (7) indicated the presence of simple compounds such as CaO (or lime), $CaSO_4$ (or gypsum), $CaCO_3$, $MgCO_3$, Na_2SO_4 and K_2SO_4 associated with the surface of the particles. The relatively low concentrations of soluble Mg, Na and K compared to calcium preclude the salts of these elements as major causes of high alkalinity in the leachate. Elseewi et al. (9) and Warren and Dudas (54) attributed high levels of pH (or alkalinity) of fly ash leachate to the dissolution of calcium oxide. Among the principal components in fly ash tested by Chue et al. (3), calcium was readily released into water independent of the pH level. Magnesium was not released at pH levels in the alkaline range.

It is well known that the concentrations of dissolved cations in fly ash leachates are controlled by the medium, mainly the pH (39). However, there are other factors that govern the release of soluble components. These include the fly ash concentration, particle size, temperature and agitation speed (54).

The behaviour of several elements examined by Natusch et al. (26) including calcium was consistent with the idea that material in the surface layer is mostly soluble and that elements go into solution progressively as their dissolvable compounds in the solid phase get into contact with the solvent. The components of the surface layer appeared to be almost solubilized within 24 hours. They also remarked that the characteristics of the initial dissolution are dominated by the nature and the quantity of surface-associated inorganic salts.

2.2.3 Short-Term Leaching

Very few studies that are concerned with initial dissolution of fly ash and the mass transfer aspects of leaching were reported. Thunem (49) tested lignite fly ash as a source of alkalinity for SO_2 scrubbing. His results demonstrated that alkaline metals (mainly calcium) from fly ash can be solubilized, and that this solubilization is a function of the pH and the mixing time.

Reed et al. (34) studied the aqueous dissolution of an alkaline fly ash (25% CaO) in a batch stirred vessel at a range of slurry density (or fly ash concentration) of 0.3-10.0 g/L at different mixing speeds. They reported that the interfacial concentration of the solute does not remain constant throughout leaching but it is a function of the amount of solids present in the reactor. They suggested that the high concentration of calcium in the ash could be the controlling factor in the mass transfer of the dissolved solute from the particle surface to the bulk liquid.

Davies and Reed (6) investigated the dissolution of two lignite fly ashes of small particle sizes in the range 10-15 μm and a high slurry density of 150 g/L (15% wt/wt) using a bench-scale complete-mix reactor. Their purpose was to collect equilibrium and kinetic data in order to determine the availability of alkaline species in the fly ash leachates for SO_2 removal in a spray drying system. They found that initial dissolution was very rapid followed by a more gradual approach to final equilibrium attributed to changes in the slurry pH.

They also found that the retention time required to reach 95% of the final equilibrium value (in terms of dissolved calcium) was 15-30 minutes with a final concentration of 300-400 mg/L and a final pH of 10-11. Although they reported some values of an estimated overall mass transfer coefficient, they did not determine the rates of dissolution under the various appropriate leaching conditions. The main conclusion of these authors is that the kinetics of fly ash dissolution is very complex since no consistent trends were observed with changing the experimental conditions. The effect of temperature was insignificant and sometimes inconsistent. These conclusions were attributed to the complexity of interactions between the various chemical species and the pH.

2.3 Previous Work on Wet Scrubbing by Fly Ash Alkalinity

Research on the utilization of fly ash alkalinity was initiated in the United States in the early 1970s. Lignite fly ash from North Dakota was first used in bench-scale and pilot plant studies to test the potential and the performance of the proposed technology (29). Results obtained from the studies of Ness and co-workers (27,29) showed that available alkalinity was sufficient to reduce the SO_2 emissions below the environmental standards when burning lignite with an average sulphur content of 0.75%. Supplementary lime is needed for fuels with higher sulphur content. In most fly ash scrubbing systems tested, the slurry pH ranged from 3-6 and the retention time was 4-16 minutes.

Most of the available literature focuses on describing the installed scrubbing units that uses fly ash alkalinity and evaluating their operating experience (19,27,28,55). Unlike scrubbing by limestone and other calcium-based reagents, the absorption of SO_2 by fly ash slurries was not investigated in detail in a laboratory bench-scale reactor.

2.4 Absorption of SO_2 into Slurries of Fine Solids

Since the work of Ramachandran and Sharma (31) on gas absorption into agitated slurries, several theoretical and experimental studies have been reported. The two authors studied the problem of simultaneous dissolution of sparingly soluble solids and gas absorption with instantaneous liquid phase reaction on the basis of the film model. Uchida and Wen (52) considered several cases of gas absorption, solid dissolution and liquid phase reaction at a finite rate.

Due to the increased interest in the pollution control, particularly the removal of sulphur dioxide from the flue gases of power plants, the problem of gas absorption into slurries of fine solid particles attracted the attention of researchers. The objective was to develop the existing lime/limestone scrubbing process and other possible alternatives by understanding the chemical and transport events taking place in the scrubber. Examples for the studies reported in the literature on the gas absorption into slurries of pertinent interest to flue gas desulphurization are given below.

Sada and co-workers studied the absorption of sulphur dioxide and carbon dioxide (separately) into aqueous slurries of calcium hydroxide (40,43). They also studied the absorption of SO_2 into aqueous slurries of magnesium hydroxide (41), calcium carbonate and magnesium hydroxide (44,45) and limestone promoted by magnesium sulphate (42). Uchida et al. (50) and Uchida and Ariga (51) studied the absorption of SO_2 into slurries of limestone in a stirred tank reactor. In all these studies, attempts have been made to interpret the experimental results through the theoretical models described in the earlier works (31,52).

The above-mentioned studies have been carried out using pure solids with predictable dissolution behaviour. In the case of fly ash, however, the dissoluton of the solid particles is more complicated due the complexity of fly ash composition.

CHAPTER 3

MATERIALS AND EXPERIMENTAL METHODS

3.1 Selection and Preparation of Fly Ash Samples

Two fly ash samples derived from Western Canadian coals were selected for this study based on their higher alkaline metal contents compared to fly ashes derived from other coals. The first type was a lignite fly ash supplied by Saskatchewan Power from its Unit No.6 at Boundary Dam near Estevan, Saskatchewan. The other type was derived from subbituminous coal and supplied by Alberta Power from its Battle River station near Forestburg, Alberta. It will be refered to as SB ash. Most exploratory experiments were carried out using SB ash which was received first.

Samples to be used in the experiments were sieved to constant weight (for 3-4 h) using Tyler's Canadian Standard Sieve Series. The different size fractions were then stored in plastic containers for use in the appropriate experiments.

3.2 Reactor Design

A stirred vessel was used to carry out the gas absorption and most of the solid leaching experiments (Few "Shake-Flask" experiments to study long-term dissolution were also carried out and will be described later). The reactor consisted of a 4-liter vessel of Pyrex glass, 14 cm in diameter and 34 cm in height equipped with a 4-bladed turbine impeller which is 6.4 cm in diameter and 1.27 cm in width. The impeller was fitted by a 1.27 cm motor shaft which, in turn, was fitted by a mechanical seal and bearings to the reactor cover. The cover was provided with adequate ports for feeding the solid particles, temperature measurement, liquid sampling and gas exit. The cover, shaft, turbine, sparger, sampling pipe and fittings were all stainless steel. A schematic diagram illustrating the experimental setup is shown in Figure 3.1.

3.3 Gas Handling System

Gases were fed to the reactor by means of a 0.5 cm diameter stainless steel ring sparger installed through the reactor cover. Before that, they passed through a long tubing to allow for better mixing. The sparger ring was provided with 16 perforations 0.05 cm diameter each. Each gas was delivered at 1.36 atm. For leaching experiments, only nitrogen was

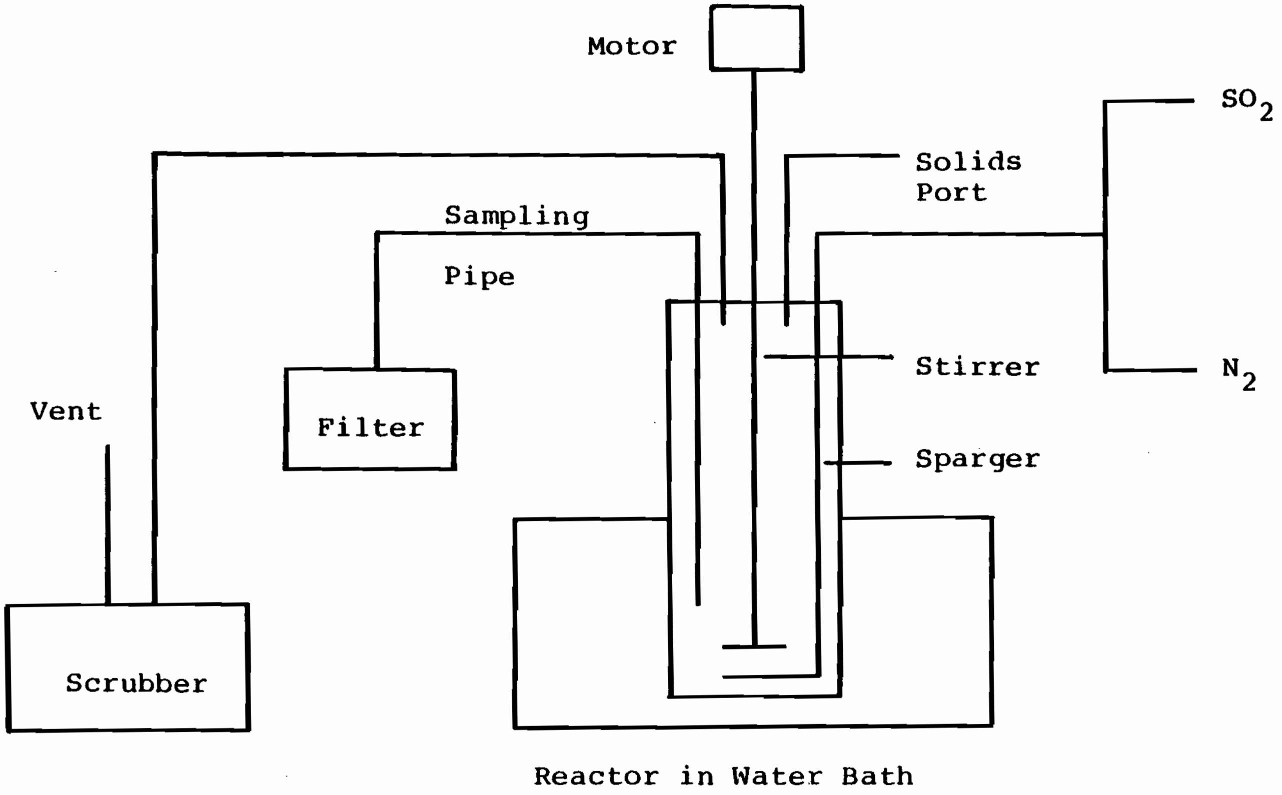

Figure 3.1 Schematic diagram of the experimental setup.

allowed to pass through the reactor. For absorption experiments, SO_2 was diluted in nitrogen to the desired inlet gas concentration by setting the appropriate flow rates of SO_2 while maintaining the flow rate of nitrogen constant. The SO_2 flow meter was calibrated by the soap-bubble method while the N_2 flow meter was calibrated with a wet-test meter. Typical calibrations of the SO_2 and N_2 flow meters are shown in Appendix A.

Effluent gases were passed through a 20 liter scrubber containing a solution of 20% sodium hydroxide to remove SO_2. A vent from the scrubber allowed the non-absorbed gases to pass to the fume hood.

3.4 Stirring, Temperature and pH

A variable speed Dyna-Mix stirrer (Fisher Scientific) capable of providing up to 2000 rpm of impeller speed was used. The speed was adjusted and monitored using a Strobotac strobe light (General Radio model 1531-AB).

All the reactor experiments were carried out at constant temperature. Isothermal conditions were maintained by immersing the reactor in a constant-volume water bath (Neslab Instruments). Cooling water was used when necessary.

For the leaching experiments, the pH of the water was adjusted to the desired level prior to the addition of the solids. For the absorption experiments, the pH of the water was not adjusted but it remained in the range of 5.4-5.6. The slurry pH was not controlled in order to quantify the changes caused by solid leaching, gas absorption or both. Adjustment of initial pH was made by the addition of several drops of 2 N HNO_3 or 0.1 N NaOH.

3.5 Slurry Preparation and Sampling

Slurries of fly ash and those of mixtures of ash and limestone were prepared by the addition of an accurately weighted amount of solids to a volume of 2 L of distilled water in the reactor at the desired conditions of the experiment (namely, agitation, temperature and initial pH). Solids were fed by a funnel through a designated port in the reactor cover and it was completed in 10-20 seconds.

In leaching experiments, samples were withdrawn from the reactor at the desired times through a sampling pipe into a vacuum filtration system. About 5-10 cm^3 of filtrate were collected through 0.45 μm pore-size membranes into a screw-capped test tubes. Part of the filtrate was used to measure the leachate pH (equal to slurry pH), and the rest was used for the determination of dissolved metal concentrations.

In gas absorption experiments, samples were withdrawn in a similar way but rather than filtration they are immediately poured into 250 cm^3 Erlenmeyer flasks containing iodine solution for the determination of absorbed sulphur dioxide concentrations.

3.6 Shake-Flask Experiments

A Volume of 200 cm^3 of distilled water was added to 500 cm^3 Erlenmeyer flasks. Accurately weighed amounts of fly ash were added and the flasks were placed in a shaker at a constant temperature of 30° C and stirring speed of 200 rpm. Samples were filtered and analyzed in the same way as described above for reactor experiments.

3.7 Analytical Methods

3.7-1 Gas Phase Analysis

The composition of the gas fed to the reactor was analyzed by gas chromatography (Hewlett Packard GC Model 5890 A) to verify the percent SO_2 in the mixture set by adjusting the individual gas flow rates. The chromatogragh was fitted with a Poropak QS column, and a thermal conductivity detector was used to detect the gases. The detector's signal was processed by a HP 3390 integrator. The exit gas was not analyzed.

3.7-2 Liquid Phase Analysis

The following three types of analyses were performed on liquid samples:

(1) Determination of dissolved metal concentrations. These metals were mainly calcium and magnesium released into solution due to solid leaching both in absence and in presence of gas absorption. The concentrations of sodium and potassium were also determined in preliminary leaching experiments. All the dissolved elements were determined by atomic absorption spectrophotometry using a Perkin Elmer model 403 spectrophotometer. This instrument uses air-acetylene flame as the source of energy and hollow cathode lamps as the light sources. Readouts were obtained in absorption units and the corresponding element concentrations (in mg/L) were calculated from the appropriate calibration curves. The calibrations were performed using standard (Fisher Scientific) solutions of the appropriate elements.

(2) Determination of absorbed SO_2 concentrations. Iodometric titration was used for this purpose and the details of the procedure are presented in Appendix B.

(3) Measurement of pH. This includes the adjustment of the initial pH and the measurement of the final pH of the solutions and slurries encountered in both the leaching and absorption experiments. The final pH levels of samples taken during an experiment were analyzed directly at the end of that experiment. A polymer combination pH electrode connected to a digital pH meter (Fisher Accumet) was used. The pH meter was standardized at room temperature against two buffer solutions (a combination of pH 2 and pH 4 or pH 4 and pH 7, according to the pH level of interest).

(4) Measurement of the total soluble alkalinity. This was determined by titration with 0.02 N HCl to the methyl orange end point.

3.7-3 Solid Phase Analysis

The following physical and chemical characterizations were conducted on the solid particles of fly ash:

1. Exploring the shape and the size of the particles. This was possible by taking scanning electron micrographs using a JEM-100 electron microscope (Jeol Ltd.,Japan).

2. Determination of the chemical composition of fractions of different particle size ranges to examine the relation between the metal content of the particles and their size. The percents of CaO and MgO among other major and minor components of fly ash were obtained by X-ray spectrophotometry. This type of analysis was performed at the Centre de Recherches minerales in Quebec City.

3. Estimation of the density using the water displacement method. A known weight of solids from the desired size fraction was added to a known volume of water in a measuring cylinder and the increase in the water volume was taken as the volume of the solids.

CHAPTER 4

Dissolution of Alkaline Metal Compounds

4.1 Introduction

In this Chapter, the experimental results on the characterization of the dissolution of the compounds of calcium and magnesium in fly ash will be presented and discussed. Both subbituminous (SB) and lignite ashes were examined and the results will be shown in terms of the concentrations of each metal as well as the leachate pH, all being functions of the leaching time.

The chemical compositions (as weight percents of metal oxides) of SB and lignite fly ashes are given in Tables 4.1 and 4.2 at different ranges of particle size. Lignite ash obviously has a higher alkaline metal content than subbituminous ash. The total alkaline metal content (defined as the sum of the percents of CaO, MgO, Na_2O and K_2O) in the reported size range has an average of 11.5% for SB ash and 20.7% for lignite. In general, the particle size has no effect on the concentrations of the reported metals in fly ash particles. However, it can be noticed that the concentrations of calcium and sodium in SB ash increased slightly as the

Table 4.1

Effect of Particle Size on the Chemical Composition of SB Ash

Component	45-53 μm	63-75 μm	75-90 μm	90-125 μm
SiO_2	60.2	61.2	60.1	61.4
Al_2O_3	21.3	21.4	22.0	22.4
Fe_2O_3	3.79	3.18	3.62	3.13
CaO	5.69	4.74	4.87	4.41
MgO	1.10	0.97	1.08	1.03
Na_2O	4.41	3.99	3.83	3.50
K_2O	1.47	1.66	1.53	1.60
TiO_2	0.50	0.48	0.48	0.49
MnO	0.03	0.02	0.03	0.02
P_2O_5	0.29	0.25	0.26	0.23
LOI(*)	0.31	0.40	0.48	0.62

(*) Loss on ignition.

Table 4.2

Effect of Particle Size on the Chemical Composition of Lignite Ash

Component	45-53 µm	53-63 µm	63-75 µm	75-90 µm
SiO_2	44.6	48.0	47.3	47.3
Al_2O_3	21.2	22.2	22.0	22.4
Fe_2O_3	7.05	5.83	6.49	6.34
CaO	13.9	12.7	12.9	12.7
MgO	4.69	4.31	4.44	4.41
Na_2O	1.96	2.00	2.01	2.03
K_2O	1.11	1.22	1.22	1.25
TiO_2	0.77	0.77	0.78	0.79
MnO_2	0.01	0.01	0.02	0.02
P_2O_5	0.26	0.26	0.26	0.25
LOI	0.55	0.82	0.83	0.74

particle diameter decreased.

Among the alkaline metals in fly ash, calcium and magnesium were found to be the only dissolvable metals important in the generation of alkalinity at the tested conditions as illustrated in Table 4.3. In this Table, the final concentrations of Ca, Mg, K and Na obtained after 60 minutes of contact between fly ash and the solution in the reactor are compared at two levels of initial pH. The particle size fraction used was 63-75 μm and the slurry density was 5 g/L. Calcium comprised 80-90% of the total alkaline metals dissolved and magnesium the balance. Almost no potassium and no sodium were found in the solution at the stated conditions.

In lignite particles, the content of calcium was three times higher than that of magnesium whereas in SB ash particles, the content of calcium was five times more than that of magnesium. In solution, however, the concentration of calcium was greater than magnesium by 5-100 times depending on the properties of the solution and dissolution conditions. This is due to the non-uniform distribution of metals in the solid particles where significant portions of calcium are associated with the surface of the particles. This is not the case for magnesium, potassium and sodium since these elements mostly exist in the interior of the glassy matrix as indicated by Hansen and Fisher (13).

Table 4.3

Concentrations of Alkaline Metal Ions (mg/L) After Leaching for 60 min in the Reactor

	From SB Ash		From Lignite	
Cation	pH 2	pH 6	pH 2	pH 6
Ca^{2+}	78	28	164	55
Mg^{2+}	5	1	35	1
K^+	1	Nil	Nil	Nil
Na^+	Nil	Nil	Nil	Nil

In Section 4.2, the effects of selected process variables on the dissolution behaviour of the alkaline components of fly ash will be evaluated. These variables are the slurry density (that is, the amount of fly ash solids added per unit volume of the liquid), the ash particle size, the initial pH of the liquid (that is, the adjusted pH of the water before the addition of the solids) and the slurry temperature. The initial rates of dissolution of the two dissolved metals were also estimated from a model based on solid-liquid mass transfer, and they will be shown in relation to the effects of these variables.

A series of long-term leaching experiments in Shake-Flasks were carried out along with the main reactor experiments. One purpose of this was to estimate the equilibrium amount of dissolved calcium compared to that obtained from a reactor experiment. This information would help in determining the length of leaching time in the reactor when most of the dissolvable metal is released into solution. Also, these experiments would give an idea about the effects of the proposed variables and therefore help in selecting the levels of variables to be used in the design of the reactor experiments.

In order to determine the appropriate stirring speed of the impeller for the reactor experiments, a set of leaching experiments was carried out at different stirring speeds. A comparison of the concentrations of calcium dissolved from SB ash at 400, 600, 800 and 1000 rpm is shown in Figure 4.1. An increase in the speed from 800 to 1000 rpm did not significantly change the concentration of the dissolved element. Therefore, the reactor experiments were all carried out at 800 rpm.

4.2 Effect of Slurry Density

The effect of slurry density on the final concentration of dissolved calcium from SB ash obtained after a long-term leaching (15 h) in a shake-flask experiment is shown in Figure 4.2. Below 7 g/L, the concentration of dissolved calcium was proportional to the amount of solids added. The maximum amount of dissolved calcium was 18 mg per gram of solids. In this range, the dissolution of calcium compounds was limited by the slurry density. Above 7 g/L, the effect of slurry density diminished and above 30 g/L, the concentration of dissolved calcium showed little change where the leachate eventually became saturated at about 200 mg calcium/L preventing further dissolution. The final pH corresponding to this saturation level was 3.8. The effect of slurry density on the dissolution of the particles is also shown in Table 4.4 as percents of dissolved calcium oxide. It is obvious that the slurry density has a strong effect on

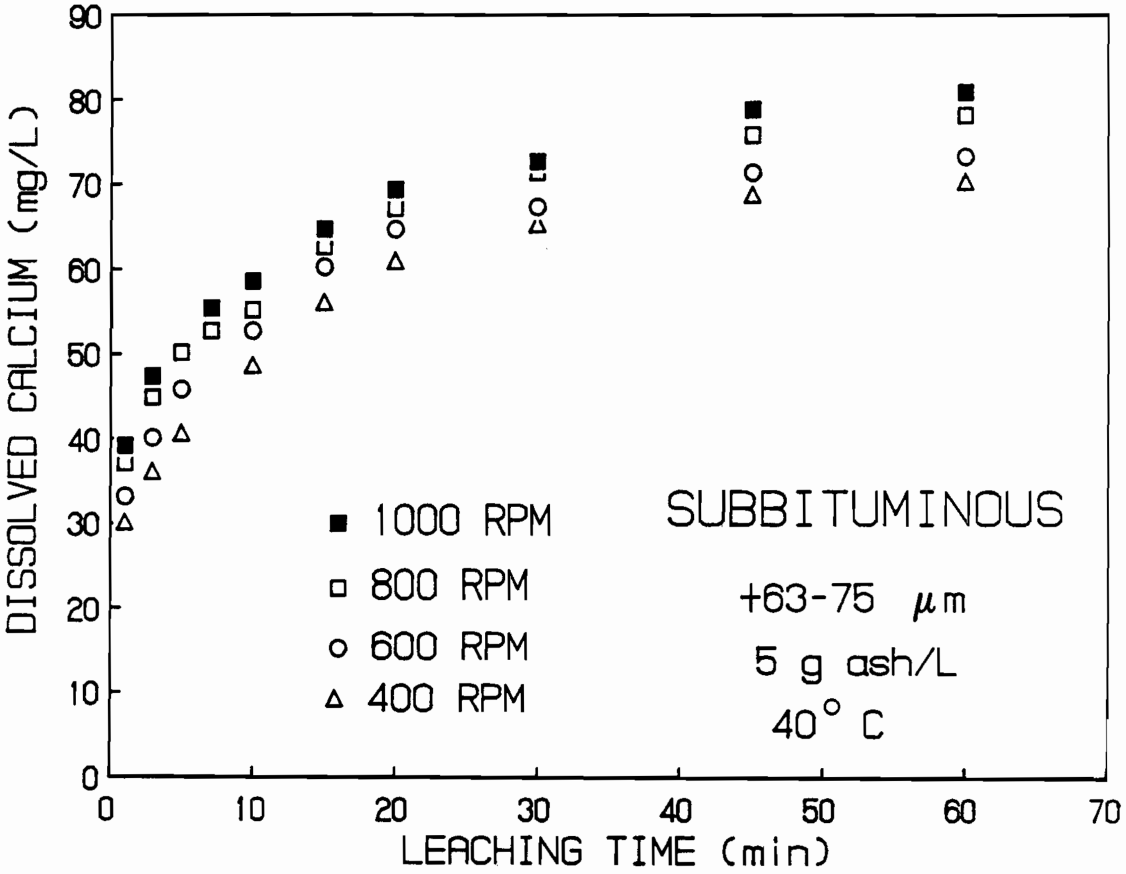

Figure 4.1 Effect of stirring speed on the dissolution of calcium from fly ash.

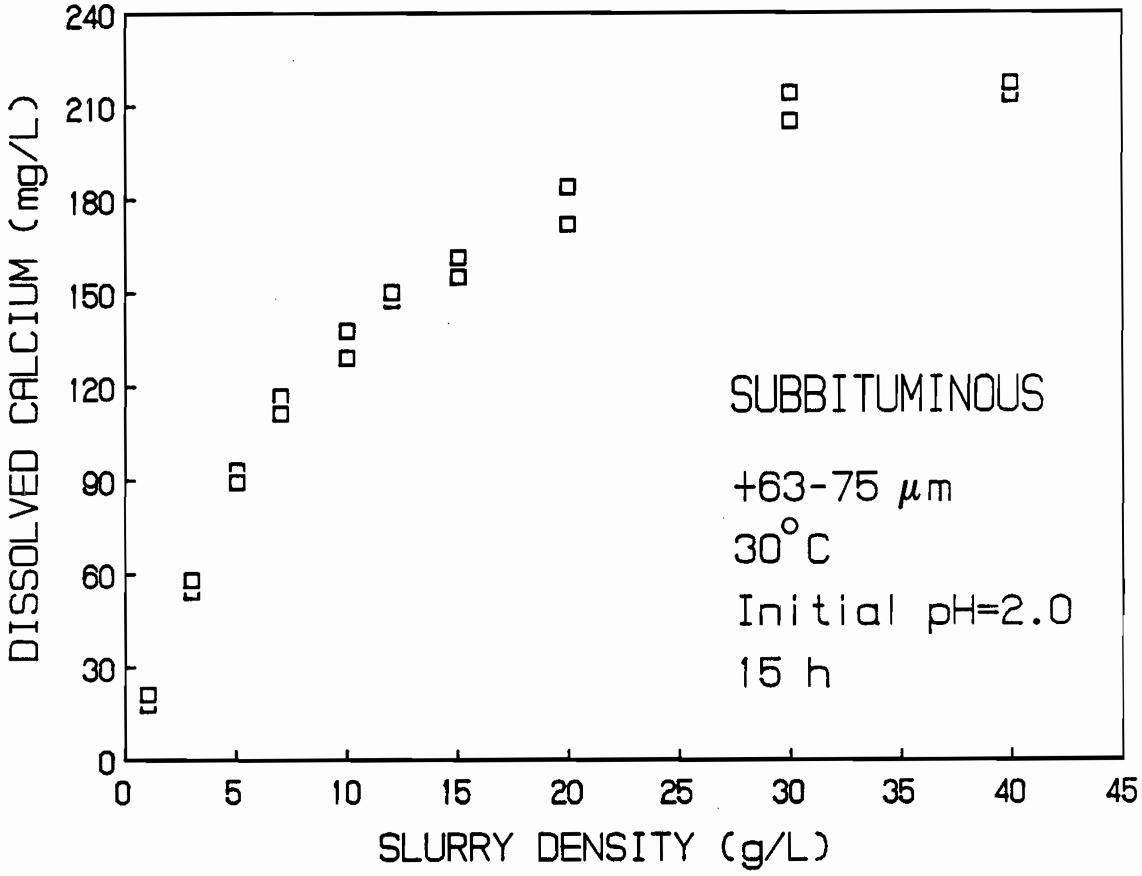

Figure 4.2 Effect of slurry density on the concentration of dissolved calcium after 15 h of leaching.

Table 4.4

Percent of Calcium Oxide Dissolved at Different Slurry Densities after 15 h

Slurry Density (g/L)	Percent CaO Dissolved
1	58.4
3	55.4
5	53.9
10	39.2
15	31.1
20	26.0
30	20.6
40	15.9

the dissolution. The percent of dissolved CaO (defined as the ratio of calcium concentration in solution expressed as CaO to that in the particles) decreased by 70% as the slurry density increased from 1 to 40 g/L. Based on these results, the reactor experiments were carried out at the slurry densities of 5, 10 and 20 g/L, representing the linear, transition and saturation regions, respectively.

The effect of slurry density on the dissolution of the compounds of calcium and magnesium from SB ash are shown in Figure 4.3 while the corresponding plots for lignite ash are shown in Figure 4.4. All these results were obtained from reactor experiments. The main feature in these Figures is the immediate increase in the concentrations of soluble metals which then tended to level off after 20-30 minutes in the case of SB and 10-20 minutes in the case of lignite. A comparison of Figures 4.3 (A) and 4.2 indicates that, for SB ash, most of the dissolved calcium available after 15 h was obtained in 60 minutes of leaching in the reactor. Therefore, 60 minutes were considered sufficient to extract the major portion of alkaline metals responsible for the soluble alkalinity in fly ash leachates.

In contrast to the final concentrations which were obtained after 60 minutes of solid-liquid contact, the initial concentrations of both calcium and magnesium as determined

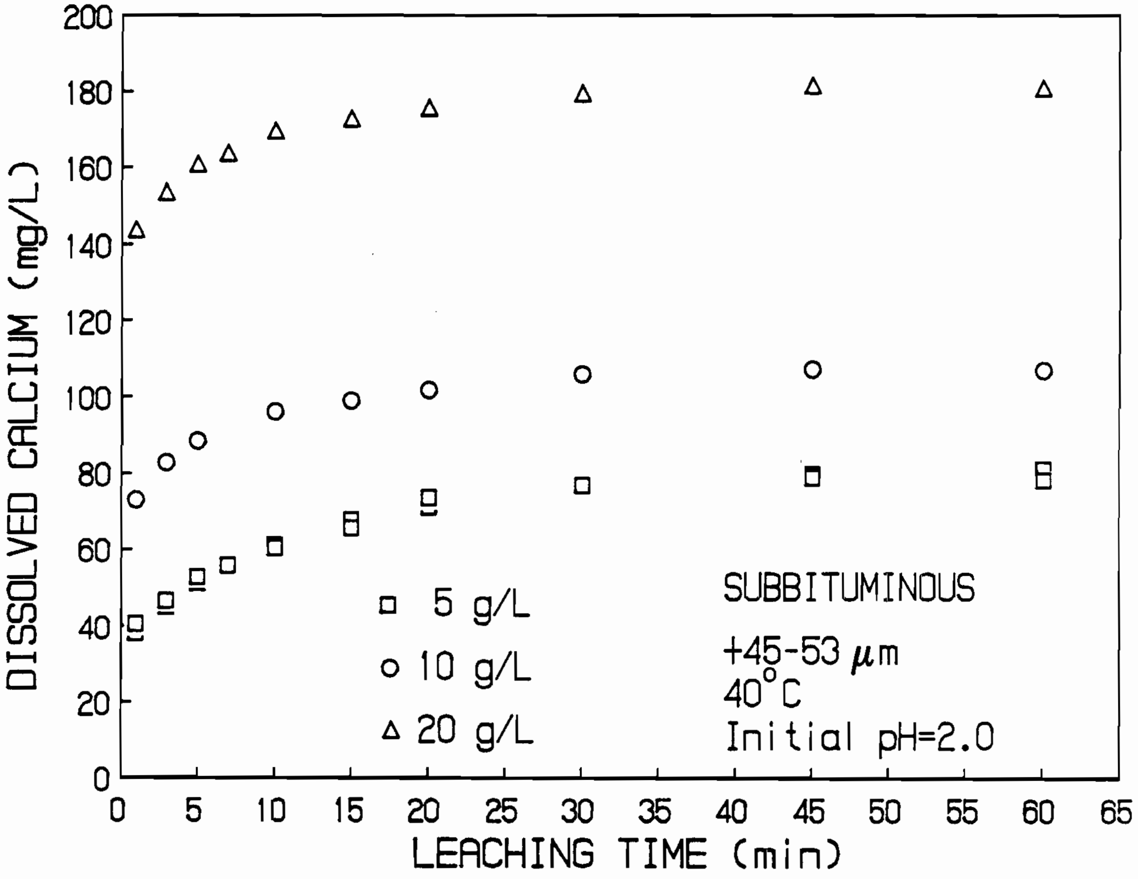

Figure 4.3 (A) Effect of slurry density on the concentration of calcium dissolved from SB ash.

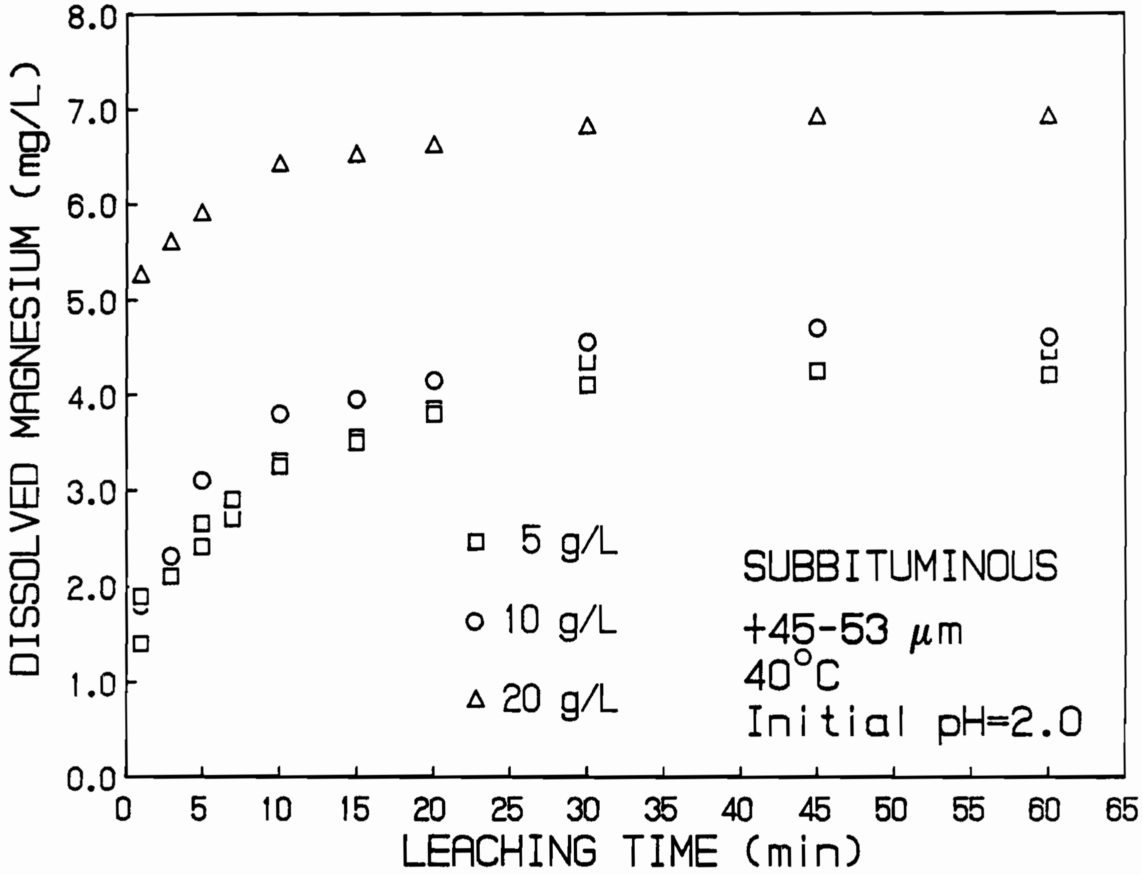

Figure 4.3 (B) Effect of slurry density on the concentration of magnesium dissolved from SB ash.

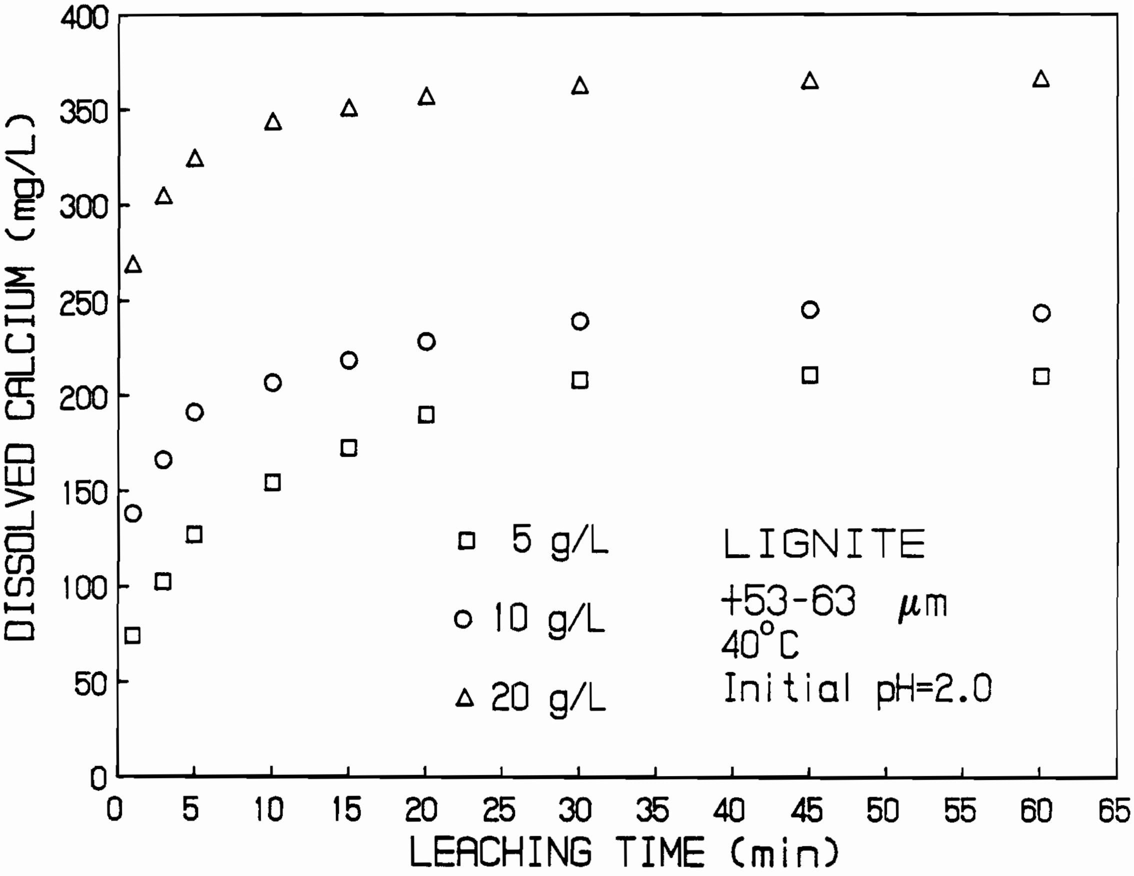

Figure 4.4 (A) Effect of slurry density on the concentration of calcium dissolved from lignite ash.

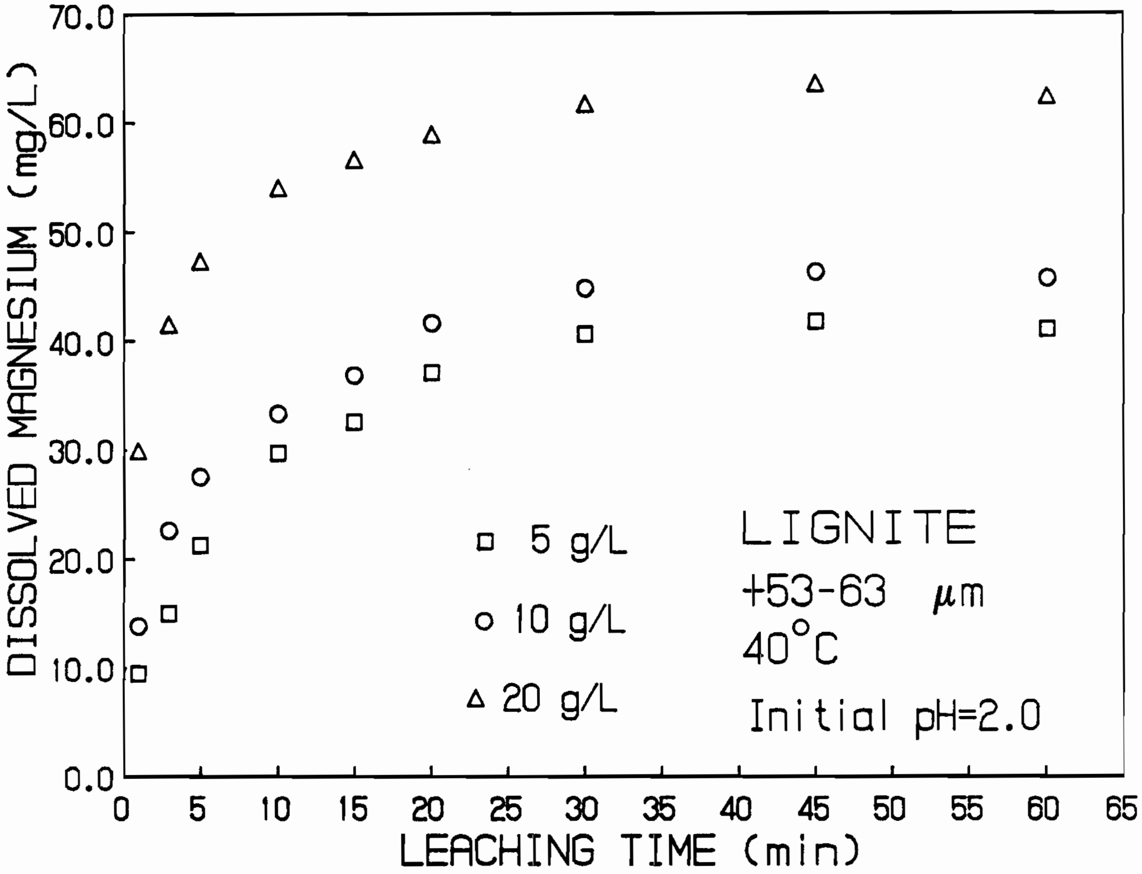

Figure 4.4 (B) Effect of slurry density on the concentration of magnesium dissolved from lignite ash.

after one minute of contact were proportional to the amounts of solids added to the reactor. For the tested slurry densities of 5, 10 and 20 g/L, the corresponding initial concentrations of calcium dissolved from lignite ash were 73, 138 and 268 mg/L and those from SB ash were 38, 73 and 143 mg/L. This initial rise in the concentrations is associated with the total surface area of the particles in the reactor as will be explained later.

The surface area of the solid particles per unit volume of slurry can be determined from the slurry density and the average specific area of the solid particles. Scanning electron micrographs showed that the particles of both fly ash types have a predominantly spherical shape (Figure 4.5) thus permitting the estimation of the specific surface area from the density and the average size of the particular fraction.

4.3 Effect of Particle Size

In order to determine the effect of the particle size, a series of experiments with particles having different size ranges were carried out while the slurry density was kept at 5 g/L. The data are plotted in Figures 4.6 and 4.7 for SB and lignite ashes, respectively. In general, a trend can be seen where the concentrations of both calcium and magnesium increased with a decreasing particle size. However, the

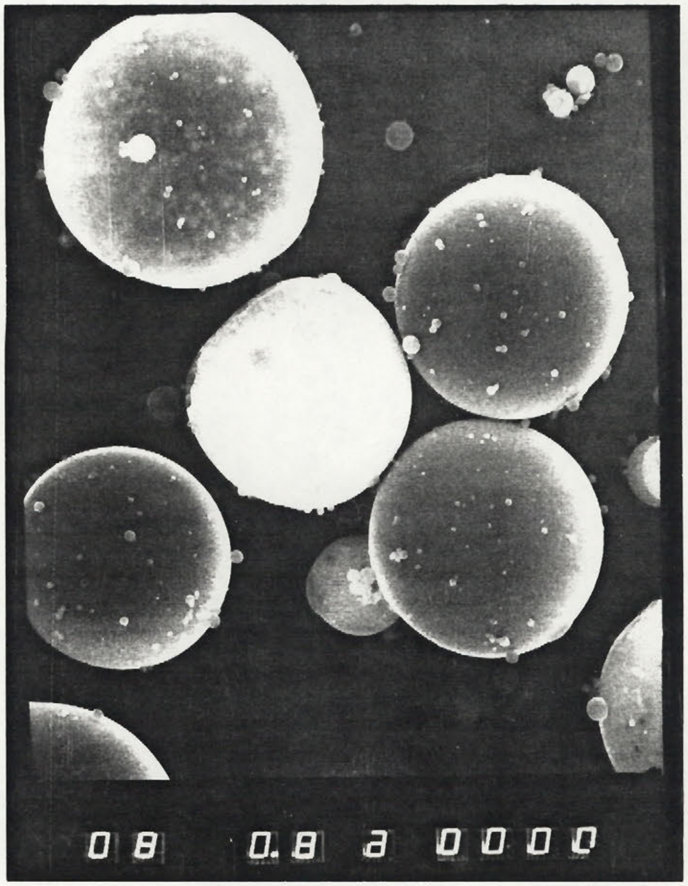

Figure 4.5 (A) Scanning electron micrograph of fresh SB ash particles

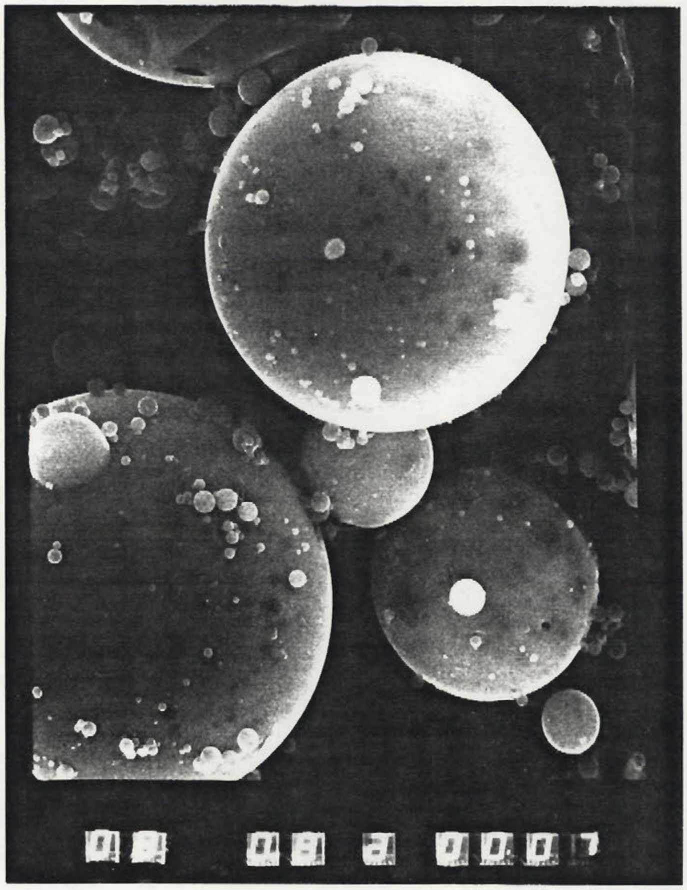

Figure 4.5 (B) Scanning electron micrograph of fresh lignite ash particles

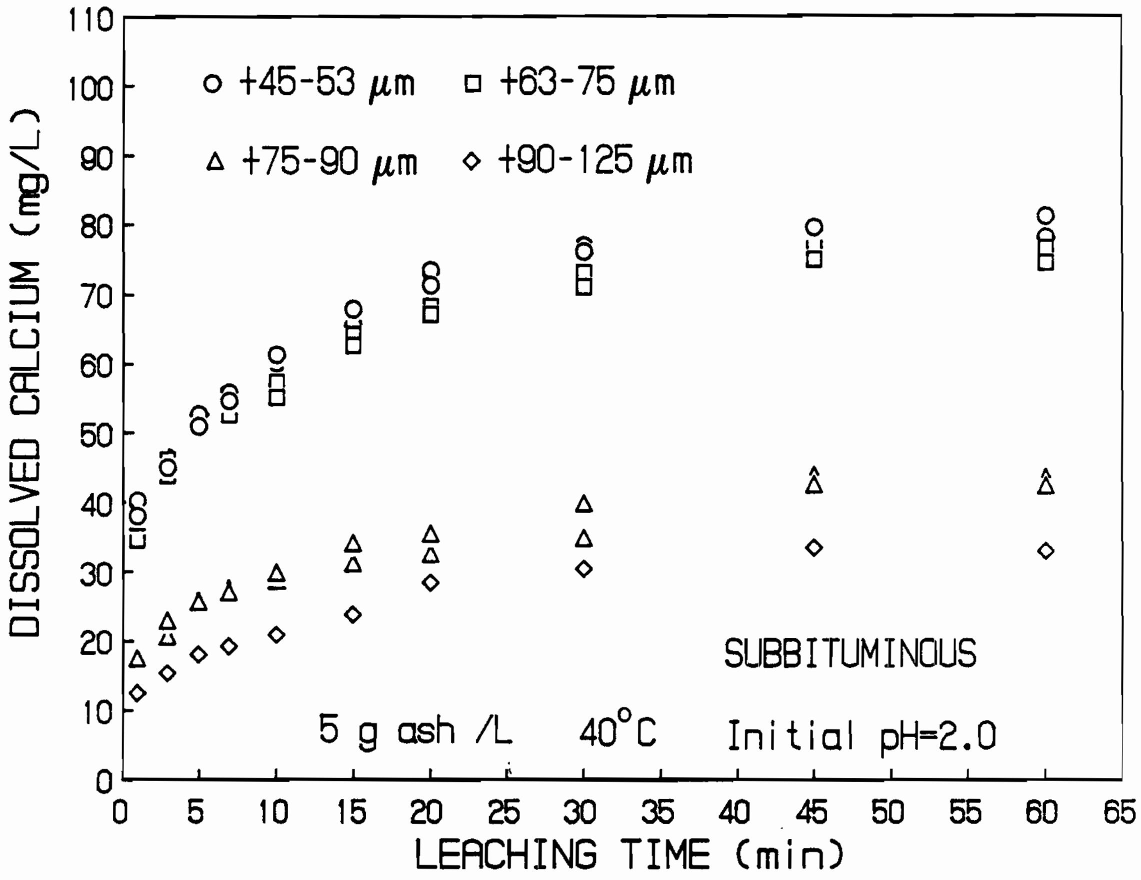

Figure 4.6 (A) Effect of particle size on the concentration of calcium dissolved from SB ash

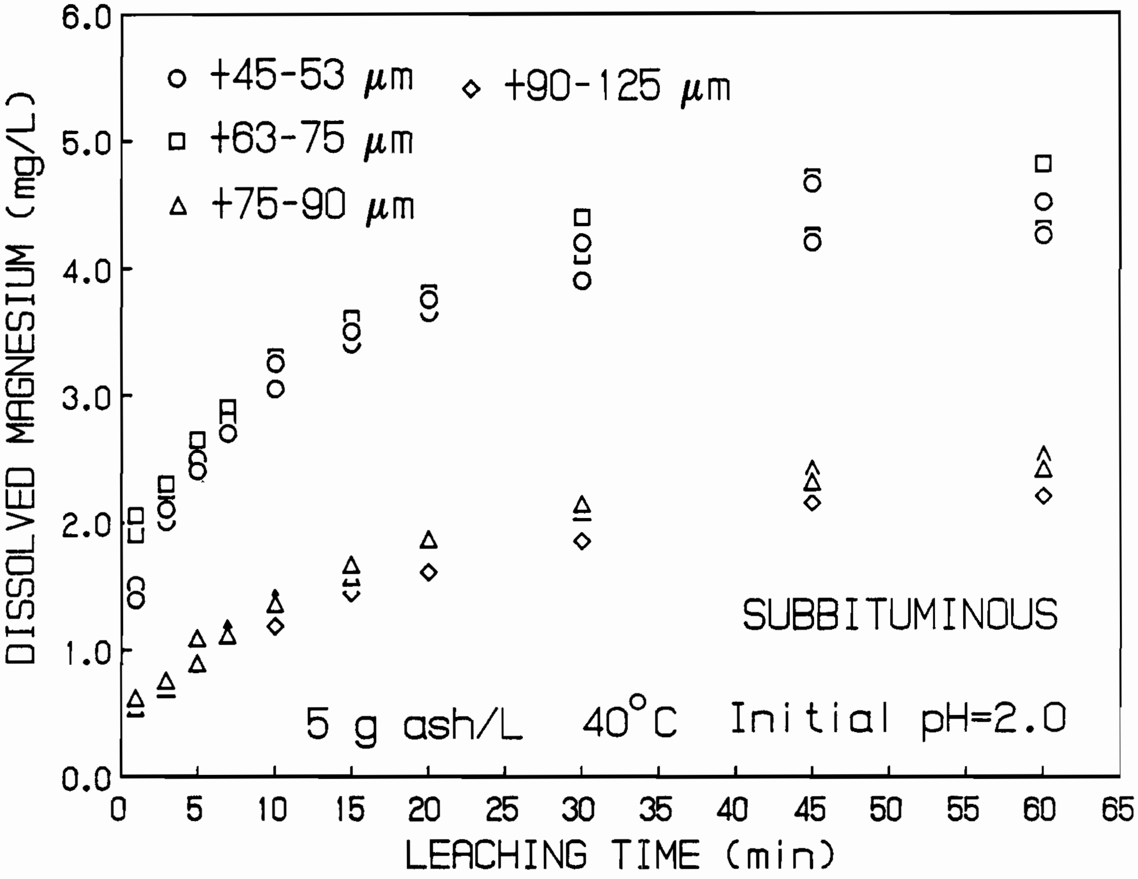

Figure 4.6 (B) Effect of particle size on the concentration of magnesium dissolved from SB ash

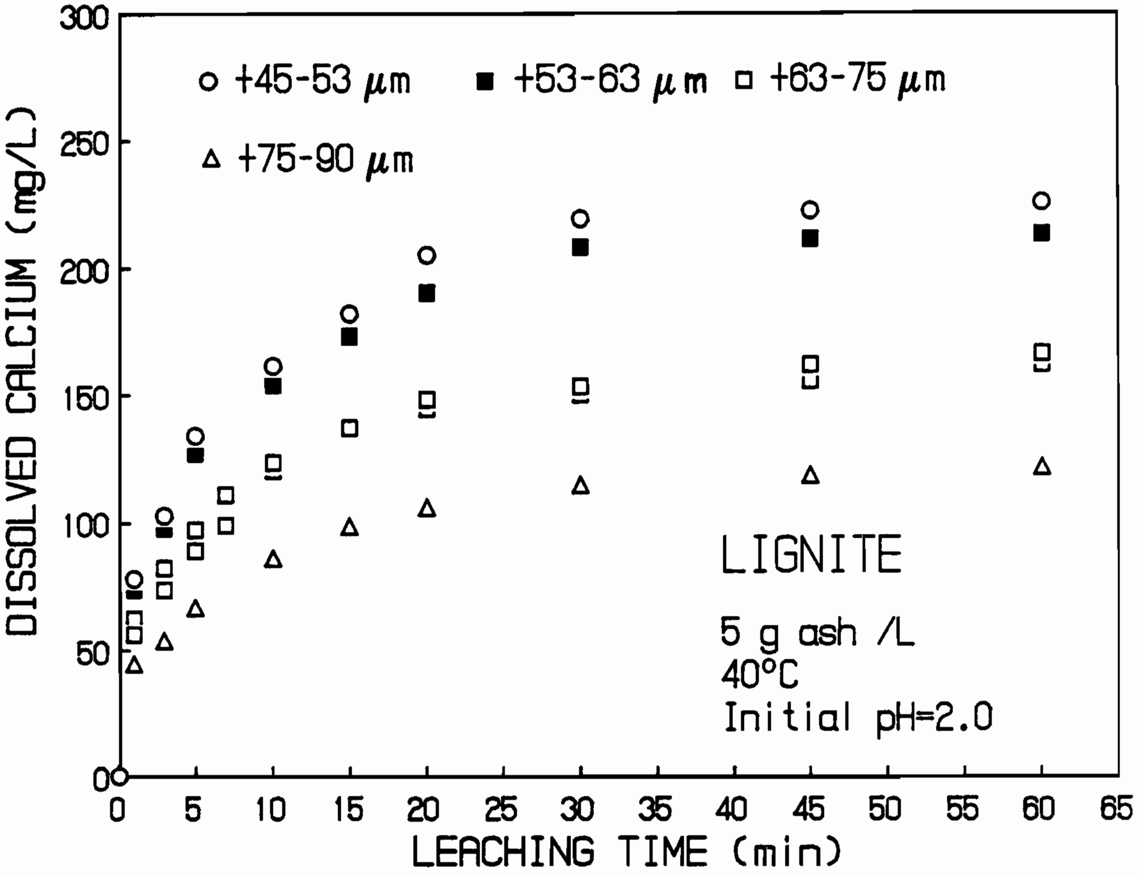

Figure 4.7 (A) Effect of particle size on the concentration of calcium dissolved from lignite ash

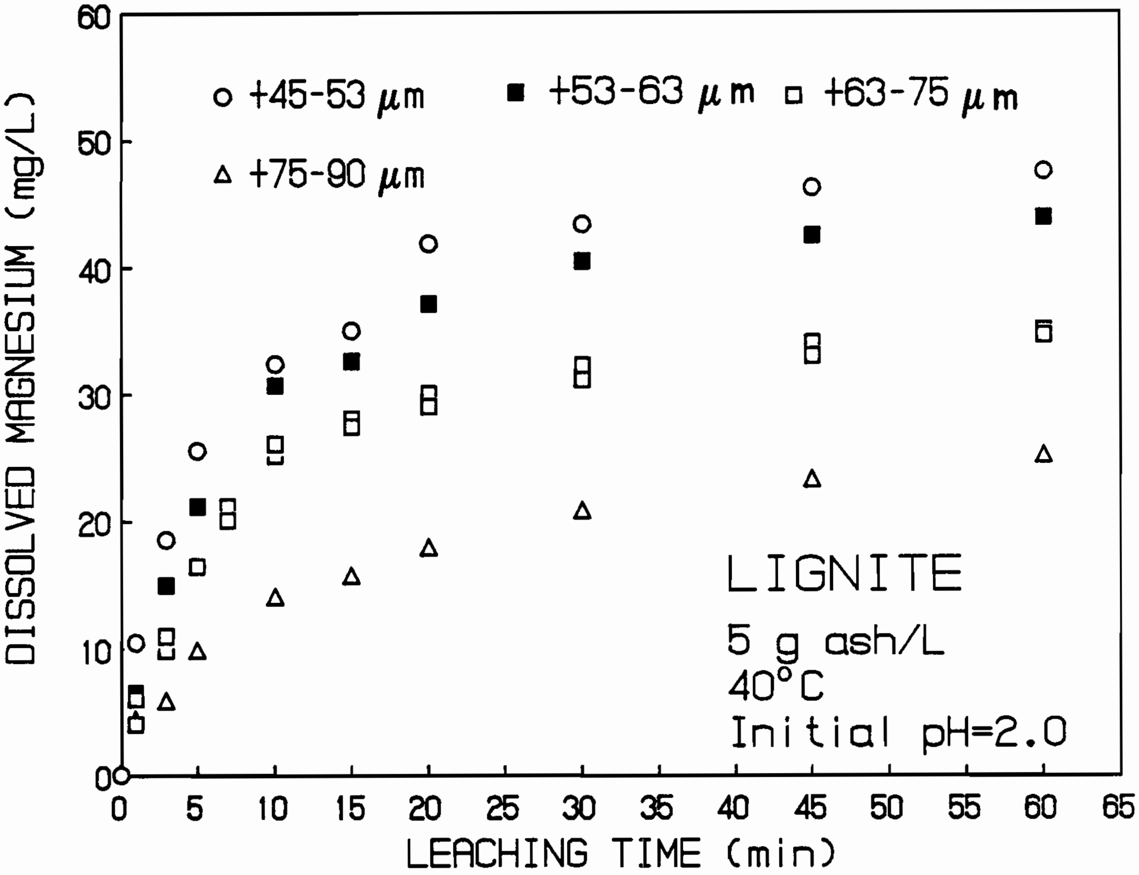

Figure 4.7 (B) Effect of particle size on the concentration of magnesium dissolved from lignite ash

change in the concentration is not proportional to the corresponding change in the particle diameter. For example, there is no difference in the concentrations of calcium or magnesium dissolved from SB ash particles having a size range of 45-53 or 63-75 μm. Also, there was no significant change in the concentrations of either metal when particles of lignite ash of the size range 45-53 or 53-63 μm were used.

4.4 The Role of Surface Area

In order to show that the initial rise in dissolved metal concentrations is due to the dissolution from the parent compounds associated with the surface of the particles, the initial concentration (obtained after one minute of contact) was plotted against the surface area per unit volume of slurry, A, expressed as cm^2/L. This area was calculated from the following relationship:

$$A = a.S \tag{4.1}$$

where "a" is the specific surface area of the particles (cm^2/g) and S is the slurry density (g solids/L). The specific surface area of a solid fraction was calculated assuming spherical particles of an average diameter in the middle of the size range. The advantage of such a plot is that it permits the combination of the results from the slurry density experiments with those from the particle size experiments. Linear relationships where obtained for calcium and magnesium dissolved from lignite ash (Figure 4.8) and from SB ash (Figure 4.9).

These linear relationships clearly demonstrate that the initial increase in the concentrations of dissolved metals is due to the release of these elements from the surface of the particles as soon as they contact the liquid phase. Contrary to the behaviour of the initial concentrations, the concentrations obtained after 60 minutes of contact did not correlate with the surface area of the particles as demonstrated in Figure 4.10.

Further confirmation that the initial rise in concentrations of calcium and magnesium was due to the dissolution of their compounds associated with the surface of the particles was obtained from an experiment in which the slurry at the end of a typical run was filtered, and the solids were reused for a second run. The solids which were initially leached were added to fresh water at the same initial pH as the first run (that is, pH 2.0). The concentrations of calcium and magnesium dissolved in the second run are compared to those obtained from fresh particles in Figure 4.11. The concentrations of both calcium and magnesium obtained from recycled solids were much less those

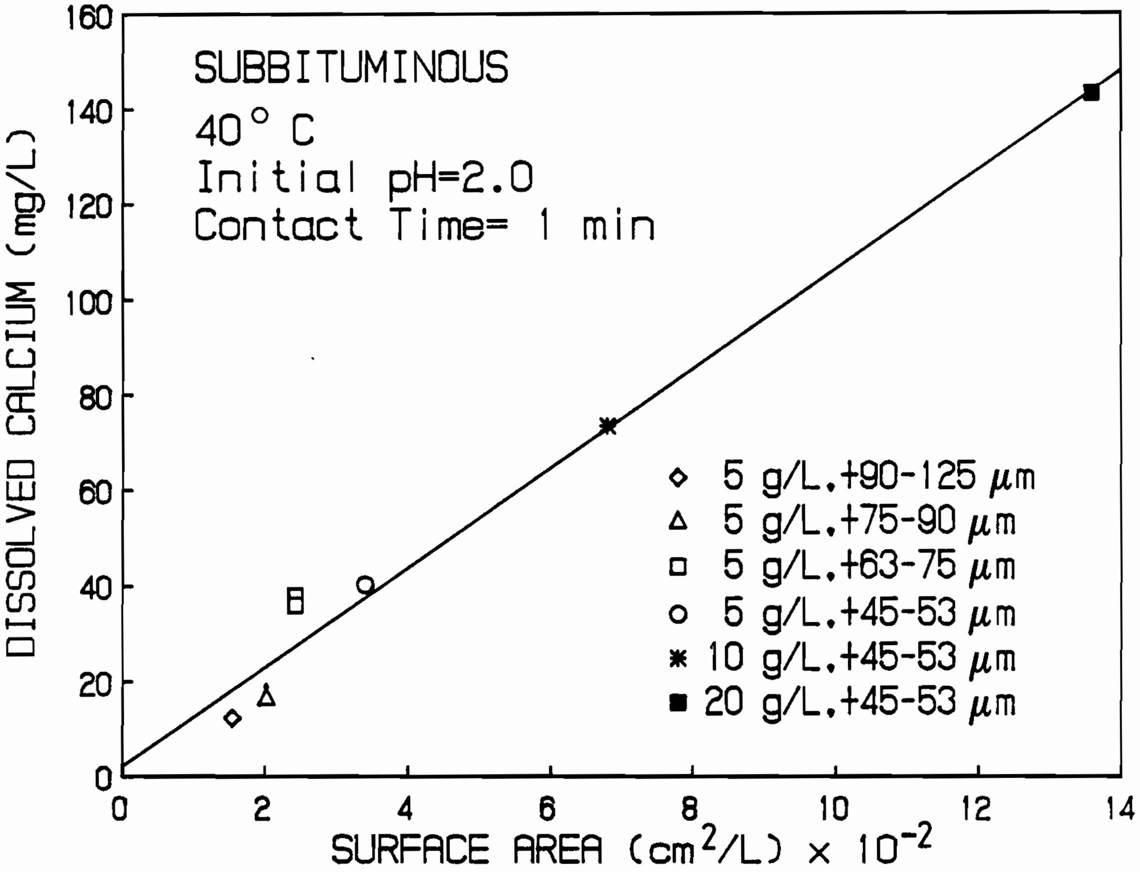

Figure 4.8 (A) The relationship between the initial dissolved calcium concentration and the surface area of SB ash particles

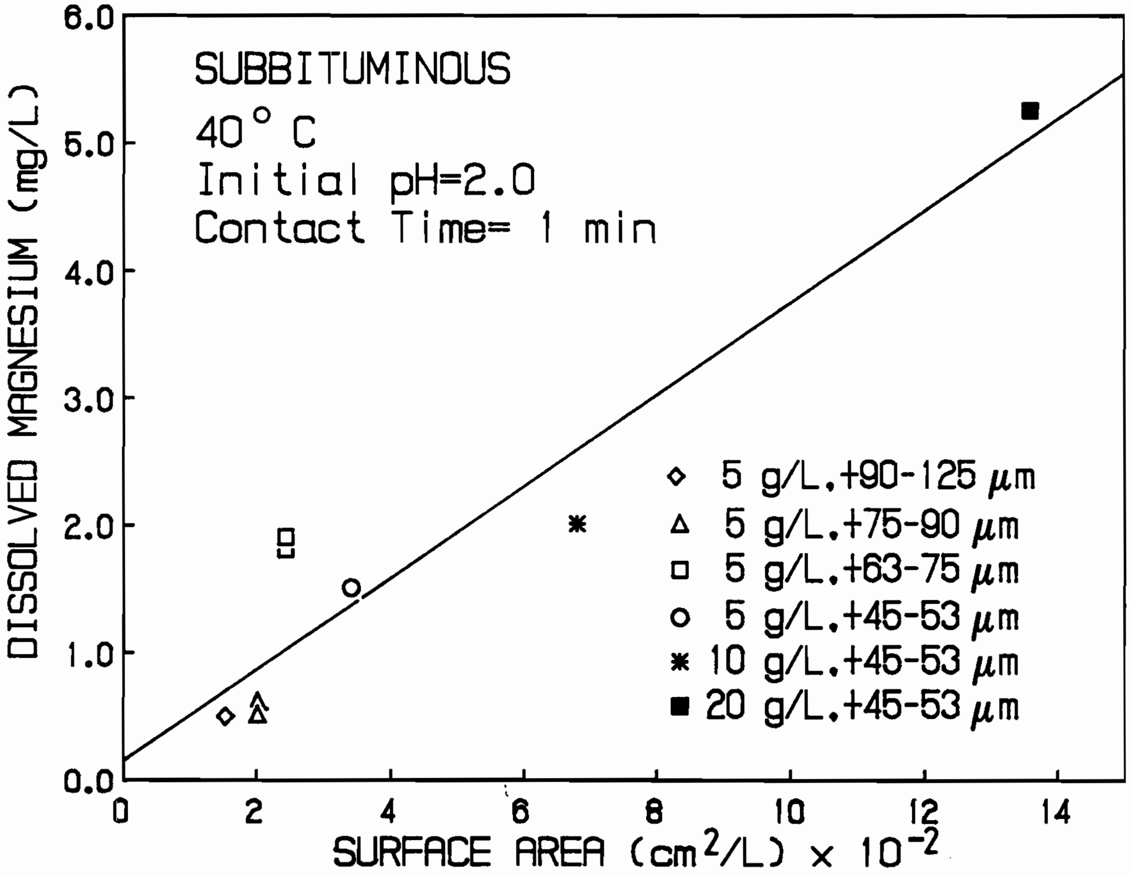

Figure 4.8 (B) The relationship between the initial dissolved magnesium concentration and the surface area of SB ash particles

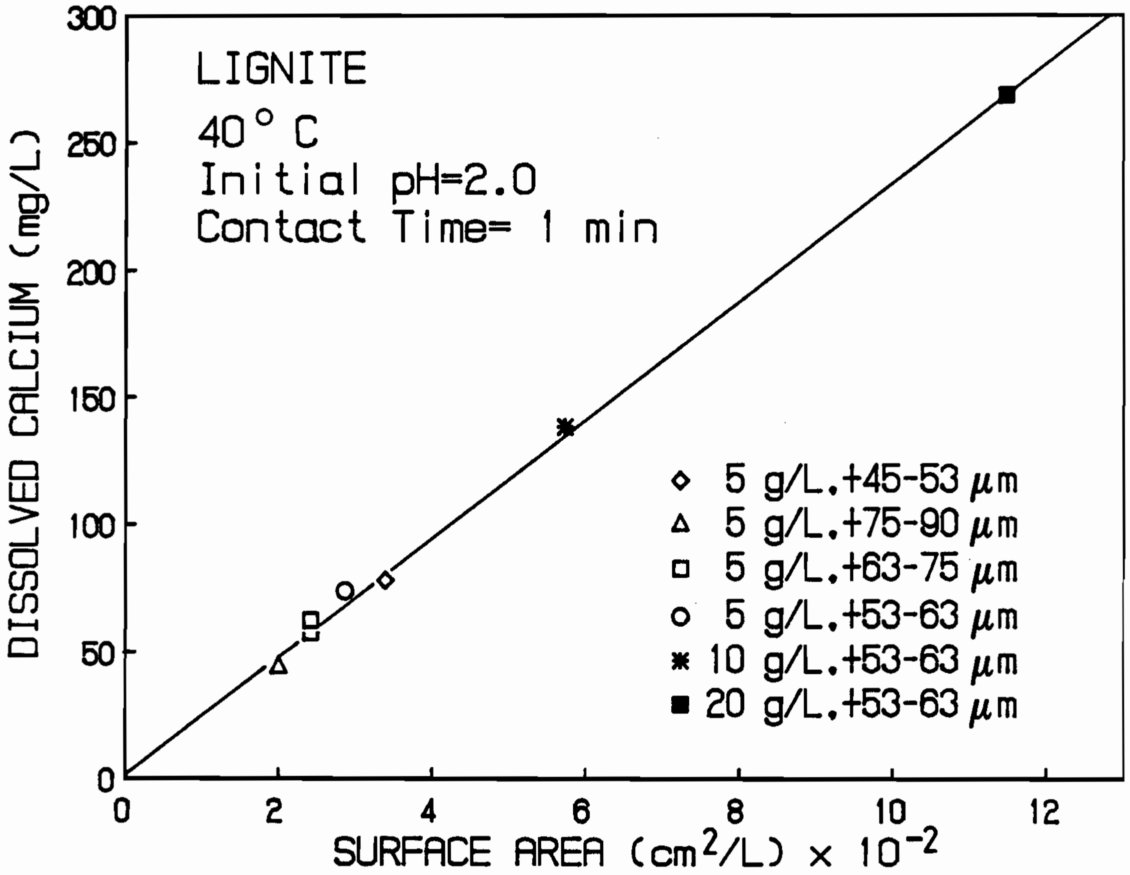

Figure 4.9 (A) The relationship between the initial dissolved calcium concentration and the surface area of lignite particles

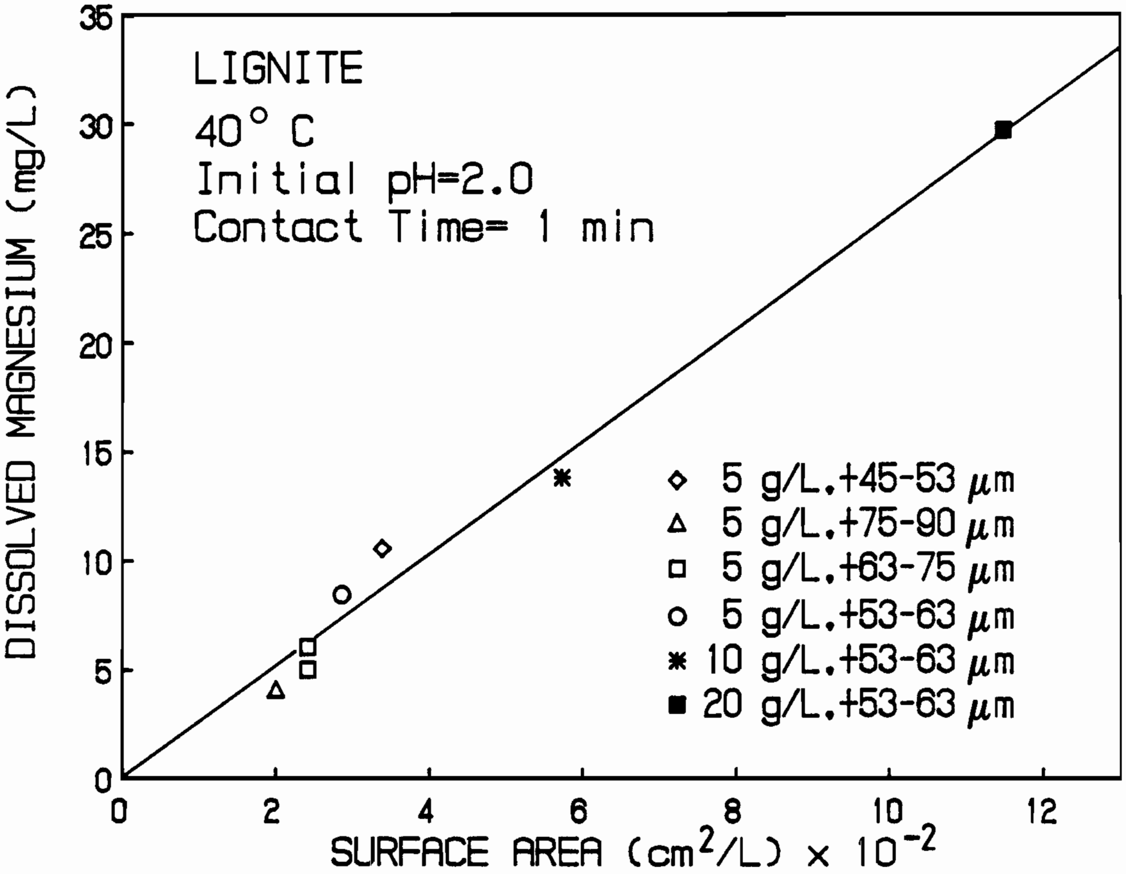

Figure 4.9 (B) The relationship between the initial dissolved magnesium concentration and the surface area of lignite particles

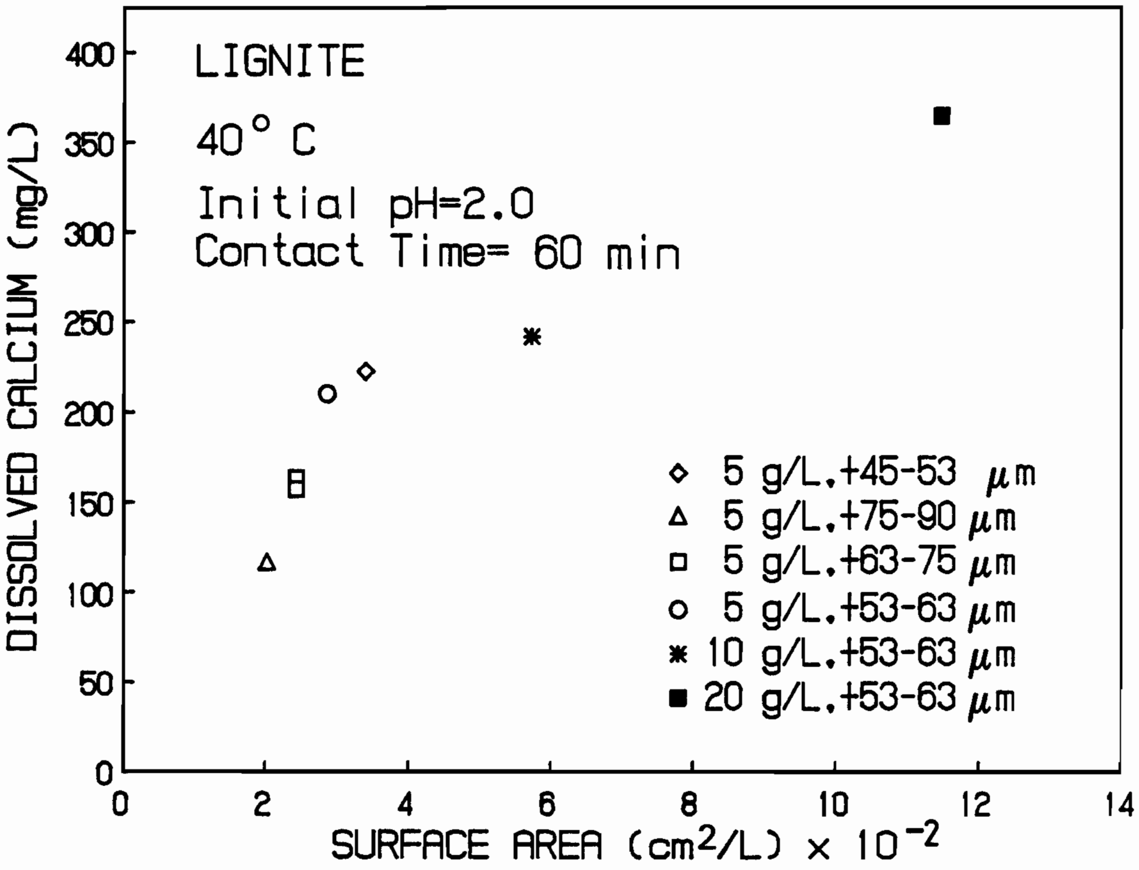

Figure 4.10 The relationship between the final dissolved calcium concentration and the surface area of fly ash particles

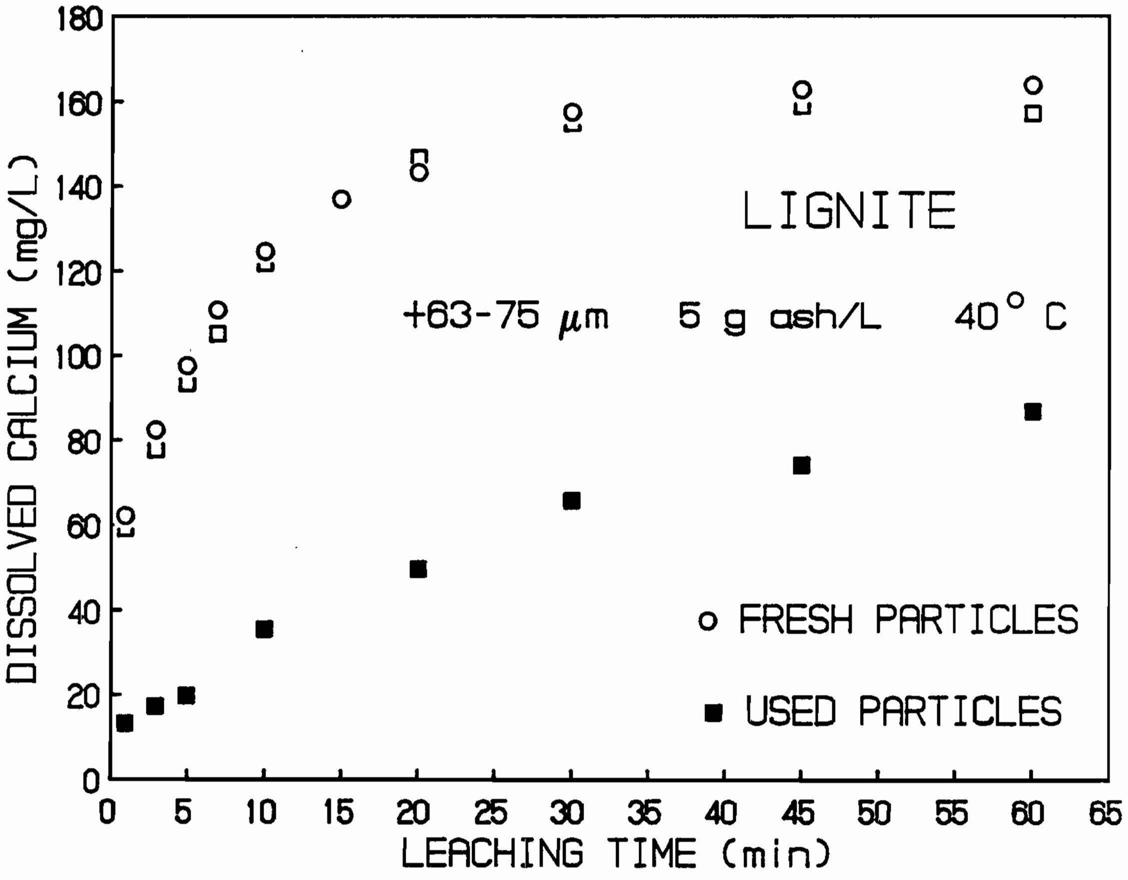

Figure 4.11 (A) Dissolved calcium concentration from fresh and used fly ash

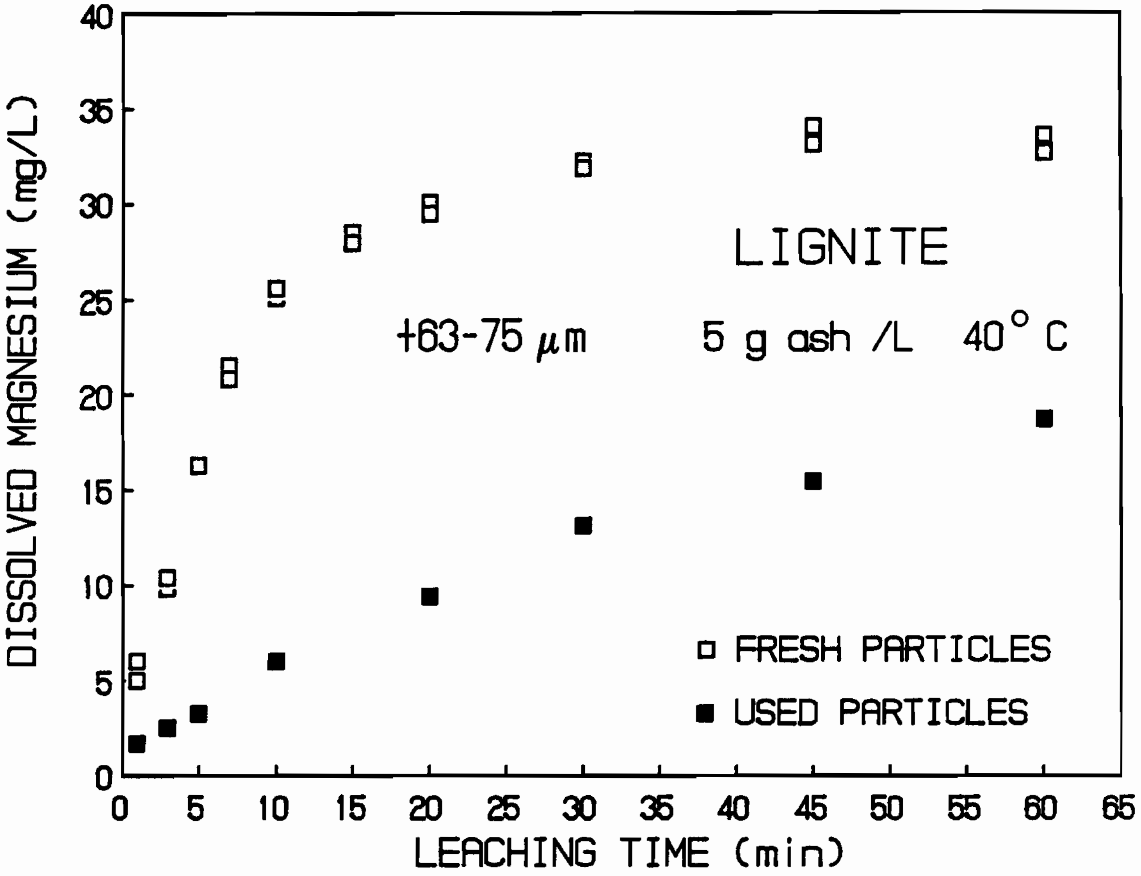

Figure 4.11 (B) Dissolved magnesium concentration from fresh and used fly ash

obtained from fresh particles after the same period of contact time. Also, dissolution from the recycled solids was slower, and no initial rise in the concentrations was observed since all the dissolvable calcium and magnesium were removed from the surface of the particles in the first leach.

Before presenting the results showing the effect of the rest of variables on the dissolution process, a simple model that was used in estimating the rates of dissolution will be presented. The effects of slurry density and particle size on the rates of dissolution will then be shown and discussed.

4.5 Rates of Dissolution

4.5.1 Dissolution Model

Observations made from the experimental results discussed above indicate that the dissolution of metal compounds in fly ash occurs in three consecutive steps. As shown above, the initial step is characterized by rapid dissolution from the surface of the particles which takes place upon immediate contact between the particles and the solution. The second step involves the dissolution from the solid layer next to the particle surface. In this step, the diffusion path within the particle and next to the surface is assumed to be very small and the dissolution is controlled by liquid-side mass transfer of the dissolving species. The final step is the slow dissolution controlled by the solid state diffusion of the solute from the interior of the particles. The results and the theory described above also agree in general with the findings of other studies (6,34,54). Since this investigation is concerned with short-term dissolution of metals responsible for providing the alkalinity to be used in flue gas scrubbing, only the initial rates of dissolution are of pertinent interest and the dissolution related to diffusion in the solid phase is not important.

In the first two steps of the dissolution process, the contact between the liquid (solvent) and the solid particles results in a high concentration of the solute at the surface of the particles. The difference between this interfacial concentration and that of the bulk liquid provides the driving force for the transfer of the dissolving species (e.g. Ca and Mg ions) to the bulk of the liquid.

In the first stage, the rate of dissolution is dominated by a high concentration difference since the bulk concentration is initially very low. The driving force, however, decreases very rapidly after the initial dissolution of the metals associated with the surface because of the increase in the bulk concentration. Moreover, at the end of the initial stage, the interfacial concentration (C_{mi}) is decreased due to the depletion of the solids causing further reduction in the driving force for transfer of the metal ions.

The initial dissolution, however, does not remove all the calcium or magnesium from the particle surface and its vicinity. The remaining amount of the alkaline metals will leach at lower rates which are limited by liquid-side mass transfer until the metals are depleted and the solid state diffusion takes over. Accordingly, in this period of time, the rate of transfer of the dissolved metal ions (expressed as mg/L.min) is given by the following equation:

$$dC_m/dt = k_La\ (C_{mi} - C_m) \tag{4.2}$$

where C_m = concentration of dissolved metal in the bulk liquid at any time, mg/L

C_{mi} = concentration of dissolved metal at the interface, mg/L, and

k_La = overall mass transfer coefficient, min^{-1}.

Assuming that the interfacial concentration, C_{mi}, is the final concentration when the leaching isotherm levels off and remains constant during the second stage when liquid-side mass transfer controls the rates, Equation 4.2 can be written in the integrated form as :

$$-\ln [(C_{mi} - C_m)/(C_{mi} - C_{m0})] = k_La\ t \qquad (4.3)$$

where C_{m0} is the concentration of the dissolved metal at zero time. Because of the immediate rise in the bulk concentration due to the dissolution from the surface in the initial stage, C_{m0} can not be considered as zero. In order to determine C_{m0} and k_La, Equation 4.3 is rearranged as follows:

$$-\ln [(C_{mi} - C_m)/C_{mi}] = -\ln [(C_{mi} - C_{m0}/C_{mi}] + k_La\ t \qquad (4.4)$$

which is equivalent to :

$$Y = A + b\ t \qquad (4.4a)$$

Typical plots of Y versus t shown in Figure 4.12 indicate that the linear relationship is valid within at least 15 minutes of leaching time beyond which diffusion inside the particles becomes the dominant mechanism. The values of k_La calculated from the slopes of these lines for the slurry density experiments are 0.07, 0.11 and 0.13 for SB ash and 0.09, 0.10 and 0.17 for lignite ash at 5, 10 and 20 g/L, respectively.

The intercept A is related to C_{m0} by this equation:

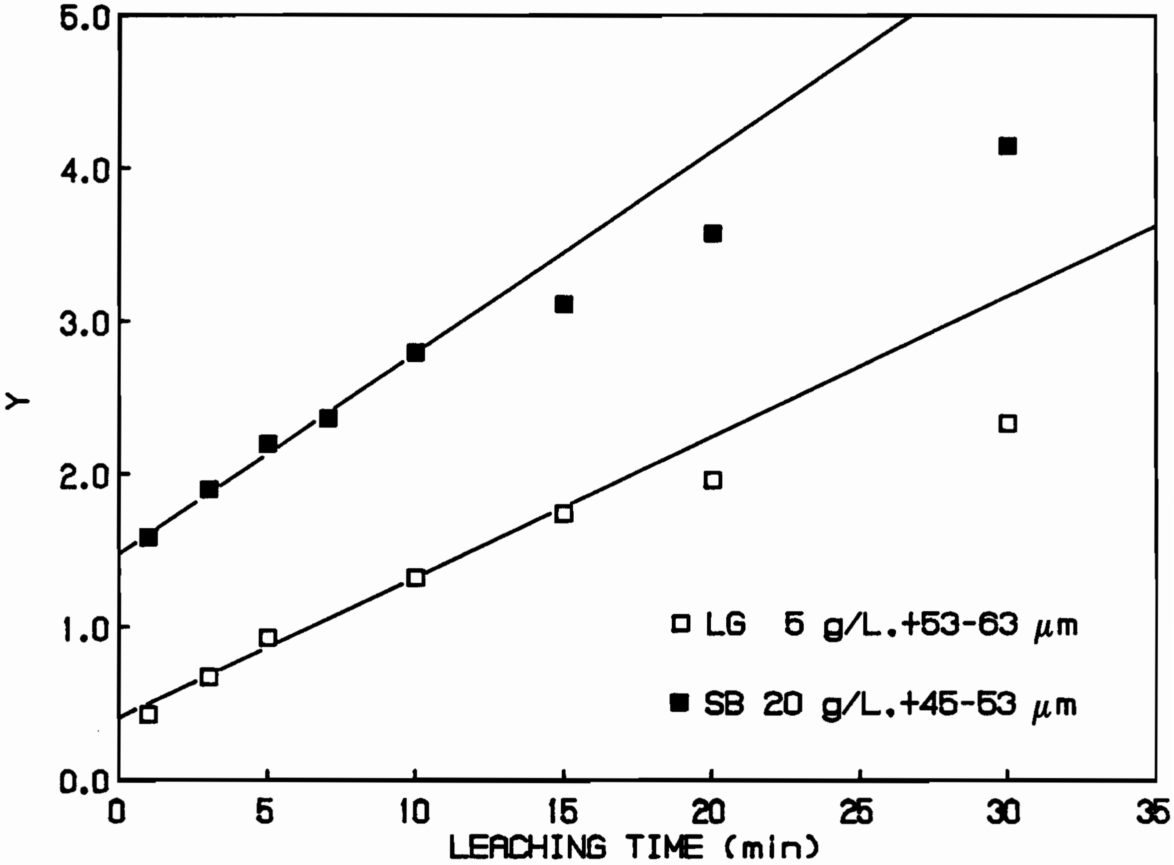

Figure 4.12 Typical plots based on the dissolution model indicating the range of model application

$$C_{m0} = C_{mi}\ [1 - \exp\ (- A)] \tag{4.5}$$

For the representative plot for 20 g/L of SB ash shown in Figure 4.12, for example, the intercept A, which was obtained from linear regression, was found to be 1.61 and C_{mi}, obtained from Figure 4.3 (A), is 180 mg/L. The calculated C_{m0} was found to be 144 mg/L. A comparison with the concentration of dissolved calcium obtained experimentally after 1 minute (which is 143 mg/L) shows that this value of C_{m0} is a good estimate. It is important to note that when C_{m0} was assumed to be zero, the model was not applicable in the period of interest.

Knowing the values of the overall mass transfer coefficient, k_La, the rates of dissolution were calculated from the following equation, which is obtained by combining equations 4.2 and 4.3:

$$dC_m/dt = k_La\ (C_{mi} - C_{m0})\ \exp\ (-k_La\ t) \tag{4.6}$$

4.5.2 Effect of Slurry Density on the Rates

The rates of dissolution (in mg/L.min) of the compounds of both calcium and magnesium from SB and lignite ash at the tested slurry densities of 5, 10 and 20 g/L are plotted in Figures 4.13 and 4.14, respectively. The

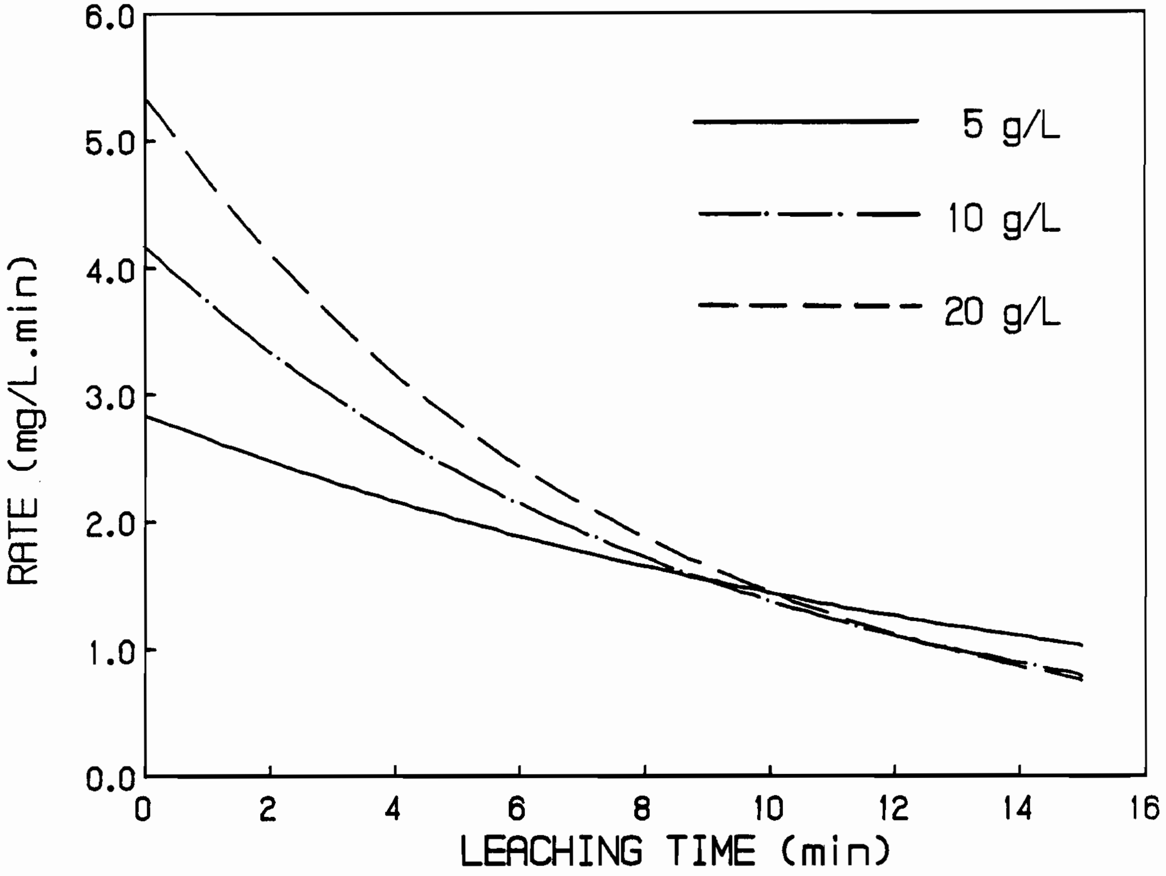

Figure 4.13 (A) Effect of slurry density on the rates of dissolution (per liter of liquid) calcium from SB ash

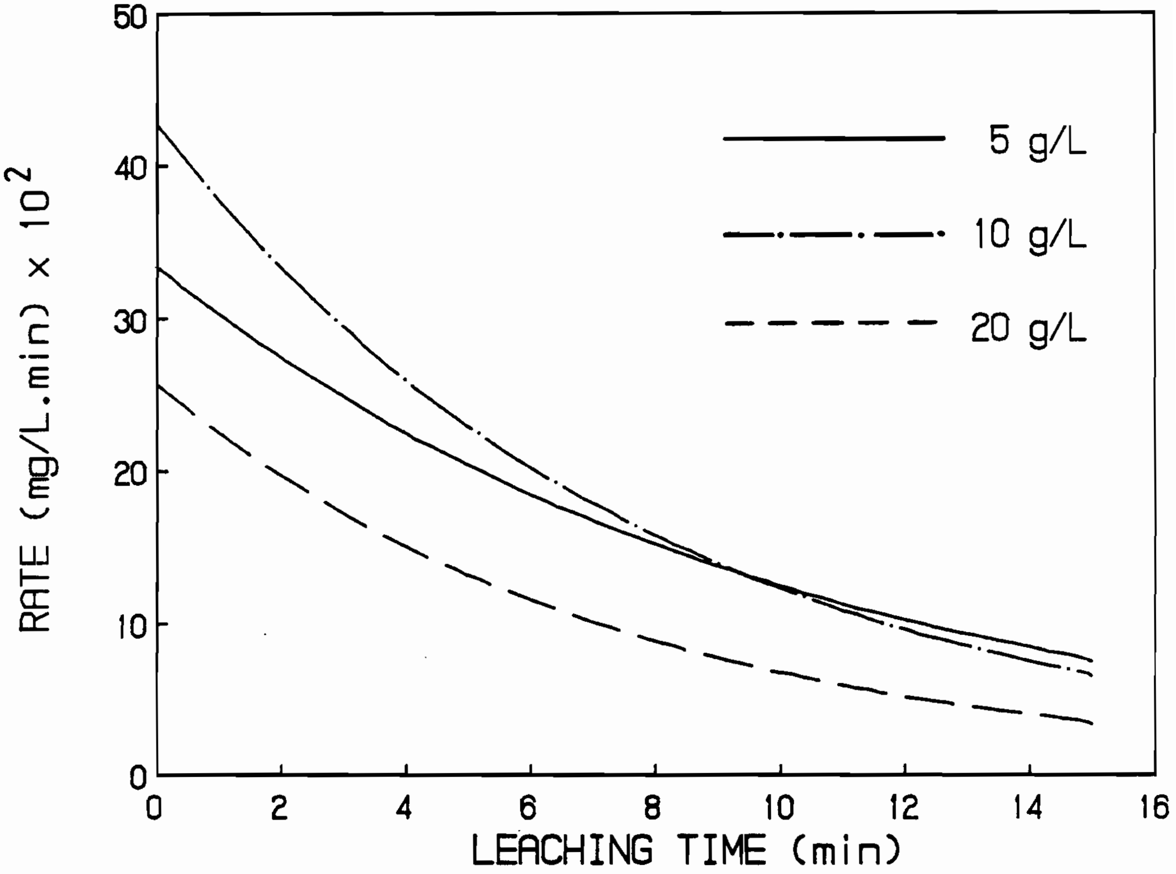

Figure 4.13 (B) Effect of slurry density on the rates of dissolution (per liter of liquid) of magnesium from SB ash

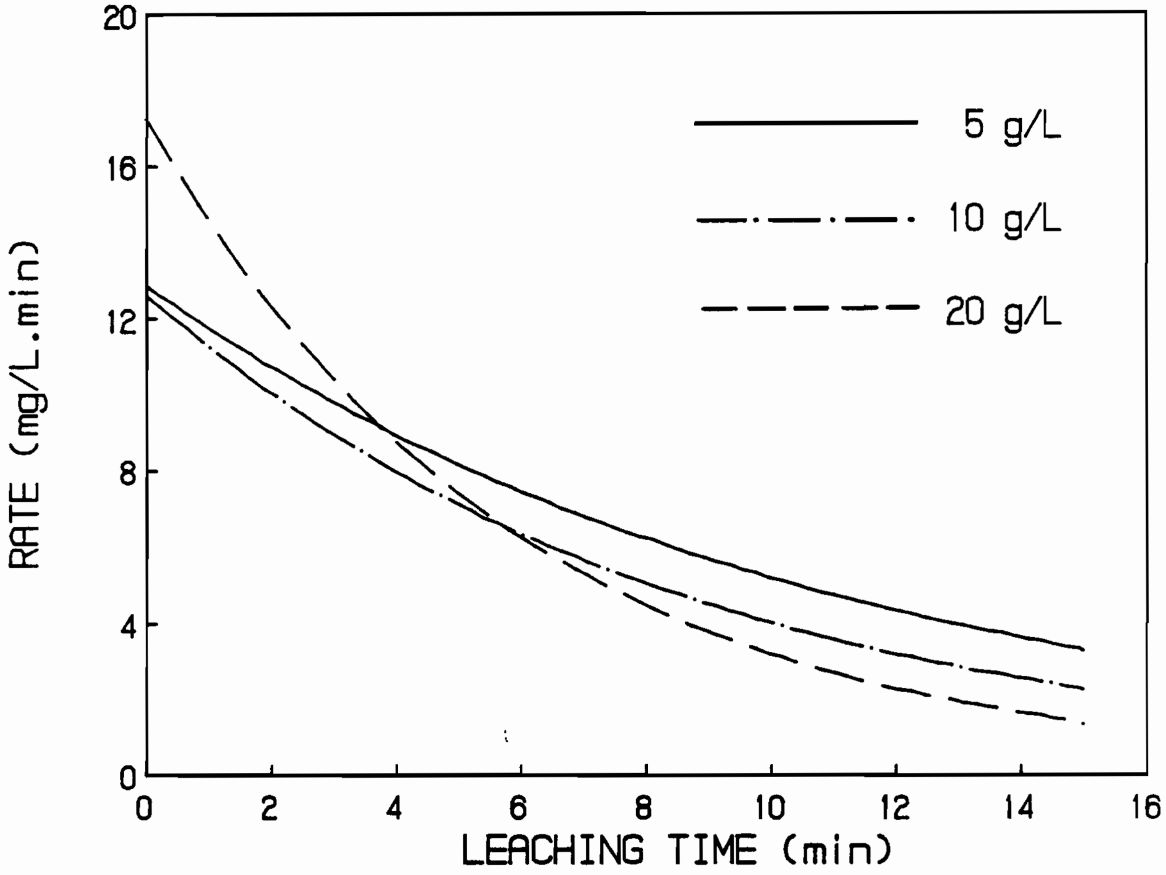

Figure 4.14 (A) Effect of slurry density on the rates of dissolution (per liter of liquid) of calcium from lignite ash

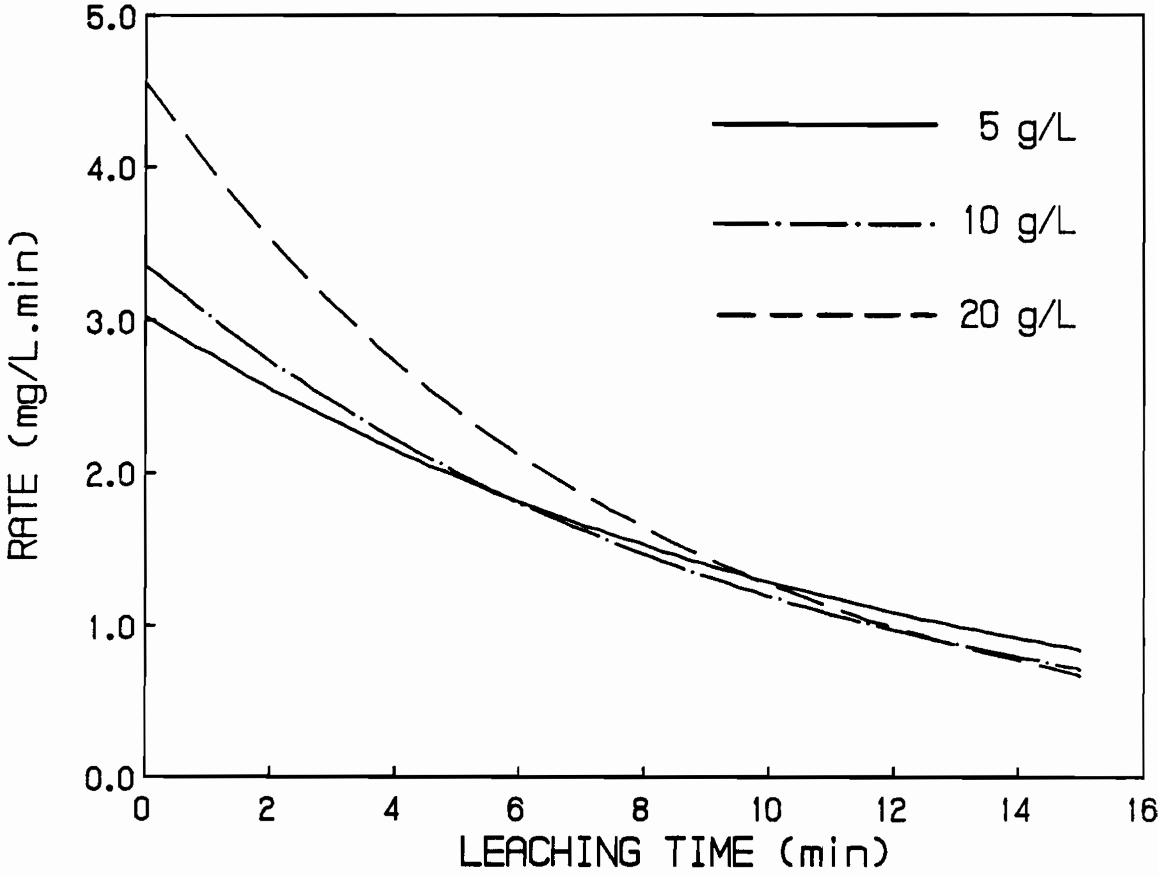

Figure 4.14 (B) Effect of slurry density on the rates of dissolution (per liter of liquid) of magnesium from lignite ash

results are shown for the first 15 minutes during which the dissolution is controlled by liquid-side mass transfer. First of all, for both types of fly ash, the rates of dissolution of calcium were much higher than those of magnesium. Also, the rates of dissolution of either metal from lignite ash were much higher than the corresponding rates for SB ash. As shown in these Figures, the rates were initially high but they decrease to a low level within 15 minutes. The Figures also demonstrate that the slurry density affects the rates only in the first few minutes of dissolution. For all cases, the rates were essentially the same at the three levels of slurry density after the initial short period of dissolution from the surface of the particles. The effect of slurry density can be noticed when these rates are in terms of the amount of solids present in the reactor as shown in Figures 4.15 and 4.16. As the amount of solids (or the slurry density) increased, the rate (per gram of solids) decreased since the concentrations of dissolved metals in the bulk liquid approach saturation.

Assuming that the overall mass transfer coefficient, $k_L a$, depends only on the particle diameter, the diffusivity of the solute, the physical properties (density and viscosity) of the liquid phase and the stirring speed (47), the dissolution rates reflect the changes in the driving force (C_{mi} - C_m) during the leaching process. When the particles come into contact with the liquid, the soluble components at

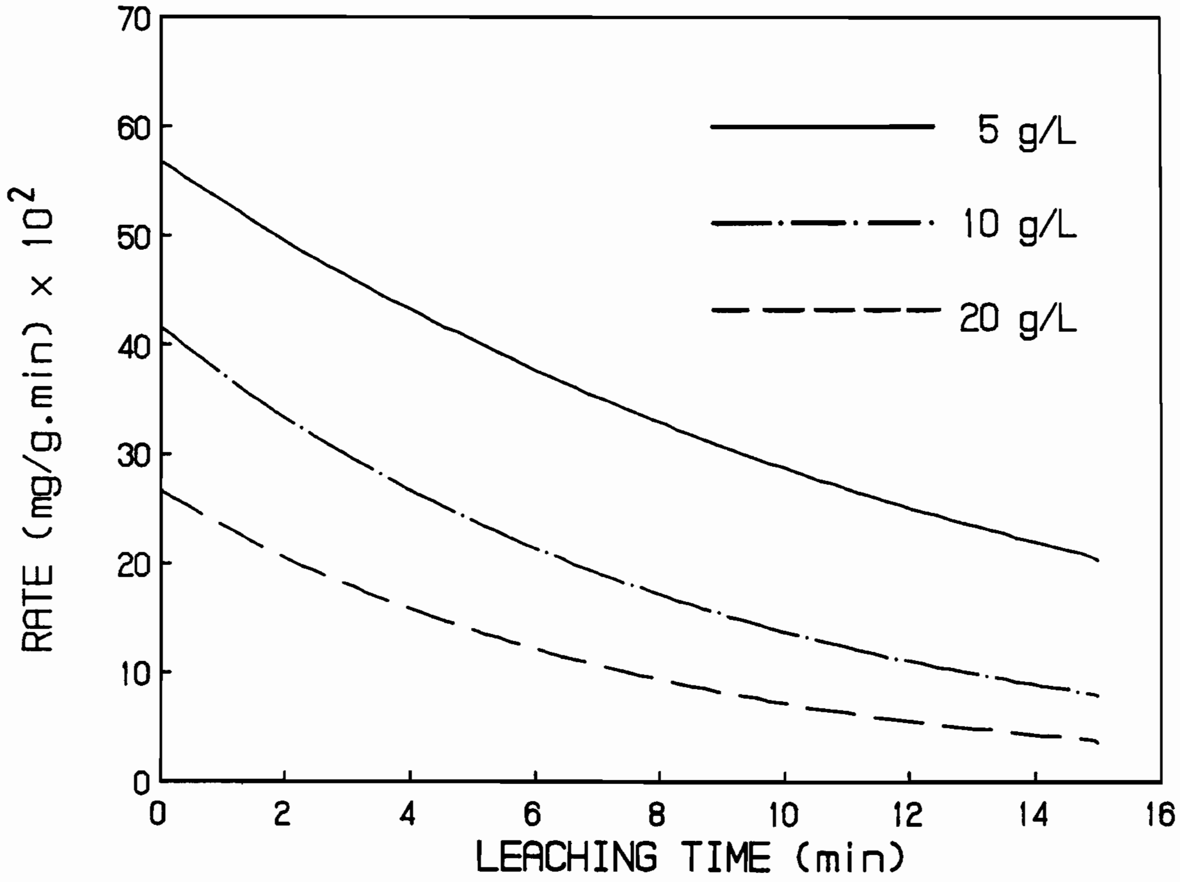

Figure 4.15 (A) Effect of slurry density on the rates of dissolution (per gram of solid) of calcium from SB ash

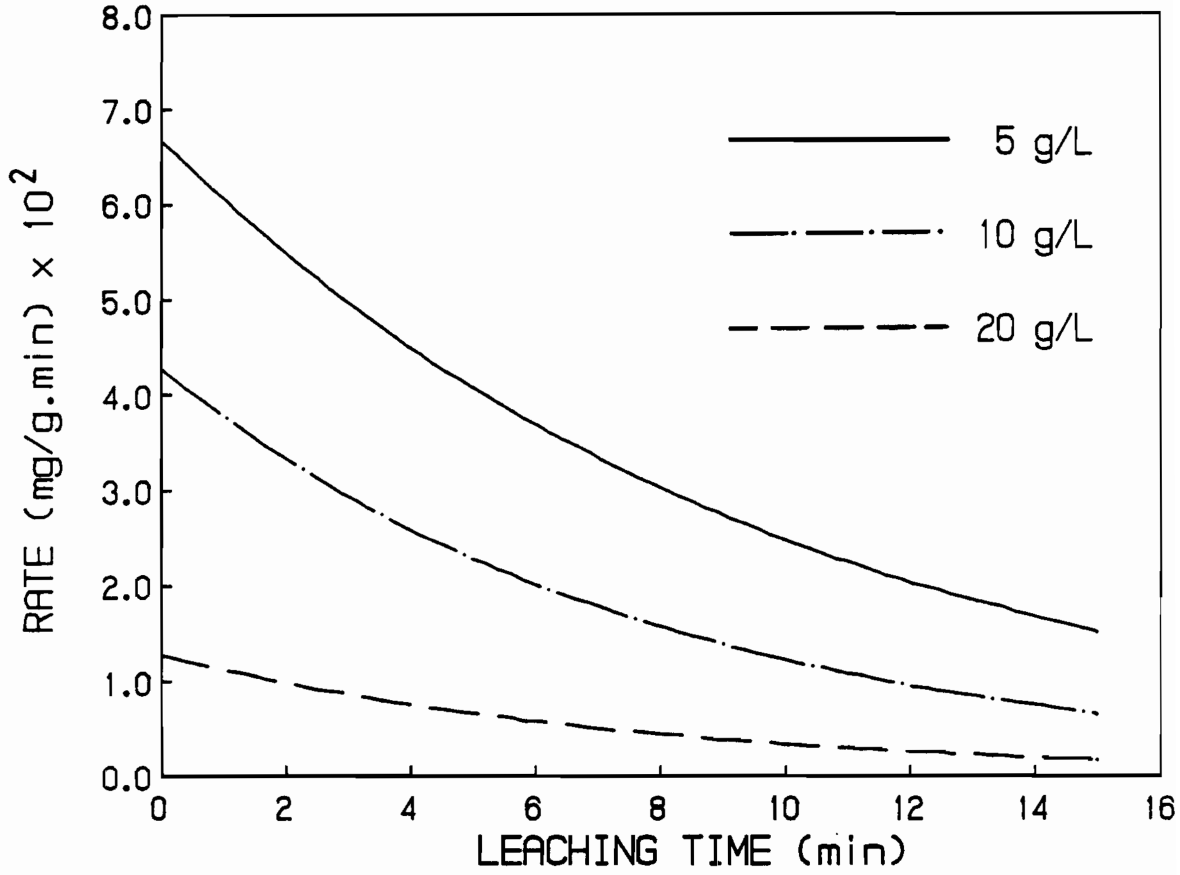

Figure 4.15 (B) Effect of slurry density on the rates of dissolution (per gram of solid) of magnesium from SB ash

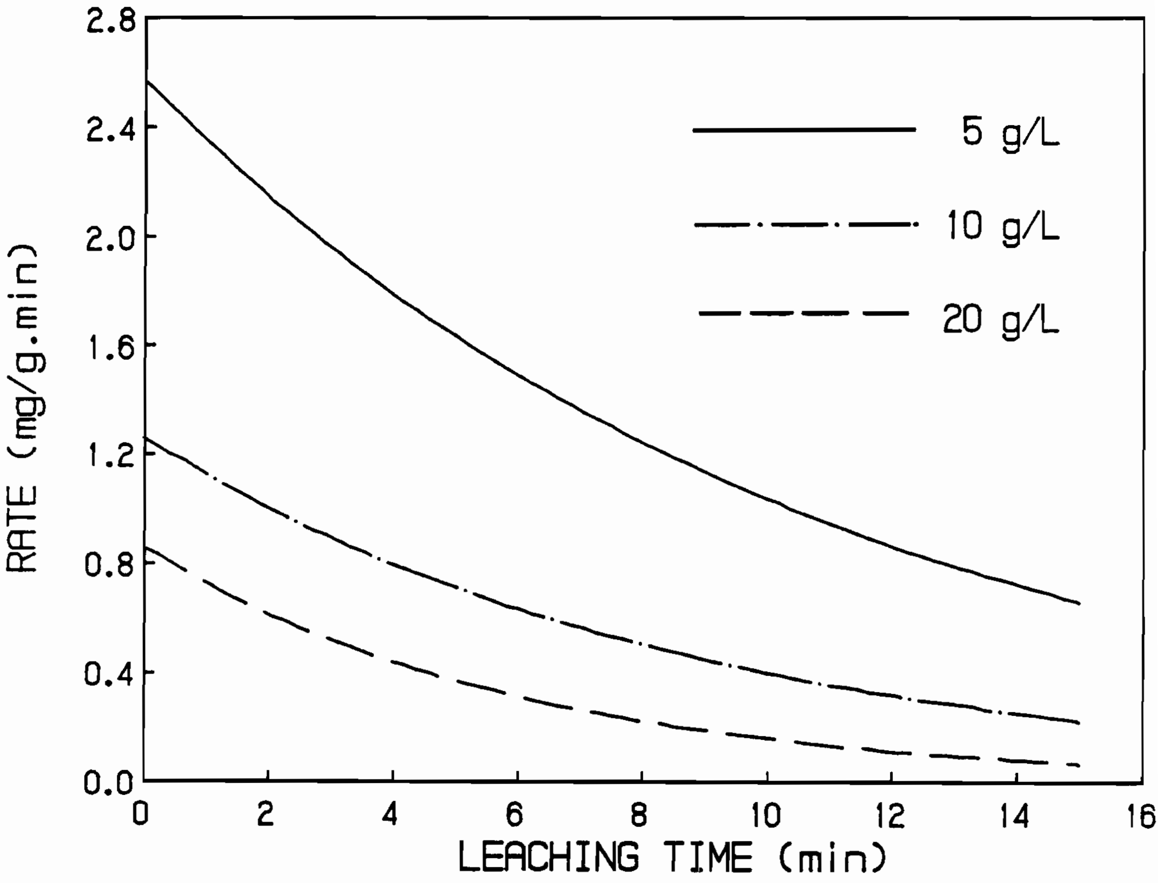

Figure 4.16 (A) Effect of slurry density on the rates of dissolution (per gram of solid) of calcium from lignite ash

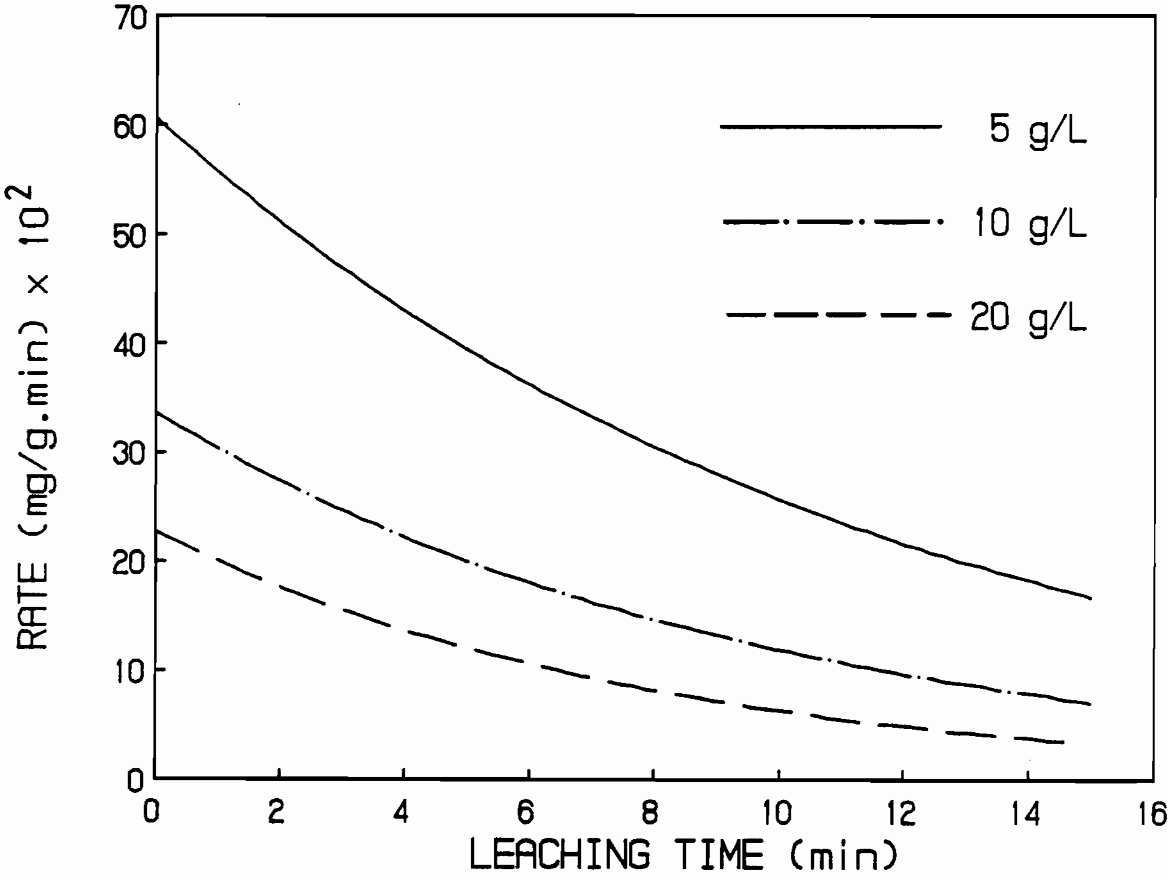

Figure 4.16 (B) Effect of slurry density on the rates of dissolution (per gram of solid) of magnesium from lignite ash

the solid surface are first dissolved and then transferred to the bulk of the liquid phase. At this initial stage, the driving force for the dissolution and the transfer in the liquid is high because of the low concentration in the bulk liquid. As the dissolution proceeds, the soluble species are depleted from the surface of the particles. Therefore, the driving force decreases since the solid surface is only replenished with the solute by diffusion from the interior of the particle, which is inherently a slow process.

Furthermore, when the slurry density is high (e.g. 20 g/L), the bulk concentration increases to a high level almost immediately after the solids are added to the liquid resulting in relatively small differences between the interfacial and the bulk concentrations (that is, small driving force) throughout the dissolution period. Consequently, the rates are slower than those obtained when the slurry density is lower.

4.6 Effect of pH

The pH of the leaching medium is the most important parameter of the liquid phase that influences the dissolution of alkaline metals from fly ash (39). In particular, the changes in the pH during leaching in batch systems (such as the one used in this study) can have a significant impact on further dissolution.

The effect of the initial pH (that is, the pH of the liquid before the addition of fly ash) on the dissolution of calcium compounds from SB ash is shown in Figure 4.17. The concentration of calcium was obtained after a long-term leaching of 15 h in shake-flask experiments. The Figure indicates that the final concentration of calcium decreased with increasing the initial pH up to 3.0 above which the concentration was independent of the pH.

Based on these observations, the reactor experiments were carried out at the initial pH levels of 2.0, 2.7, 3.0 and 6.0 for SB ash and at the levels of 2.0 and 6.0 for lignite ash. The results are shown in Figures 4.18 and 4.19 for the respective types of fly ash. The concentrations of calcium dissolved from both fly ashes were much higher when a solution of low pH was used compared to a solution of medium pH, which is expected from the long-term data. At the initial pH of 2.0, both fly ashes released 3 times as much calcium compared to that at pH 6.0. The differences in soluble concentrations were larger for magnesium especially from lignite since very little dissolved at pH 6.0. Figure 4.18 also indicates that the initial pH levels of 3.0 and 6.0 resulted in identical metal concentrations which is supported by the long-term

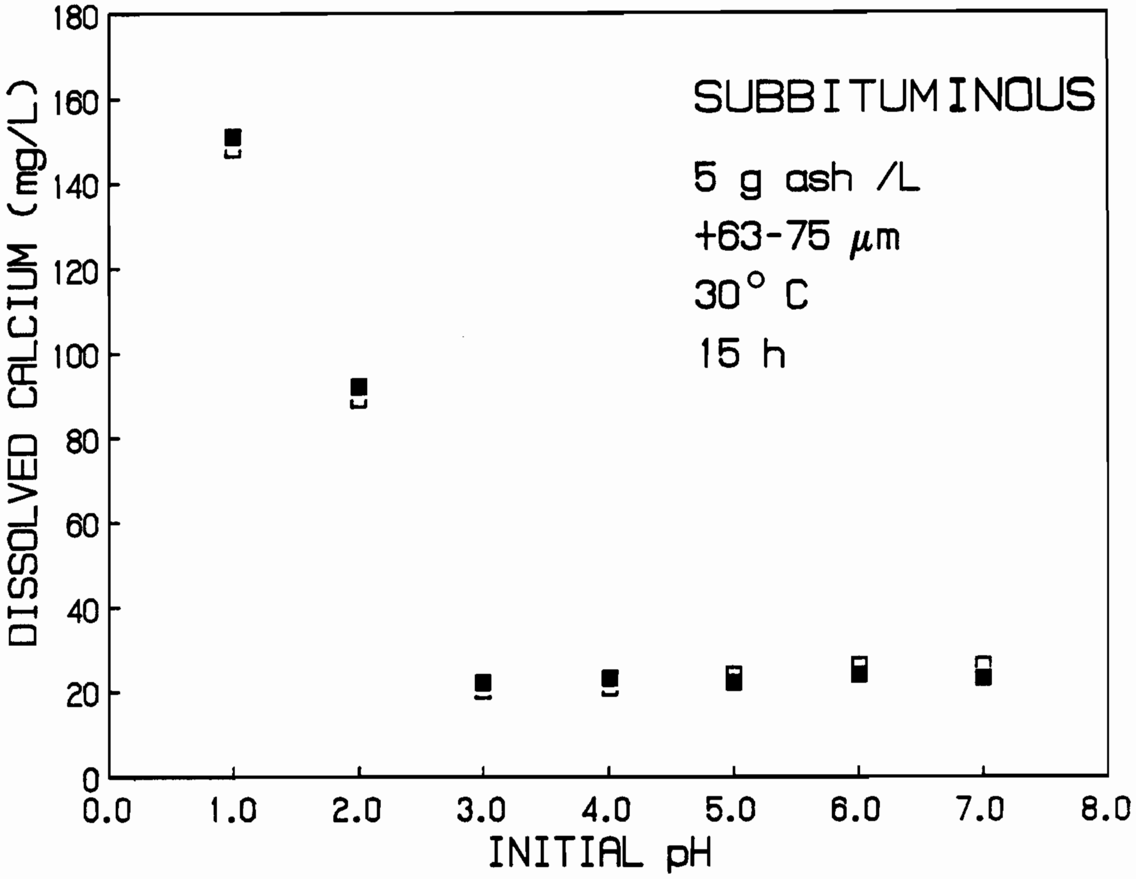

Figure 4.17 Effect of initial pH on the concentration of dissolved calcium after 15 h

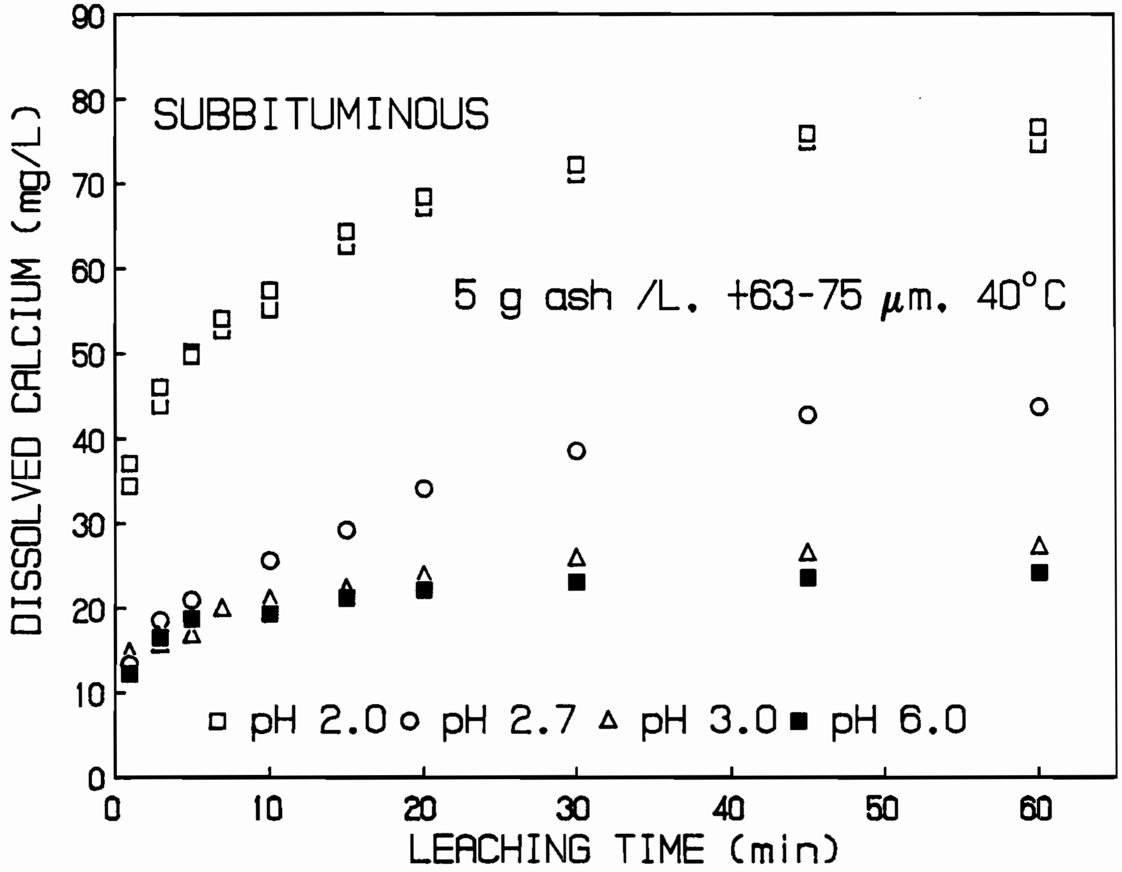

Figure 4.18 (A) Effect of the initial pH on the concentration of calcium dissolved from SB ash

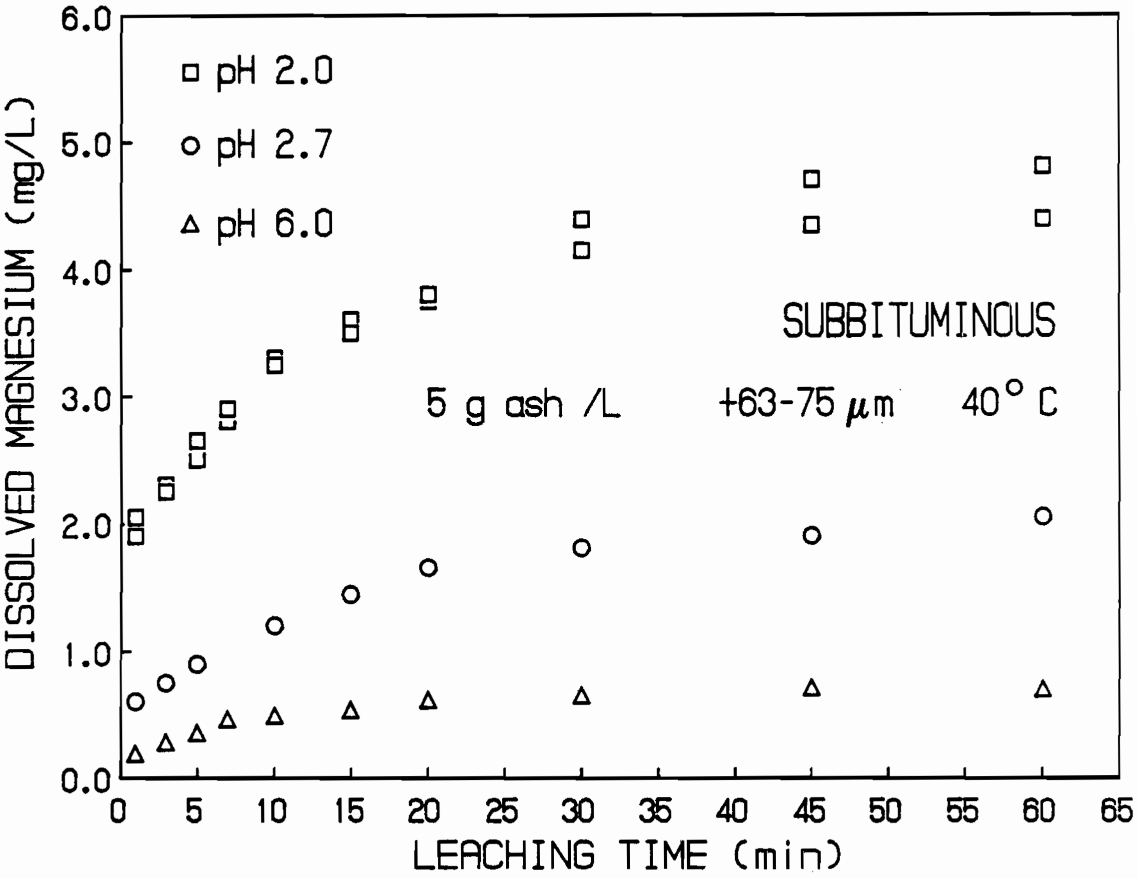

Figure 4.18 (B) Effect of the initial pH on the concentration of magnesium dissolved from SB ash

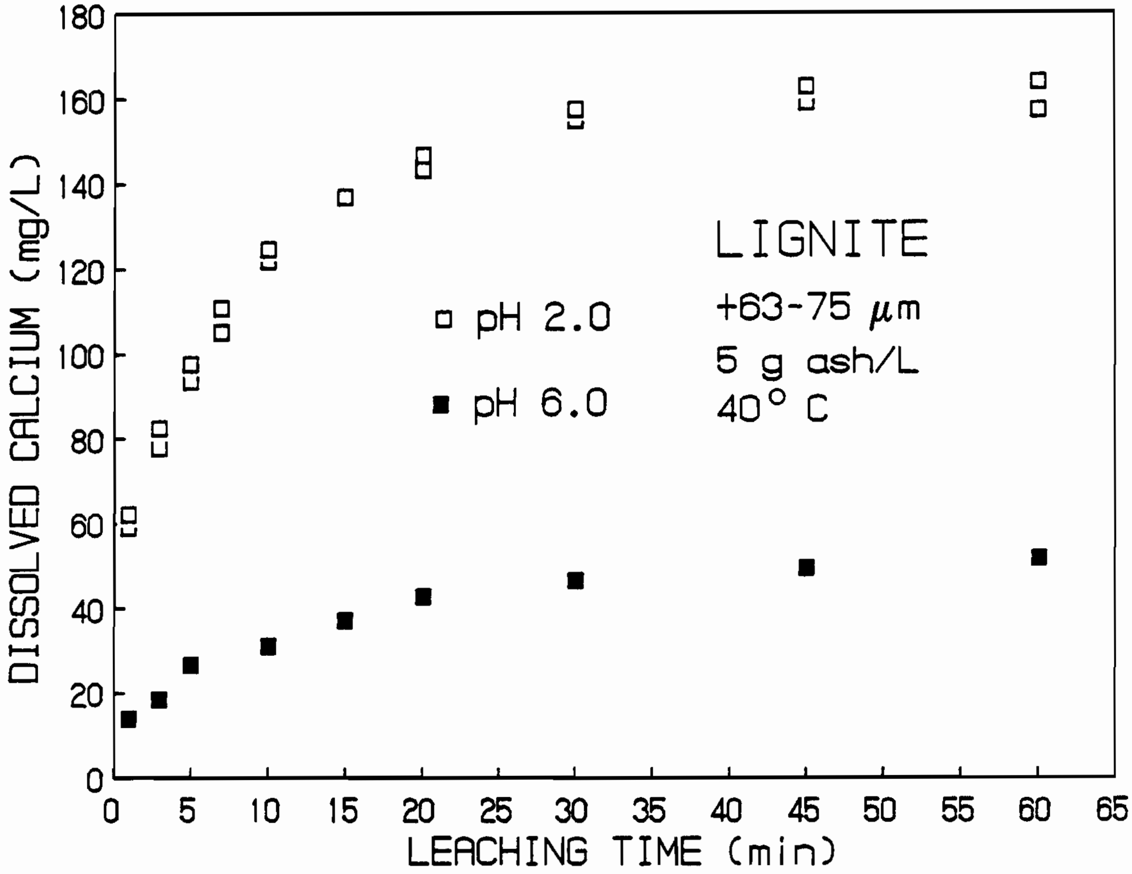

Figure 4.19 (A) Effect of the initial pH on the concentration of calcium dissolved from lignite ash

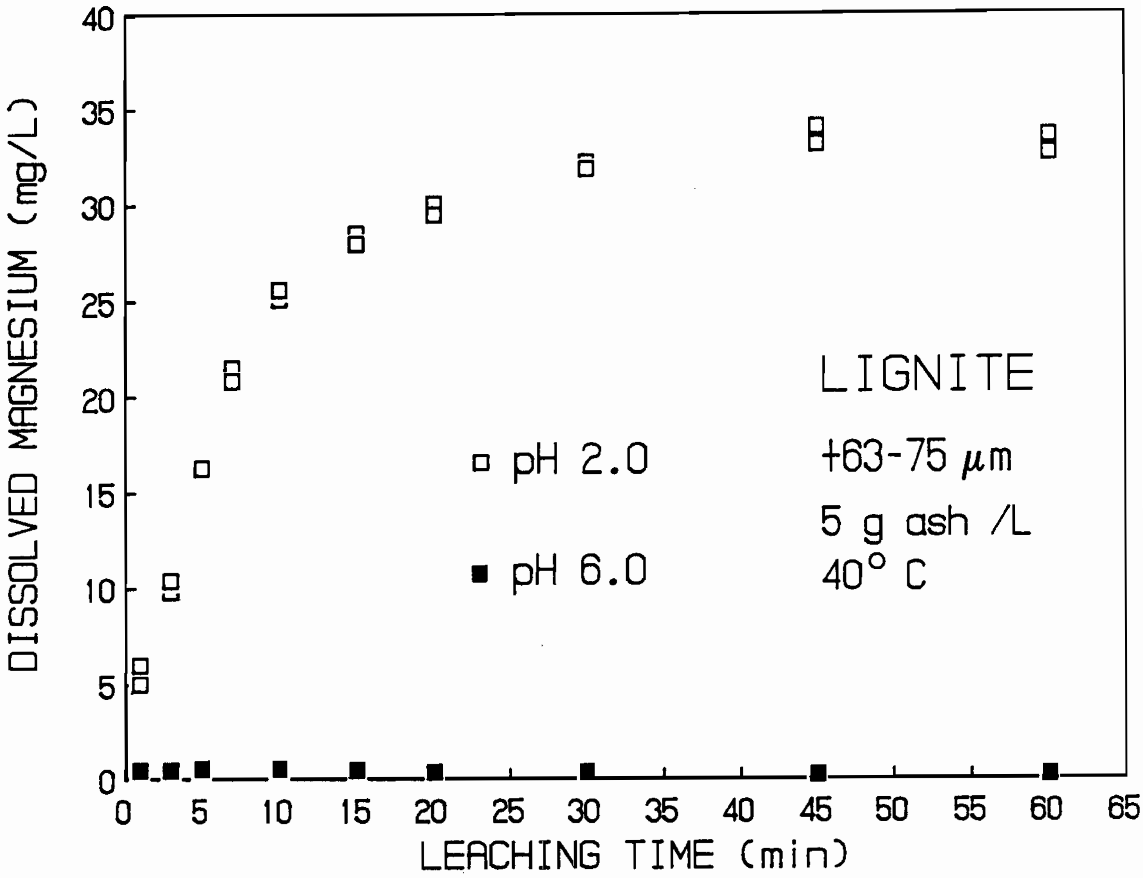

Figure 4.19 (B) Effect of the initial pH on the concentration of magnesium dissolved from lignite ash

data. The intermediate pH of 2.7 resulted in intermediate concentrations of both elements. Since the slurry phase was not buffered during the leaching process, the pH kept increasing as the dissolution of alkaline metals proceeded. The changes in the slurry pH which took place in the reactor ranged from less than a pH unit to several pH units depending on the type of fly ash and the initial pH of the liquid. Figures 4.20 and 4.21 show the profiles of the slurry pH during the leaching of lignite and SB ash, respectively. In fact, these changes have a strong impact on the concentrations of dissolved metals.

To illustrate this effect, the dissolution of calcium from SB ash which is shown in Figure 4.18 can be considered. The initial concentrations (obtained after one minute of leaching) were approximately the same for both initial pH levels of 2.7 and 3.0 (about 13 mg/L). However, the final concentration (obtained after 60 minutes of leaching) when the initial pH was 2.7 was almost twice as much as that obtained when the initial pH was 3.0 (43 versus 24 mg/L). The reason for this difference can be found in Figure 4.20 where the slurry pH did not significantly increase during leaching which started at 2.7 but it went up to pH 7.5 when leaching was initiated at 3.0. In the latter case the dissolution was retarded as the hydroxide ion concentration was building up in the solution.

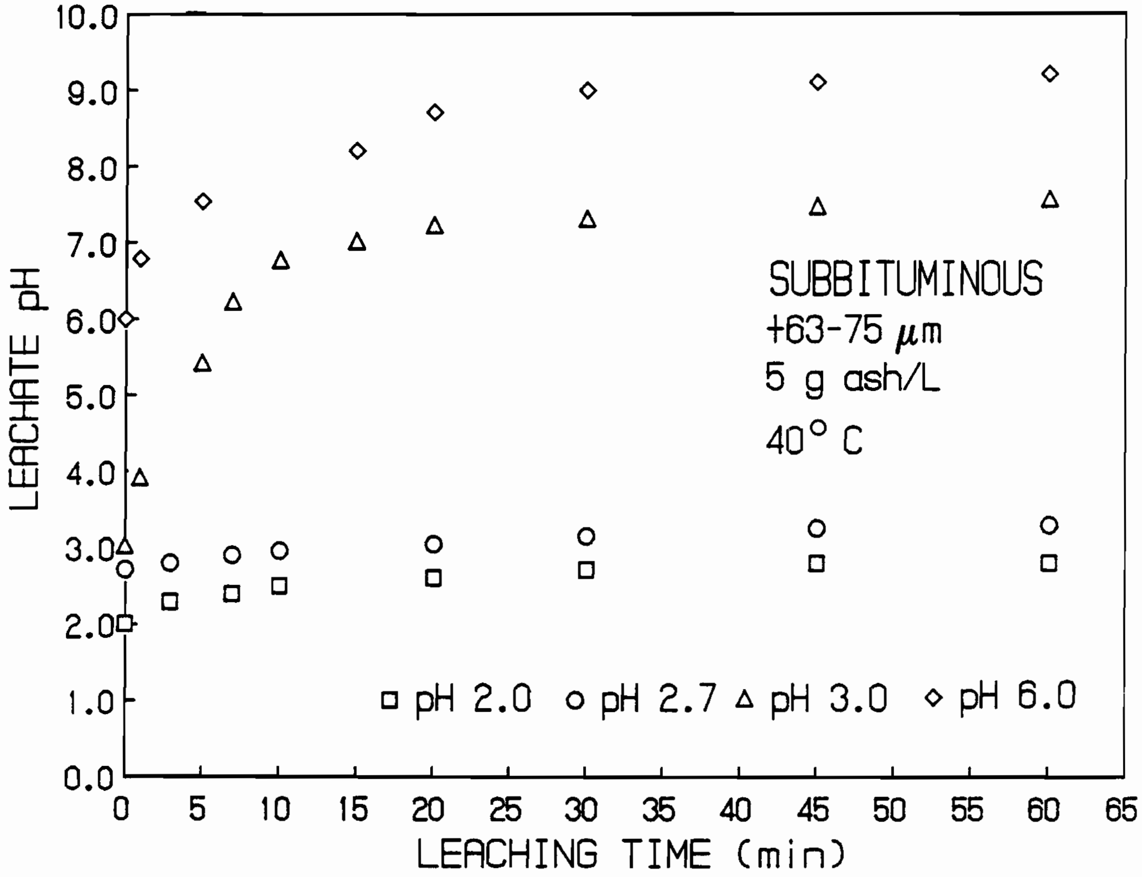

Figure 4.20 Profiles of the leachate pH during the dissolution of SB ash alkaline components

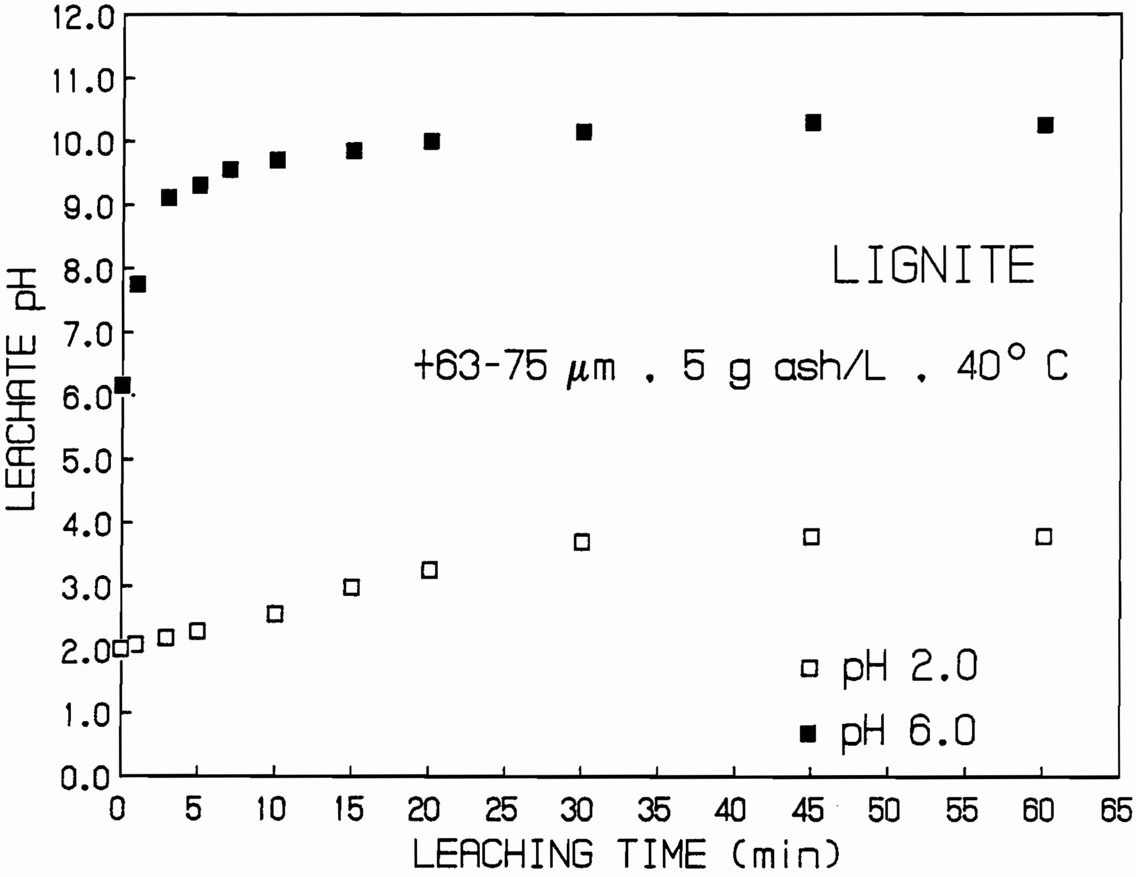

Figure 4.21 Profiles of the leachate pH during the dissolution of lignite alkaline components

Figures 4.22 and 4.23 show the dissolution rates of the dissolved metals from SB and lignite ashes, respectively, at the different pH levels tested in the experiments. There was essentially no magnesium dissolved from lignite at the initial pH of 6.0. The highest rates were obtained at the initial pH of 2.0 at which the highest concentrations were obtained. Since the mass transfer coefficient is independent of the pH, the high rates are due to the increased driving force which results from the increase in the solubilities of the metal ions when the pH is lowered.

4.7 Effect of Temperature

The effect of slurry temperature on the dissolution of alkaline metals was examined using SB ash and the results are plotted in Figure 4.24. The initial pH was 2.0 and the slurry density was kept at 5 g/L. Increasing the temperature from 20 to 60° C increased the concentrations of both metals by 30-40% after a leaching time of 60 minutes. The experimental data are statistically significant at the 95% level of confidence.

It is important to note that the influence of temperature on dissolution was not limited to the initial period where most of the dissolved elements were released

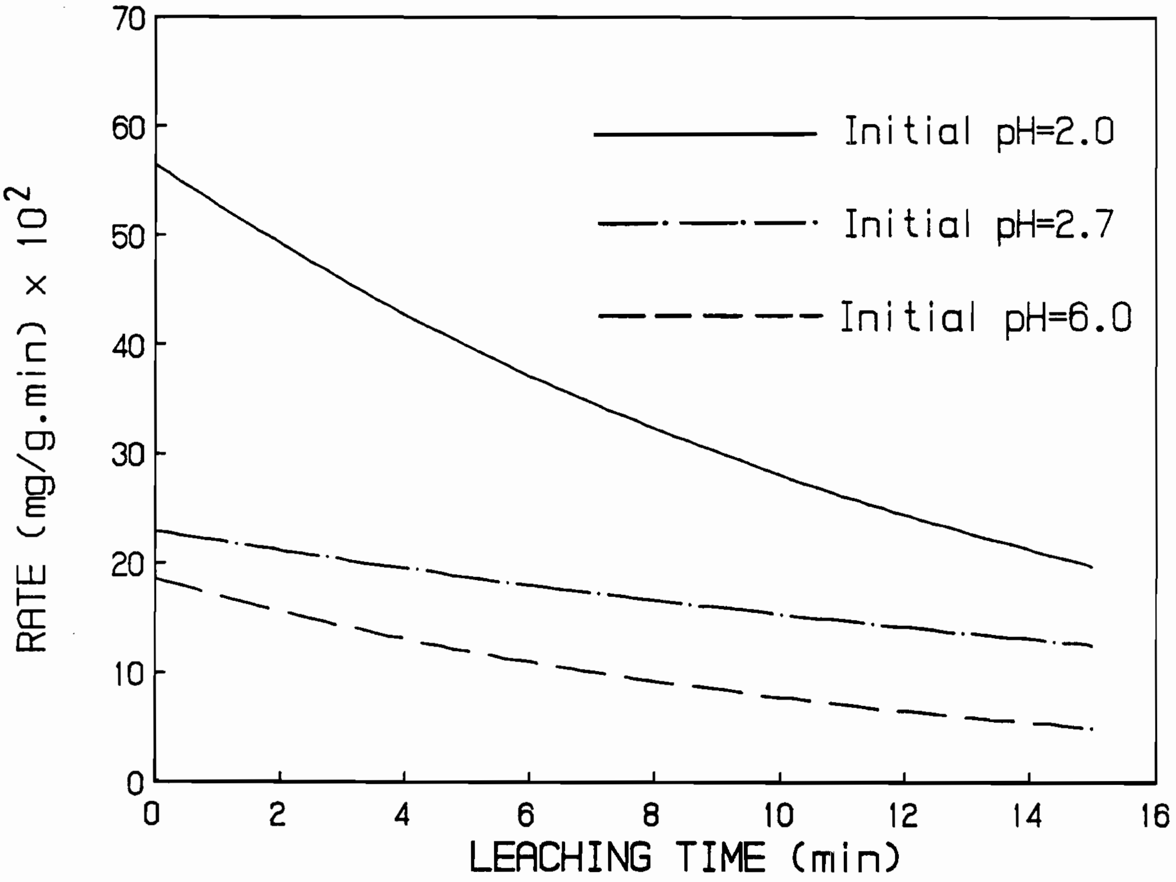

Figure 4.22 (A) Effect of the initial pH on the dissolution rates of calcium compounds from SB ash

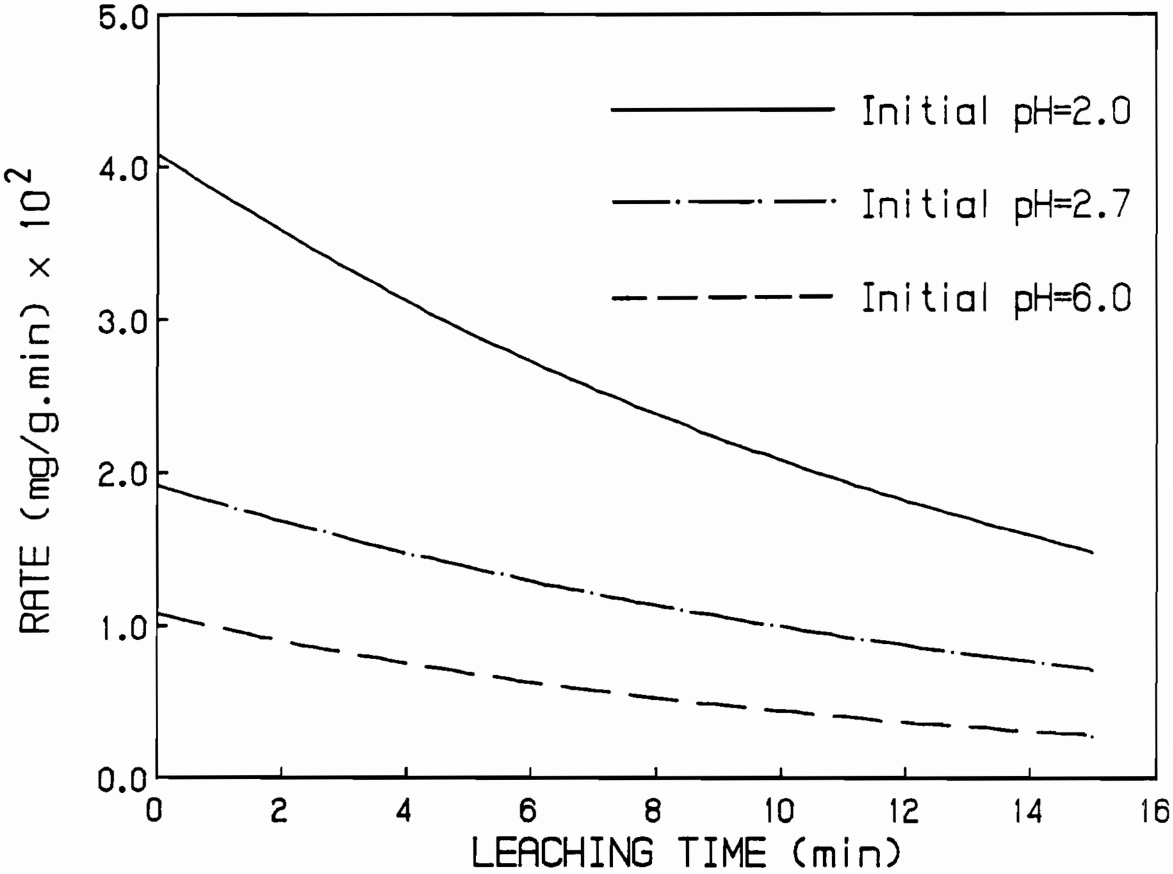

Figure 4.22 (B) Effect of the initial pH on the dissolution rates of magnesium compounds from SB ash

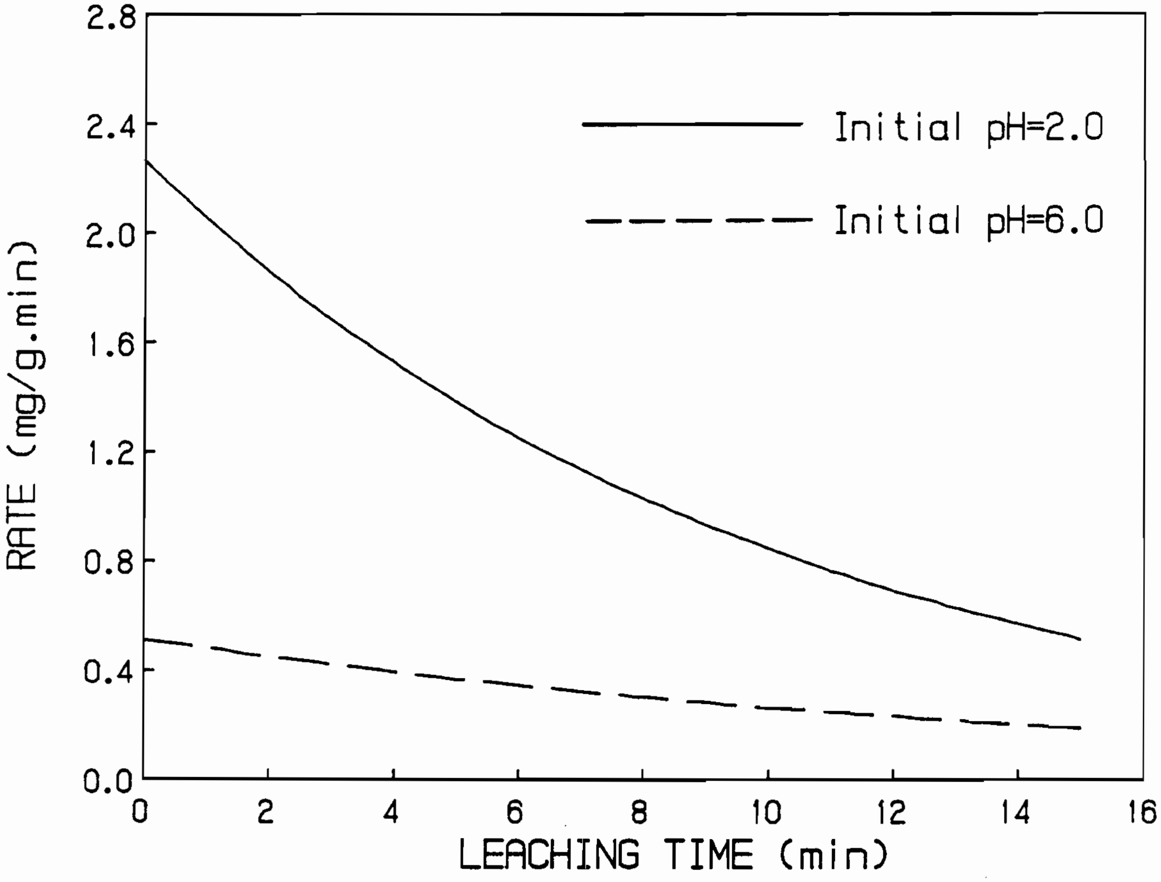

Figure 4.23 (A) Effect of the initial pH on the dissolution rates of calcium compounds from lignite ash

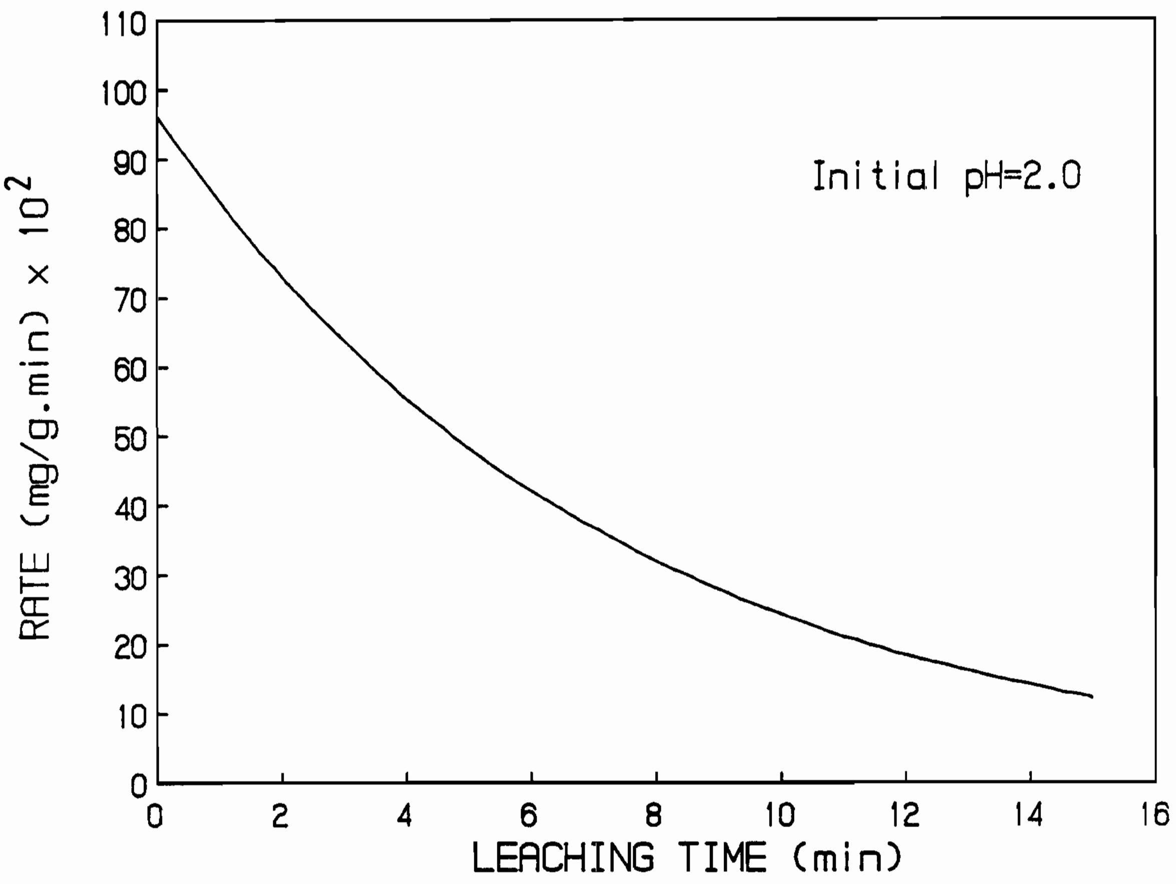

Figure 4.23 (B) Effect of the initial pH on the dissolution rate of magnesium compounds from lignite ash

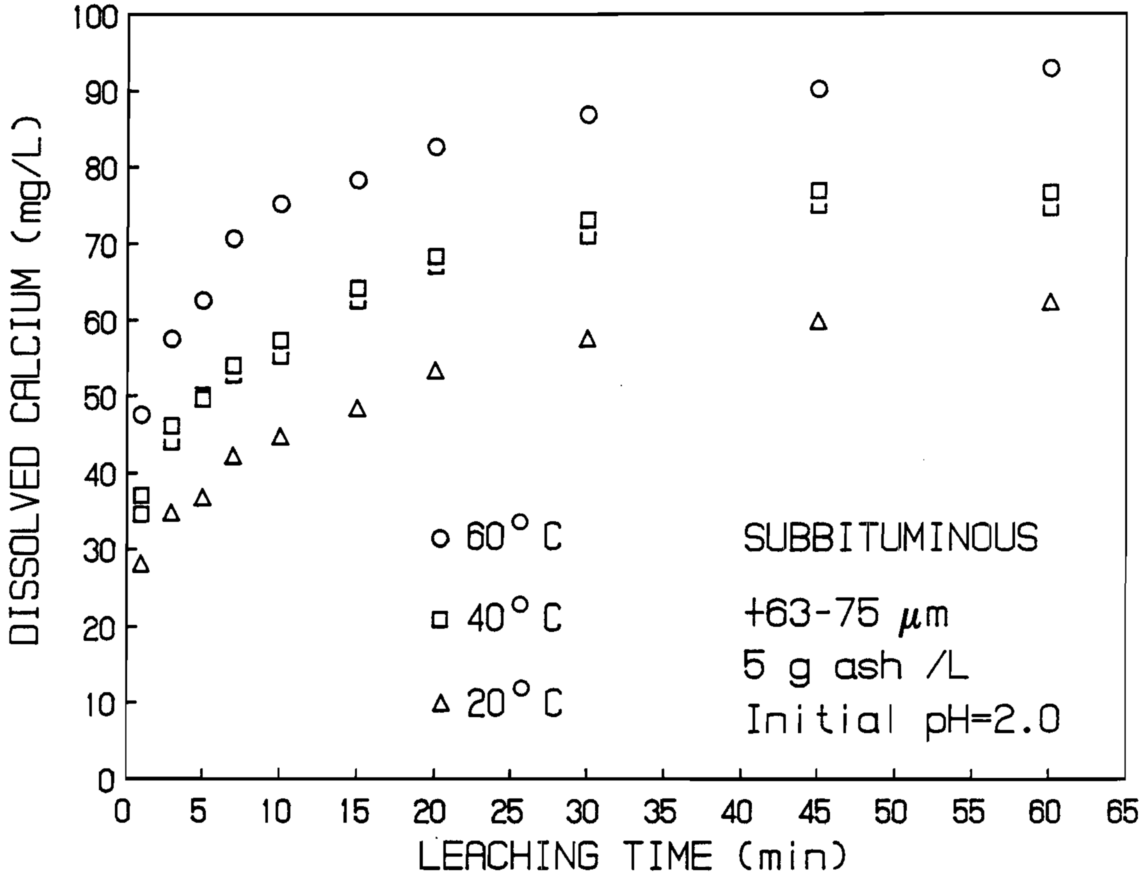

Figure 4.24 (A) Effect of Slurry temperature on the concentrations of dissolved calcium from SB fly ash

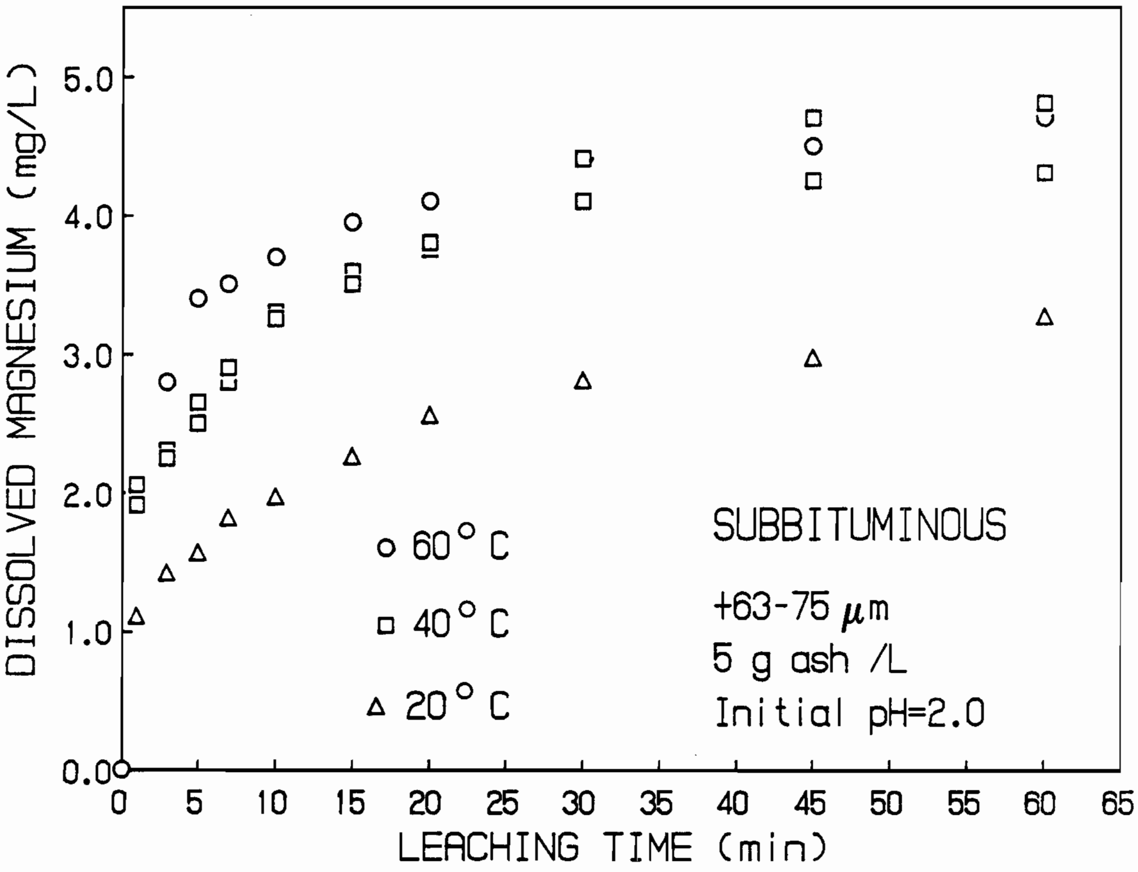

Figure 4.24 (B) Effect of slurry temperature on the concentrations of dissolved magnesium from SB fly ash

from the surface of the particles. With an increase in temperature, both the solubilities and the ionic diffusivities of the dissolving compounds and species present at the surface and in its vicinity will also increase.

4.8 Soluble Alkalinity

The total soluble alkalinity of solutions of fly ash leachates was determined and the data were correlated to the combined concentrations of dissolved calcium and magnesium present in these solutions. Total soluble alkalinity was determined for samples taken during a leaching experiment carried out in the reactor. In this experiment, 5 g/L of lignite ash were added to an aqueous solution at an initial pH of 5.5 and 40° C and the solids are allowed to leach for 60 minutes. A good correlation was obtained between the total soluble alkalinity and the combined dissolved metal concentration as shown in Figure 4.25. This Figure demonstrates that the combined concentration of calcium and magnesium in fly ash leachate can be considered as an expression of the soluble alkalinity available for SO_2 absorption in flue gas desulphurization.

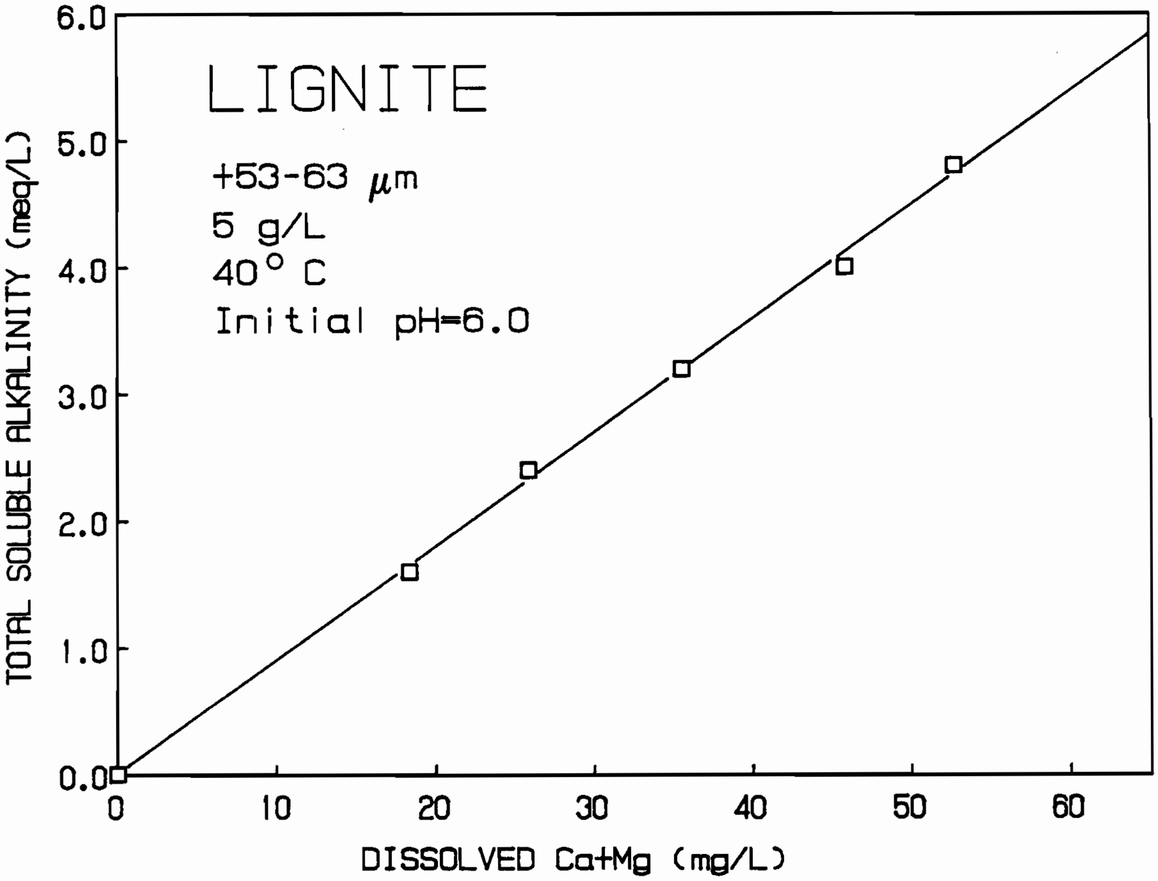

Figure 4.25 The relationship between the total soluble alkalinity and the combined Ca and Mg concentrations

4.9 Summary and Conclusions

The dissolution of the alkaline metal compounds from two Canadian subbituminous and lignite fly ashes was investigated. The effects of selected process variables on the concentrations of dissolved metals were evaluated. The rates of dissolution of these components were estimated on the basis of a solid-liquid mass transfer model at various experimental conditions. Calcium and magnesium are the only metals in the investigated fly ashes to dissolve in significant amounts providing soluble alkalinity. Lignite provides considerably higher alkalinity than subbituminous as expected from the respective metal compositions. The exact value of this alkalinity, however, depends on the slurry density, the particle size, the solution pH and the slurry temperature. The rate of dissolution of calcium and magnesium from both fly ashes was initially rapid because the dissolved metals come from surface-associated compounds. Subsequently, the rate was found to be controlled by mass transfer from the surface of the solids to the bulk liquid.

CHAPTER 5

ABSORPTION OF SULPHUR DIOXIDE INTO FLY ASH SLURRIES

5.1 Introduction

In this chapter, the results of the experimental work on the absorption of sulphur dioxide into slurries of fly ash will be presented and discussed. Theoretical analysis of the system in terms of chemical and hydrodynamic aspects will also be discussed. Lignite fly ash was used in most of the experiments because it provides higher available alkalinity for SO_2 absorption. Subbituminous fly ash was also used in some of the experiments.

Since limestone is the major source of alkalinity used in the sulphur dioxide scrubbing industry, a series of experiments with mixtures of fly ash and limestone were carried out. Both lignite and SB ashes were used in these mixtures. Absorption into a clear solution of fly ash leachate and into pure water were also carried out to determine the effect of the solids on gas absorption.

The percent overall SO_2 removal will be shown as a function of absorption time. This parameter is an expression of the absorption capacity of the liquid medium and is defined by the following equation:

$$\% \text{ Overall Removal} = (C_T\ V_L/G.\ t) \times 100 \tag{5.1}$$

where C_T = concentration of S(IV) in solution at time t, mmol/L.

V_L = volume of the liquid phase in the reactor, L

G = input rate of SO_2 calculated from gas flow rates assuming ideal gas behaviour, mmol/min, and

t = contact time between the gas and the liquid phases, min.

The total concentration of S(IV) includes both the concentrations of $SO_{2(aq)}$ and bisulphite ions and it was determined experimentally by the iodometric titration as described in Appendix B. Since the reactor was purged with nitrogen before the SO_2 flow started and there was no oxygen in the feed gas, no oxidation took place in the reactor and therefore no sulphate was formed.

The initial pH (the pH of the water before the addition of solids) was 5.4-5.6 for all the experiments on gas absorption. The solids were added three minutes before SO_2 was sparged in and the pH increased to 10 in the case of lignite and to 7 in the case of SB ash. No considerable differences in absorption were found when the solids were allowed to leach for 1, 3 or 10 minutes before the introduction of the gas. All experiments showed that as soon as the gas was introduced into the liquid phase, the slurry pH dropped sharply due to the rapid absorption of SO_2 and then stabilized at a value in the acid range. The profiles of slurry pH during absorption under important process parameters will be shown.

All the data reported in this Chapter were obtained at a stirring speed of 800-900 rpm, which is the same speed used to obtain the solid dissolution data presented in Chapter 4. Figure 5.1 indicates that a higher stirring speed is unnecessary.

In Sections 5.2 and 5.3, the effects of selected variables on absorption will be evaluated. These variables are the slurry temperature, slurry density (or solid concentration), particle size and the inlet SO_2 concentration. In the case of slurries of mixtures of fly ash and limestone, the variable is the weight percent of limestone in the solids used to make the slurry. Concentrations will be presented as functions of time.

Section 5.4 is devoted to the discussion of fly ash leaching during gas absorption and the comparison of the

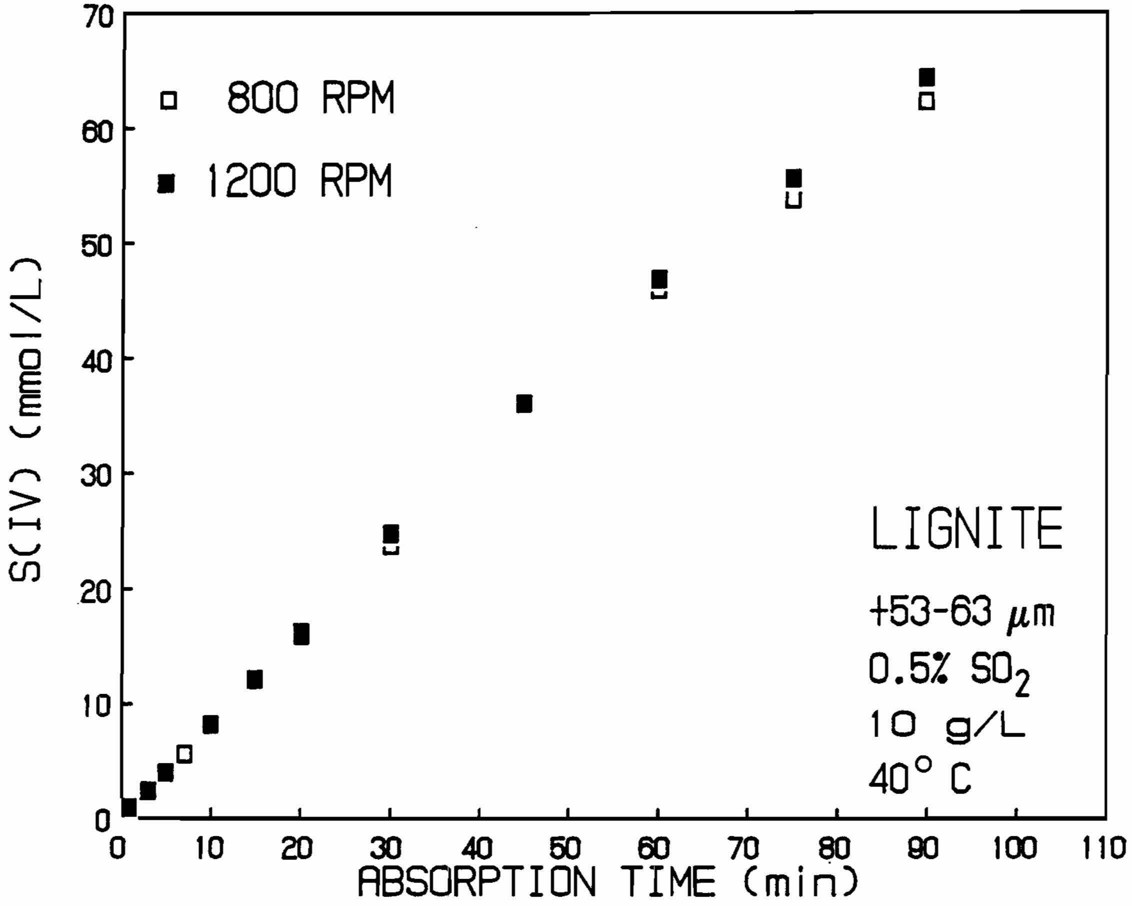

Figure 5.1 Effect of the sirring speed on the concentration of aqueous sulphur species due to SO_2 absorption

leaching behaviour in the presence and in the absence of SO_2. In the last Section, an analysis of the experimental results from the chemical and the hydrodynamic points of view will be presented and discussed.

5.2 Absorption in Water

Figure 5.2 is a plot of the concentration of the total sulphur species in solution that resulted from the absorption of SO_2 gas in water against time. In this experiment, an inlet concentration of SO_2 of 0.5% (which has a partial pressure of 0.005 atm) was allowed to equilibriate with pure (distilled) water in the stirred tank reactor at 40° C. It can be seen that the solution was saturated with dissolved SO_2 and its hydrolysis products in 20 minutes at a maximum concentration of 11 mmol/L.

The obtained value is in agreement with the solubility of sulphur dioxide reported in the literature. At 1 atm and room temperature, a maximum of 1.8×10^3 mmol/L of dissolved SO_2 is absorbed in water (4). Therefore, at a partial pressure of 0.005 atm (which was used in this work) 9 mmol/L as the total SO_2 solubility is expected. The value of the unhydrolyzed $SO_{2(aq)}$ at 40° C is 3.8 mmol/L as calculated by Henry's law (30). From the above-mentioned experiment, the value of $SO_{2(aq)}$ is 3.3 mmol/L at 40° C and pH 2.4 which

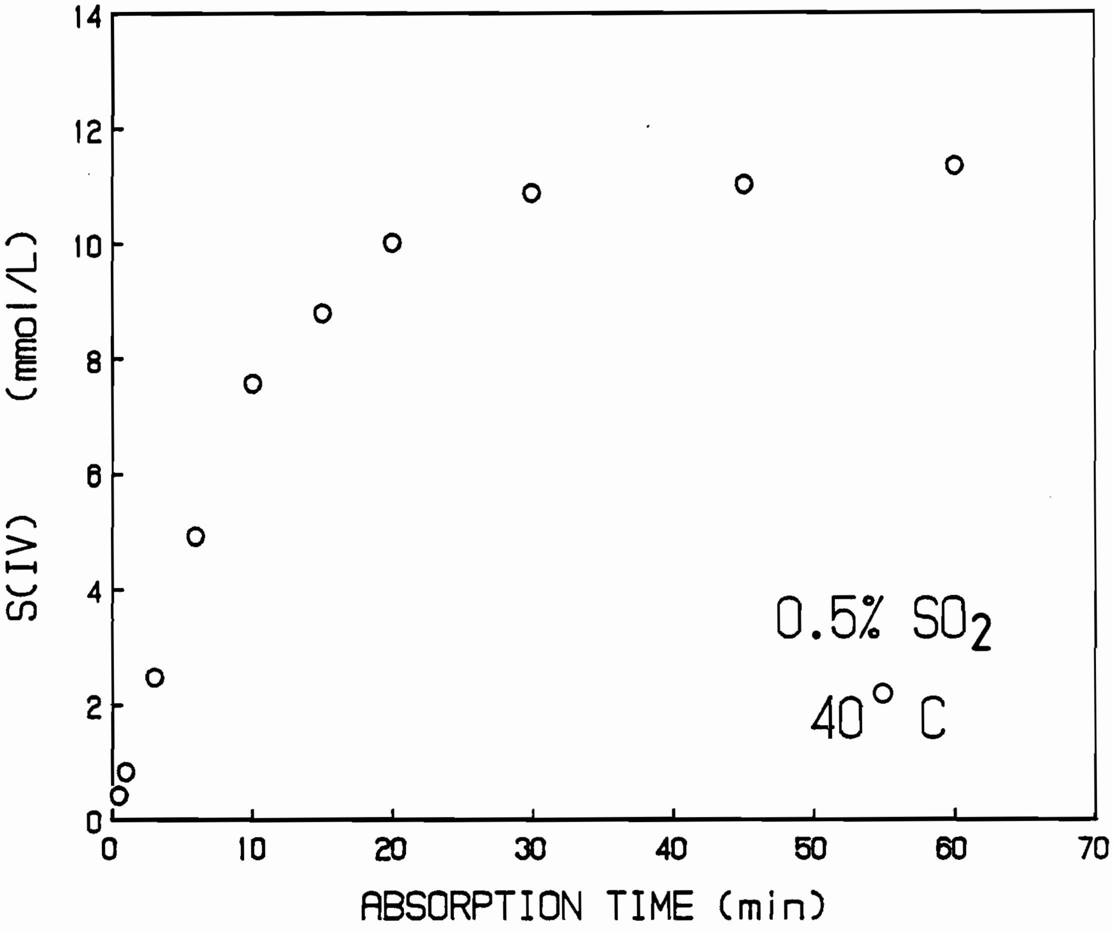

Figure 5.2 Absorption of SO_2 in water

prevailed most of the contact time between SO_2 and the water.

5.3 Effect of Selected Variables on Absorption

5.3.1 Effect of Slurry Temperature

The effect of slurry temperature on the total concentration of aqueous sulphur obtained by the absorption of SO_2 into lignite slurries is shown in Figure 5.3. The experiments were carried out at 20, 40 and 55° C while keeping the slurry density at 10 g/L and the SO_2 inlet concentration at 0.5%. Temperature had small influence on the absorption process. This indicates that the process is controlled by mass transfer rather than controlled by the chemical reaction that occurs during the hydrolysis of SO_2. The same conclusion was reached by Uchida et al. (50) in their study on the absorption of SO_2 into limestone slurries.

In fact, temperature is expected to have a dual effect on the overall process of sulphur dioxide removal by slurries of sparingly soluble solids. The dissolution of alkaline compounds in the solid particles gets a small enhancement as temperature is increased due to the increase in their solubilities and diffusivities (discussed in Chapter 4). However, the solubility of sulphur dioxide decreases (refer to Chapter 1, Section 1.3). For example, the solubility

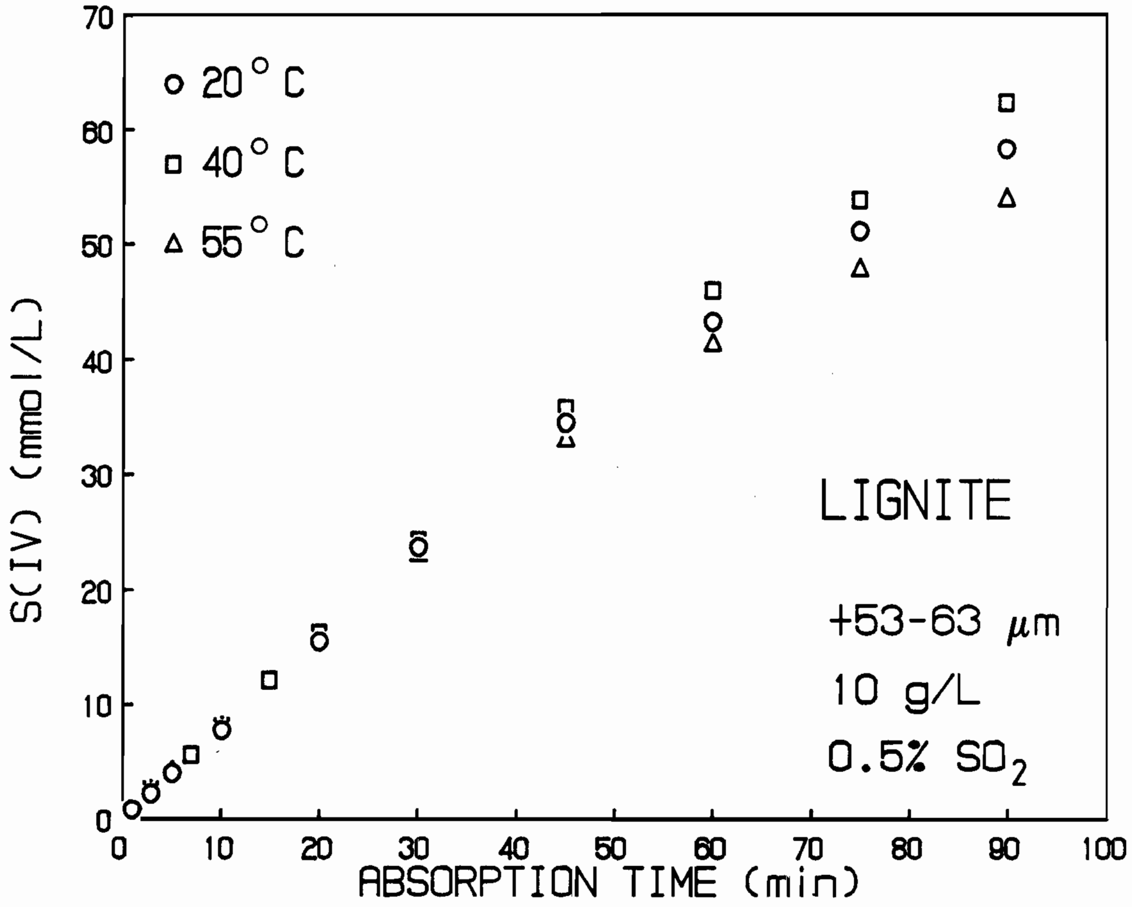

Figure 5.3 Effect of slurry temperature on the concentration of aqueous sulphur species due to SO_2 absorption

of the gas is decreased by about 50% when the temperature is increased from 20 to 40° C. The outcome of these two opposing effects will depend on the characteristics of the medium and the experimental conditions including the temperature level.

In the tested ranges of temperature of 20-40 and 40-55° C and over a contact time of 90 minutes, Figure 5.3 indicates that the concentrations of aqueous sulphur species were approximately the same since the data are statistically insignificant at the 95% level of confidence. The intermediate temperature of 40° C was chosen for all the experiments reported in the rest of this Chapter.

5.3.2 Effect of Slurry Density

Slurries of both lignite and SB ash were tested for the effect of slurry density on absorption at the levels of 5, 10 and 20 g/L at 40° C and 0.5% as inlet SO_2 concentration. The results are shown in Figures 5.4 and 5.5 for lignite and SB ashes, respectively. The Figures indicate that the concentration of aqueous sulphur species increased with increasing slurry density except for the first 20-30 minutes where absorption was independent of the amount of solids present in the liquid phase. At each level of slurry density, the concentration of aqueous sulphur species increased gradually after that initial period heading towards

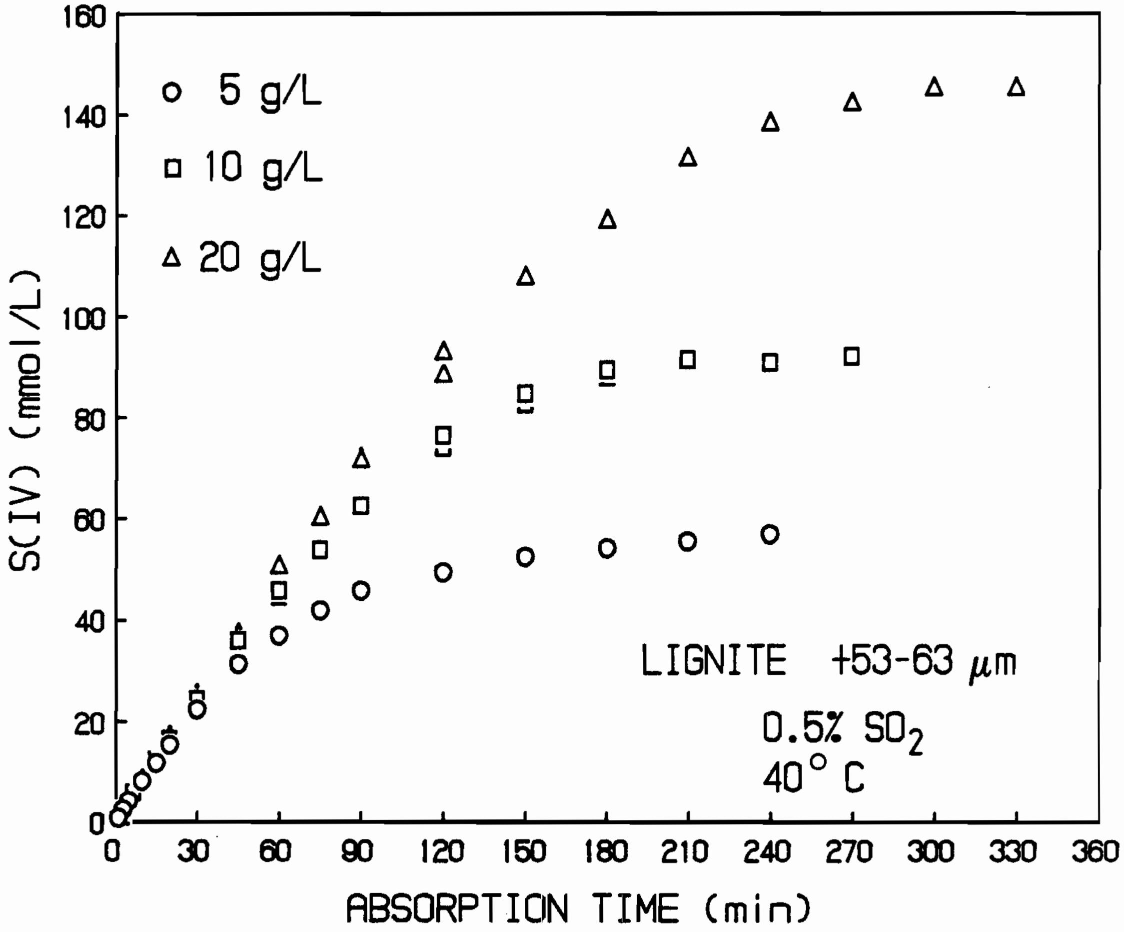

Figure 5.4 Effect of slurry density on the concentration of aqueous sulphur species from absorption into lignite ash slurries

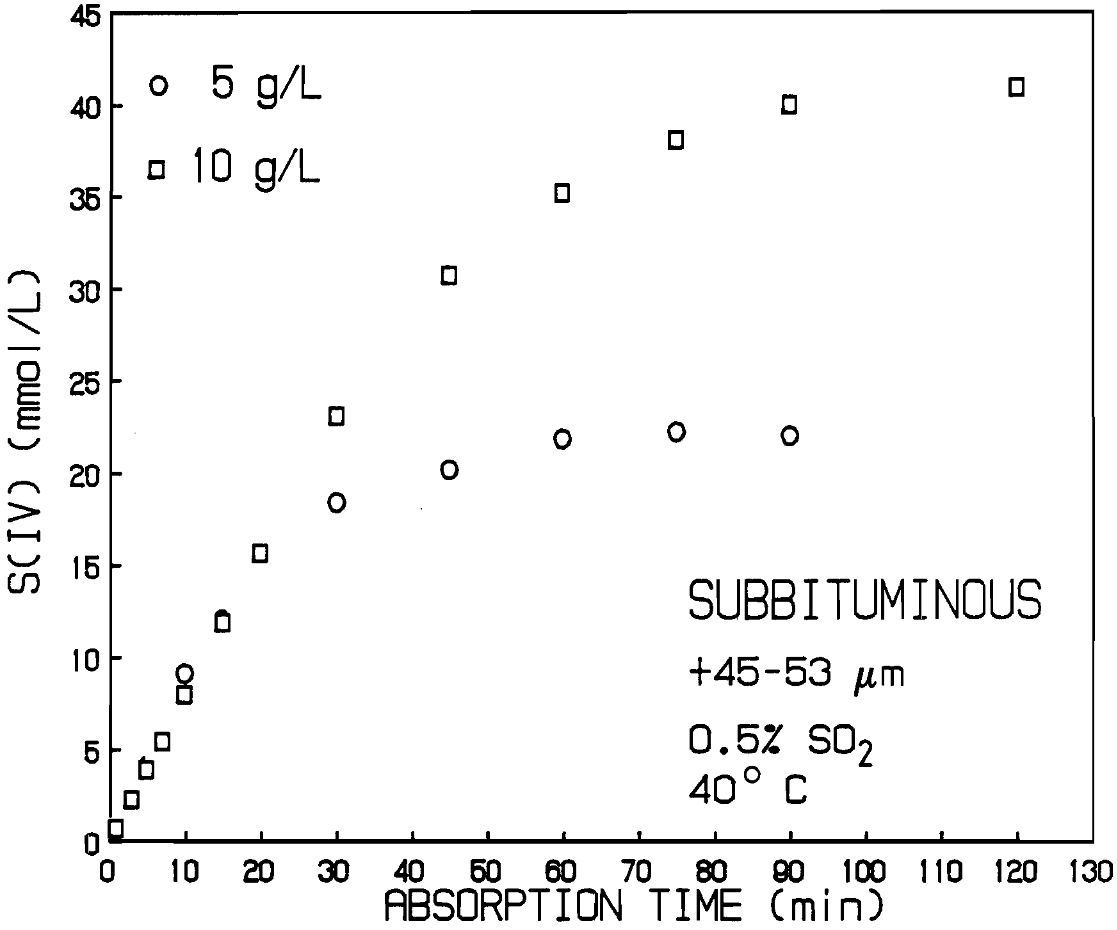

Figure 5.5 Effect of slurry density on the concentration of aqueous sulphur species from absorption into SB ash slurries

a constant level. The time needed to saturate the solution is a function of alkali availability.

The percent overall removals of SO_2 are plotted in Figures 5.6 and 5.7 for lignite and SB ash, respectively. A comparison of the overall removals in each Figure and the respective concentration in Figures 5.4 and 5.5 indicate that the initial periods in which the concentrations were independent of slurry density correspond to 100% overall removal. This implies that in the first 15-30 minutes (depending on the type and the amount of solids), there was sufficient alkalinity to absorb all the sulphur dioxide gas introduced into the system and the absorptive capacity of the slurries was close to 100% at the tested SO_2 inlet concentration of 0.5%. However, this absorptive capacity gradually decreased at later times with variable degrees depending on the type and amount of solids present.

For example, at a contact time of 90 minutes, the total amount of SO_2 absorbed in a slurry containing 10 g/L was 85% of the total amount fed to the reactor when lignite ash was used and 54% when SB ash was used. At a slurry density of 5 g/L, the total amount absorbed was only 63% for lignite and 33% for SB ash. First of all, this indicates that lignite ash provides a larger amount of alkalinity compared to SB ash (See Chapter 4). In addition, the rate of consumption of the

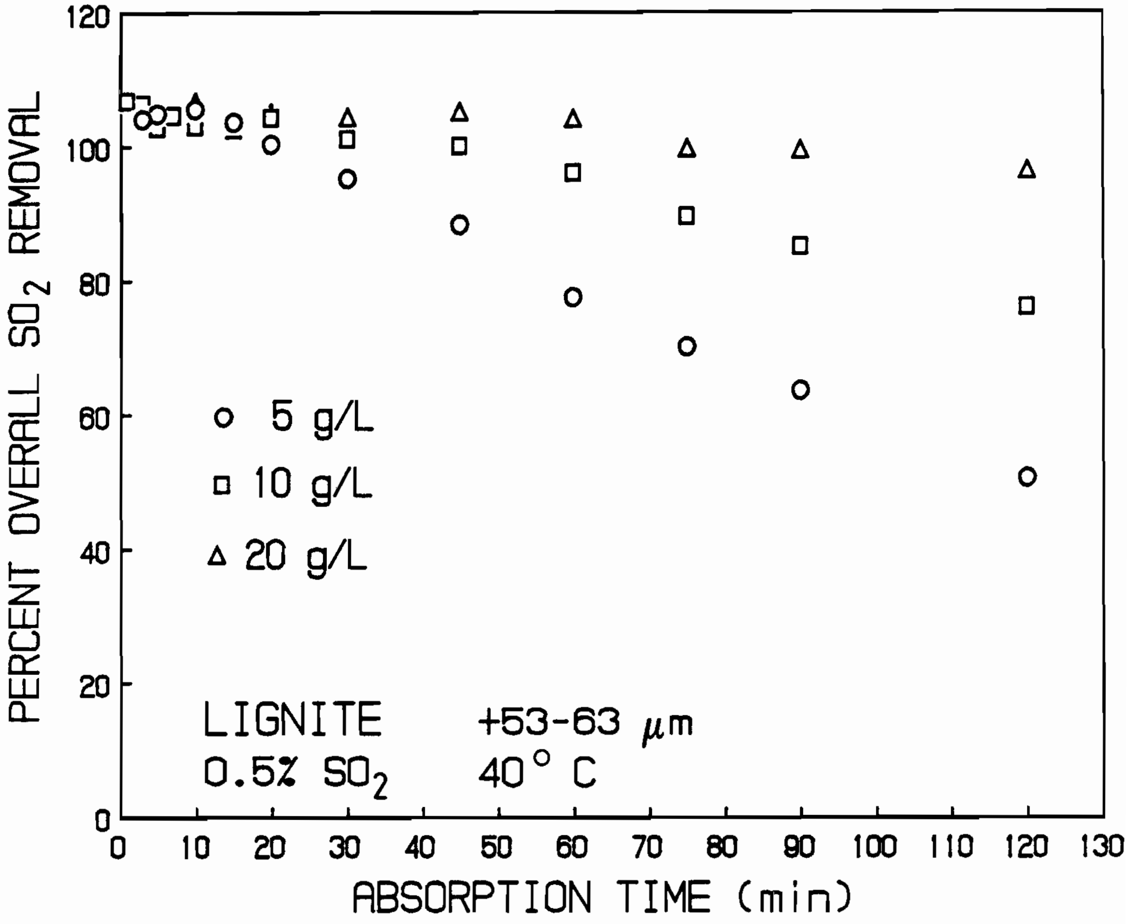

Figure 5.6 Percent overall removal of SO_2 by lignite slurries

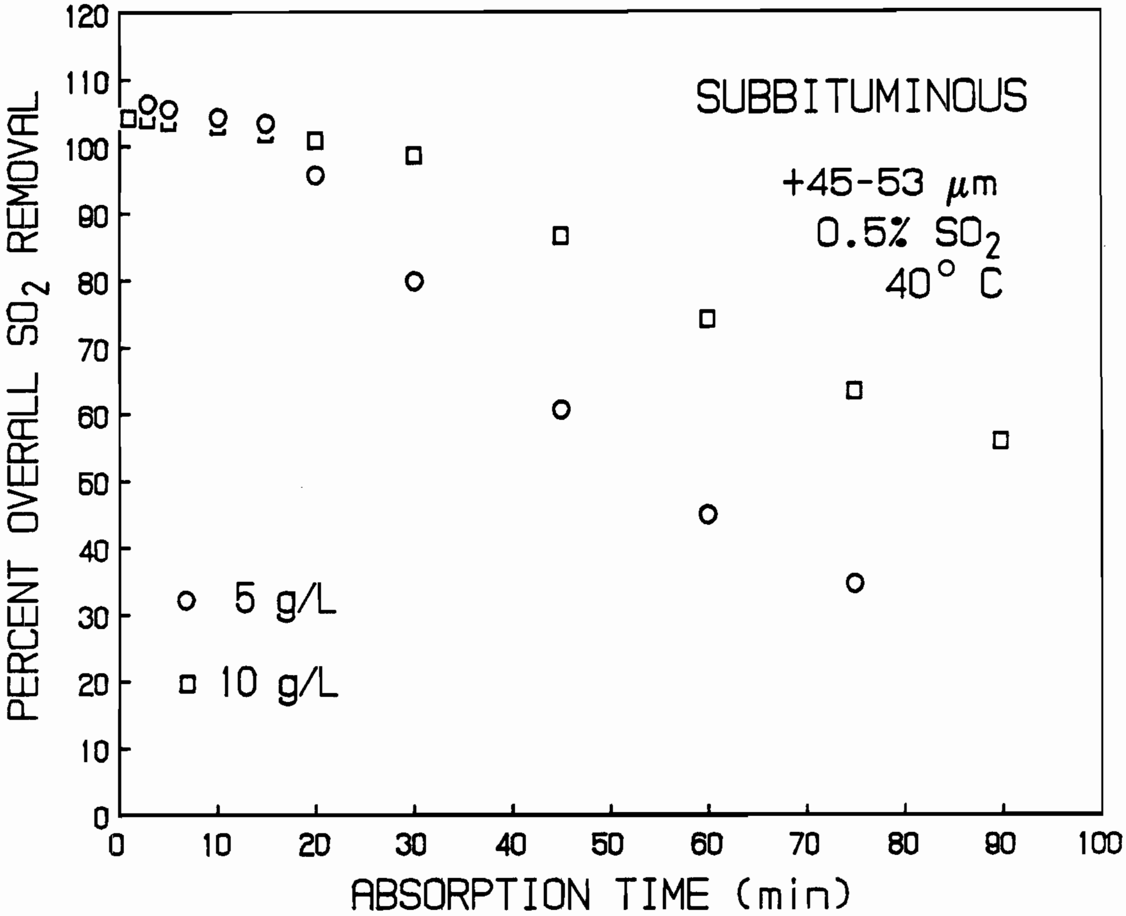

Figure 5.7 Percent overall removal of SO_2 by SB slurries

soluble alkalinity by the reactions with the aqueous sulphur species is greater than the rate of dissolution of alkaline compounds where these compounds are progressively depleted from the solid particles.

5.3.3 Absorption into Clear Solution

The role of solids in the process of gas absorption is to provide the alkalinity that will increase the absorption capacity of the liquid volume which is achieved through the dissolution of the alkaline metal compounds in fly ash. An experiment was also carried out in which the absorbing medium is a clear solution of lignite ash leachate. First, a leaching experiment was conducted according to the procedure described in Chapter 3 where 10 g solids/L were added to the liquid at an initial pH of 5.5 and 40° C and then allowed to leach in the reactor for 60 minutes at the usual stirring speed of 800 rpm. The slurry was filtered, the solids were discarded and the filtrate was added to the reactor as a medium for SO_2 absorption.

The data on the concentration of aqueous sulphur species obtained from this experiment were compared to those obtained from absorption into a lignite slurry containing 10 g/L of solids and the results are shown in Figure 5.8. Data on the absorption into pure water at similar experimental

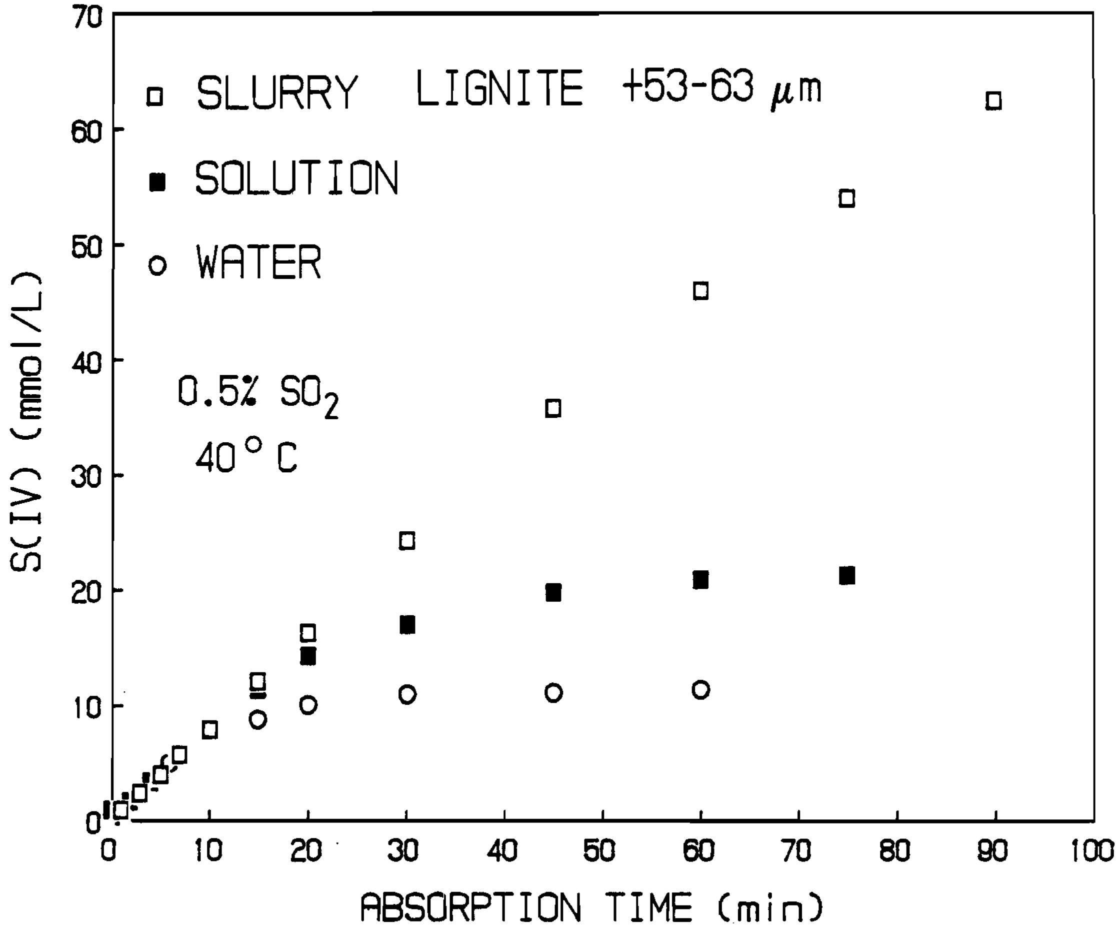

Figure 5.8 Absorption into clear solution of fly ash alkalinity compared to absorption into a slurry

conditions were also plotted in the same Figure for comparison purposes. It is interesting to note that during the first 15 minutes of contact, the rate of absorption was the same regardless of the type of the absorbing medium as can be concluded from the initial slopes of the plotted data (this will be explained in Section 5.6).

The solution of ash extract absorbed twice as much SO_2 as that absorbed by pure water at the stated conditions. When a slurry was used as the absorbing medium, the amount of the gas absorbed was increased to more than four times as much as that of the solid-free solution.

This large difference in the absorption capacities of the slurry and the solution media reflects a corresponding large difference in the amount of the soluble alkalinity available for gas absorption in the two media. Since this alkalinity is produced by the continuous dissolution of the alkaline metal compounds in fly ash as indicated by Figure 4.25, the use of a slurry rather than a solution is necessary to provide as much of the alkalinity as possible. In order to achieve this, the conditions favourable for dissolution of these components, especially the pH, should be provided.

5.3.4 Variation of Slurry pH During Absorption

Table 5.1 presents the values of the slurry pH during SO_2 absorption into the slurries of lignite and SB ashes reported earlier. It can be seen that during the initial stage of absorption, there was a sharp drop in the pH which started as soon as the gas was introduced into the reactor and lasted for about five minutes. After that, the slurry pH stabilized and remained constant until the end of the experiment.

The level of the slurry pH in the prevailing latter stage is determined by the effects of two processes that occur simultaneously, namely the gas absorption and the solid dissolution. The absorption of SO_2 and its subsequent hydrolysis to the bisulphite ion results in the production of hydrogen ions which consume the alkalinity that is produced by the dissolution of the alkaline compounds in fly ash. The relatively low pH that is attained results in favourable pH conditions for further dissolution. The use of lignite slurries resulted in smaller pH drop than in the case of SB ash slurries because lignite ash offers more alkalinity that would prevent further decrease in the slurry pH.

The fact that this pH is quite low eliminates any possibility of absorbing a fraction of CO_2 which is present in the actual power plant flue gas in 50-100 times as much as

Table 5.1

Variation of the Slurry pH During Absorption at Different Fly Ash Slurry Densities

Time	Lignite (g/L)			SB (g/L)	
(min)	5	10	20	5	10
0(*)	9.6	9.9	10.3	7.1	7.2
1	7.0	7.1	7.35	-	-
3	3.7	3.7	3.8	3.0	3.3
5	3.55	3.5	3.7	2.8	3.1
10	3.4	3.35	3.55	2.7	2.95
15	-	3.25	-	2.7	2.9
20	3.2	3.35	3.4	2.6	2.85
30	3.1	3.3	3.4	2.65	2.9
45	3.0	3.3	3.3	2.6	2.8
60	3.0	3.25	3.35	2.7	2.9
75	2.95	3.25	3.35	2.65	2.9
90	3.05	3.2	3.4	-	2.85

(*) Before the introduction of the gas.

SO_2. Carbon dioxide may be absorbed in the scrubbing solution when the pH is higher than 7 (23). In industrial scale scrubbing processes in the presence of oxygen in the flue gas, lower pH will speed up the oxidation from sulphite to sulphate. This step is very important since a sludge of sulphite is difficult to dewater and environmentally unsuitable for landfill disposal due to its high chemical oxygen demand (23,35). Scrubbing by fly ash systems reported in the literature (27) were operated at lower pH levels (pH 3 in most cases) compared to the conventional limestone systems which usually operate at pH 4-6.

5.3.5 Effect of the Particle Size

Three fractions of lignite ash , namely, 53-63, 63-75 and 75-90 μm were examined for the effect of particle size on the absorption of sulphur dioxide and the results are shown in Figure 5.9. The slurry density was kept at 10 g/L and the inlet SO_2 concentration was 0.5%. The data indicate that under the tested conditions, the particle size does not affect the amount of SO_2 absorbed. The only role of the solids was to provide the necessary alkalinity through the dissolution of the alkaline metal compounds (See Section 5.5).

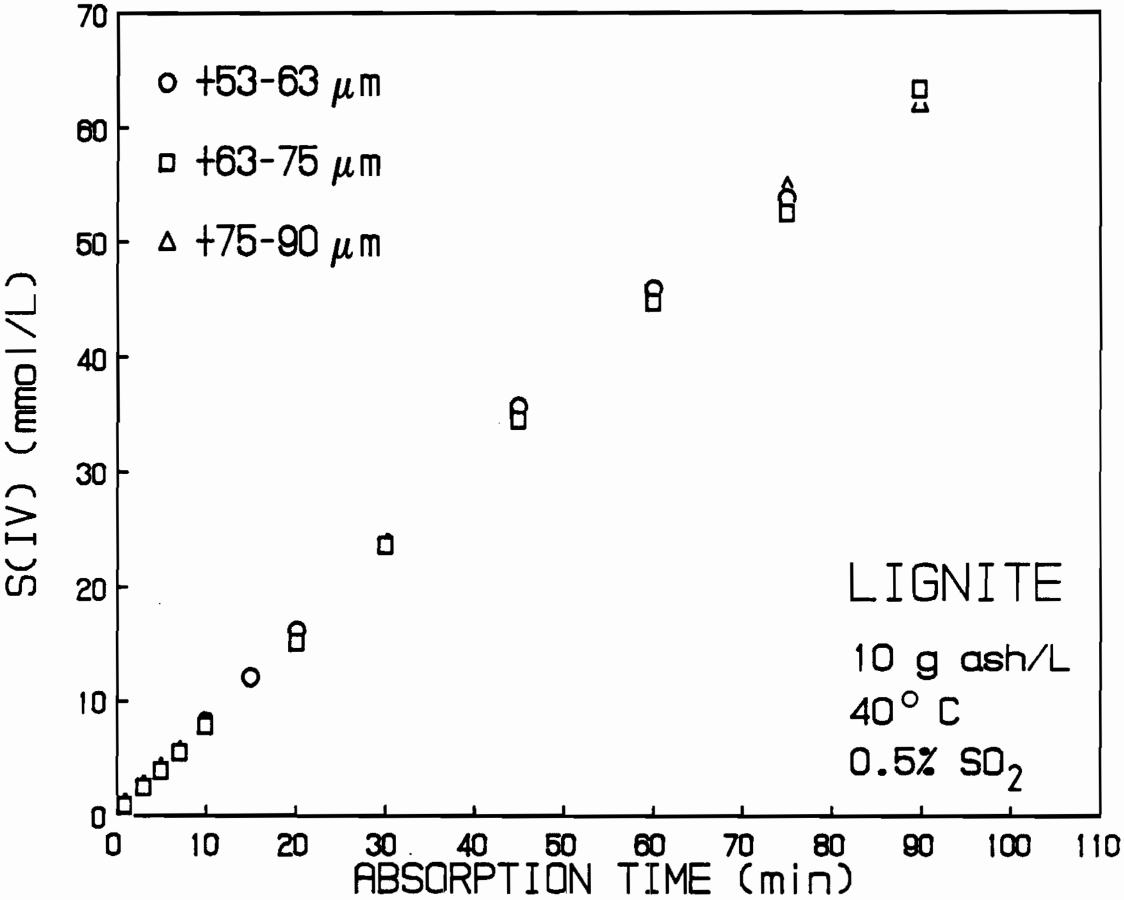

Figure 5.9 Effect of particle size on the concentration of aqueous sulphur species from SO_2 absorption

5.3.4 Effect of SO_2 Inlet Concentration

The concentration of aqueous sulphur species was measured as a function of absorption time at three levels of SO_2 concentrations in the gas phase, namely, 0.5, 1.0 and 1.5% (by volume) which correspond to the partial pressures of 0.005, 0.01 and 0.015 atm, respectively. The experiments were conducted at 40° C and a slurry density of 10 g/L and the results are shown in Figure 5.10. The concentration of aqueous sulphur species increased with increasing the inlet concentration of SO_2 in the tested range. The obtained equilibrium values of 92, 160 and 225 mmol/L correlate linearly with the inlet concentrations.

The overall percent SO_2 removals at the different gas inlet concentrations are plotted in Figure 5.11. At the lower SO_2 inlet concentration of 0.5%, 100 percent removal was obtained in the first 30 minutes of contact. At the higher gas inlet concentrations, the percent removal dropped rapidly to 70-80% in the same period of time due to the low pH attained in the liquid phase. The variation of the slurry pH is presented in Table 5.2.

These results indicate that at the particular slurry density of the experiments, the liquid phase does not contain sufficient alkalinity to remove the large amounts of SO_2 in

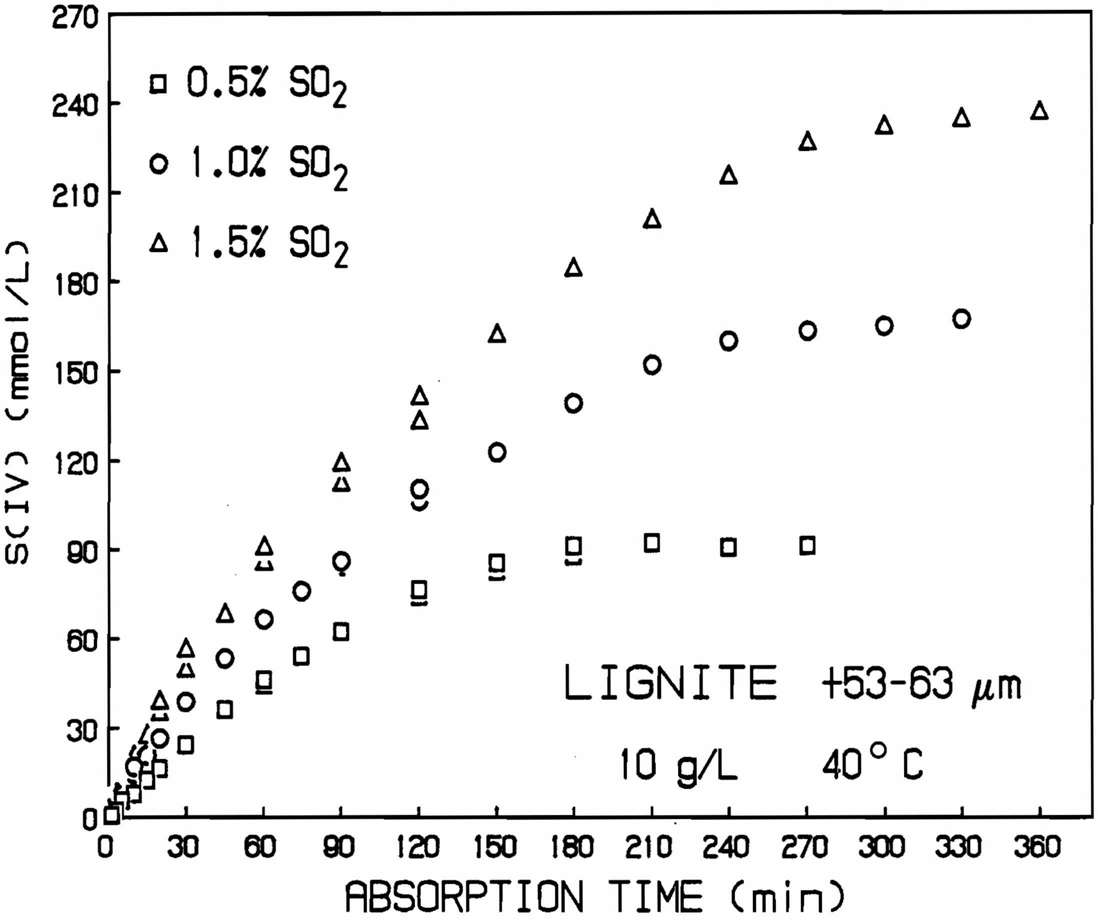

Figure 5.10 Effect of SO_2 inlet concentration on the concentration of aqueous sulphur species

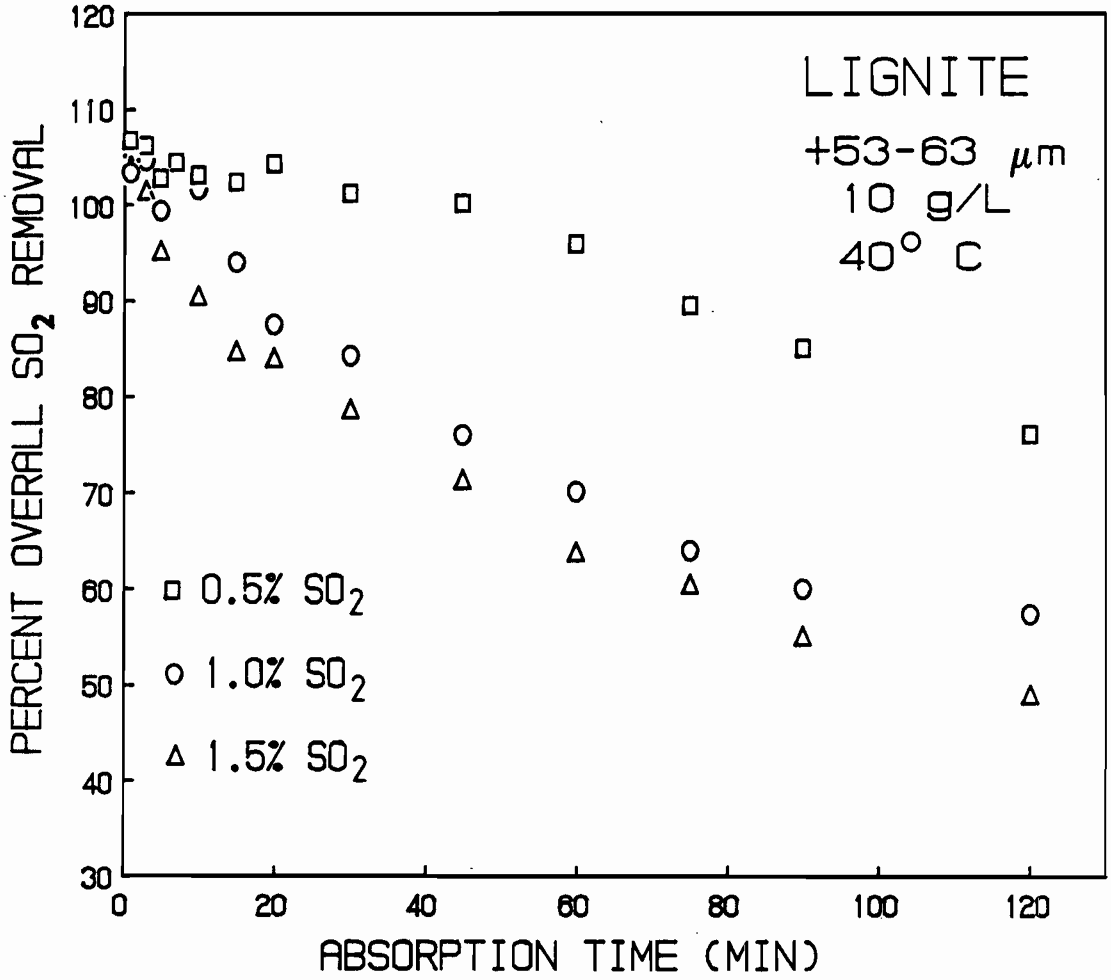

Figure 5.11 Percent overall removal of SO_2 at different gas inlet concentrations

Table 5.2

Variation of the Slurry pH at Different Inlet SO_2 Concentrations

Time (min)	0.5%	1.0%	1.5%
0	9.9	9.75	10.1
1	7.1	6.6	6.8
3	3.7	2.9	2.7
5	3.5	2.8	2.6
10	3.35	-	2.5
15	3.25	2.75	-
20	3.35	-	2.5
30	3.3	2.6	4.45
45	3.3	2.6	2.4
60	3.25	2.65	2.45
75	3.25	2.6	2.5
90	3.2	2.7	2.5

the feed gas. In order to scrub all the incoming SO_2, the soluble alkalinity should be increased. This can be done by increasing the slurry density, adding a supplement source of alkalinity (e.g. limestone) or both. The level of the operating pH may also be optimized to obtain maximum absorption at the particular conditions of the process.

5.4 Absorption into Limestone-containing Slurries

In this Section, the results obtained from the experiments on absorption into mixtures of fly ash and limestone will be presented and discussed. The experiments were carried out using either lignite or SB ash at 10 g/L of total solids in the reactor and 0.5% SO_2 as the inlet gas concentration for a maximum contact time of 120 minutes. Absorption in pure limestone (analytical grade calcium carbonate of fine particles below 45 μm) was also examined and the data are compared to that from absorption into slurries of mixtures. Also, the results from absorption into slurries of ash alone are replotted for comparison purposes.

Figure 5.12 presents the results of absorption in mixtures of lignite ash and limestone. For the first 60 minutes, there was no difference in the amount of SO_2 absorbed with the four different slurries. At 90 minutes of contact, the concentrations of aqueous sulphur species obtained using

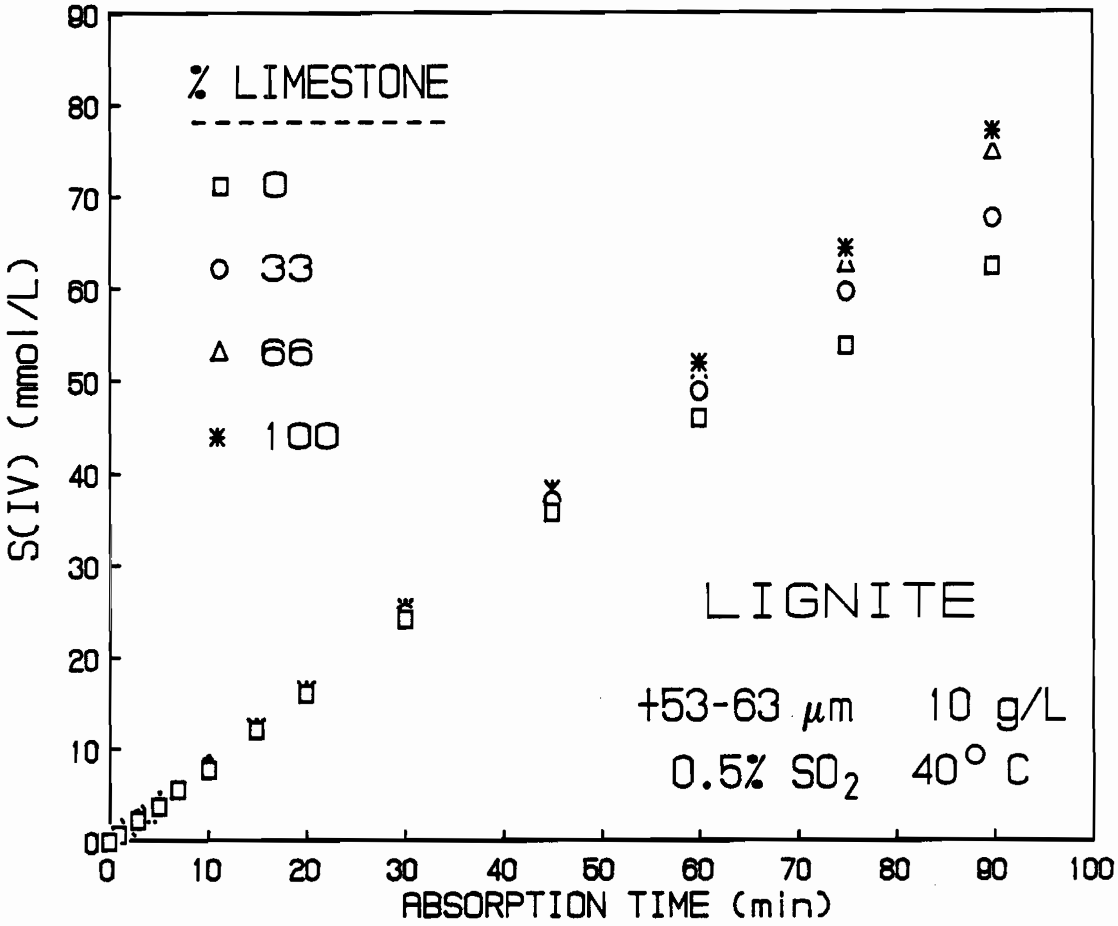

Figure 5.12 Absorption of SO_2 into slurries of lignite ash and limestone mixtures

mixtures containing 66% limestone was the same as the concentration obtained using a slurry of pure limestone because of the high availability of alkalinity as a result of the dissolution of calcium carbonate from limestone. Also at 90 minutes, absorption into a slurry of lignite ash alone produced aqueous sulphur concentrations only 20% less than pure limestone. This indicates that lignite ash is a rich source of alkalinity and has the potential of being used without a supplement alkali in some applications.

The percent overall removals of SO_2 in lignite-limestone mixtures are shown in Figure 5.13. Complete overall removals (or absorptive capacities) were obtained with the mixture of 66% of limestone and 90% removal was possible with the mixture of 33% after 90 minutes of absorption. In a slurry of lignite alone at the same conditions, 85% of the incoming gas was absorbed in the liquid phase.

The effect of the addition of limestone on the absorption of SO_2 into slurries of SB ash is shown in Figure 5.14. In general, the concentrations of aqueous sulphur species increased as the limestone ratio was increased. After a contact time of 90 minutes, a slurry of SB ash alone absorbed half the amount of SO_2 which was absorbed by a slurry of pure limestone at the same conditions. Using a mixture of 50% produced an intermediate concentration and a mixture of

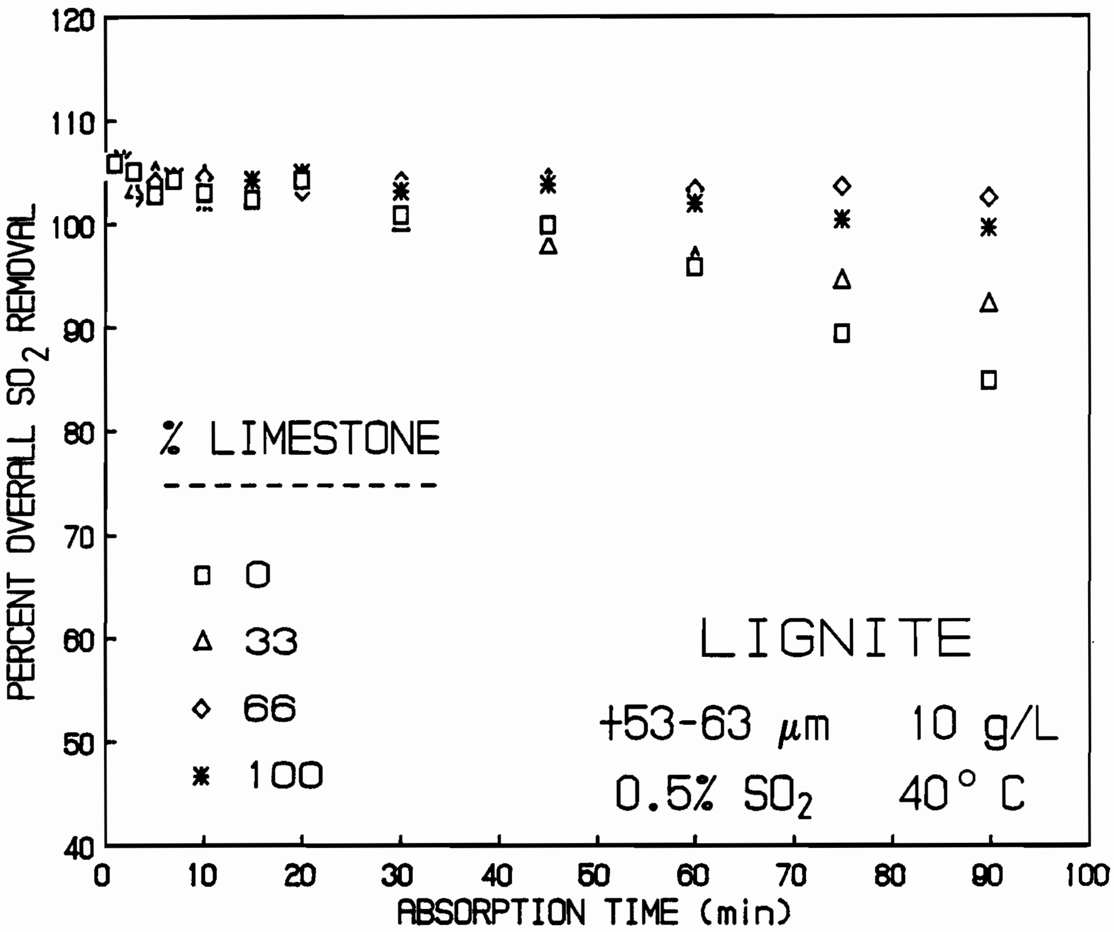

Figure 5.13 Percent overall removal of SO_2 by slurries of lignite ash and limestone mixtures

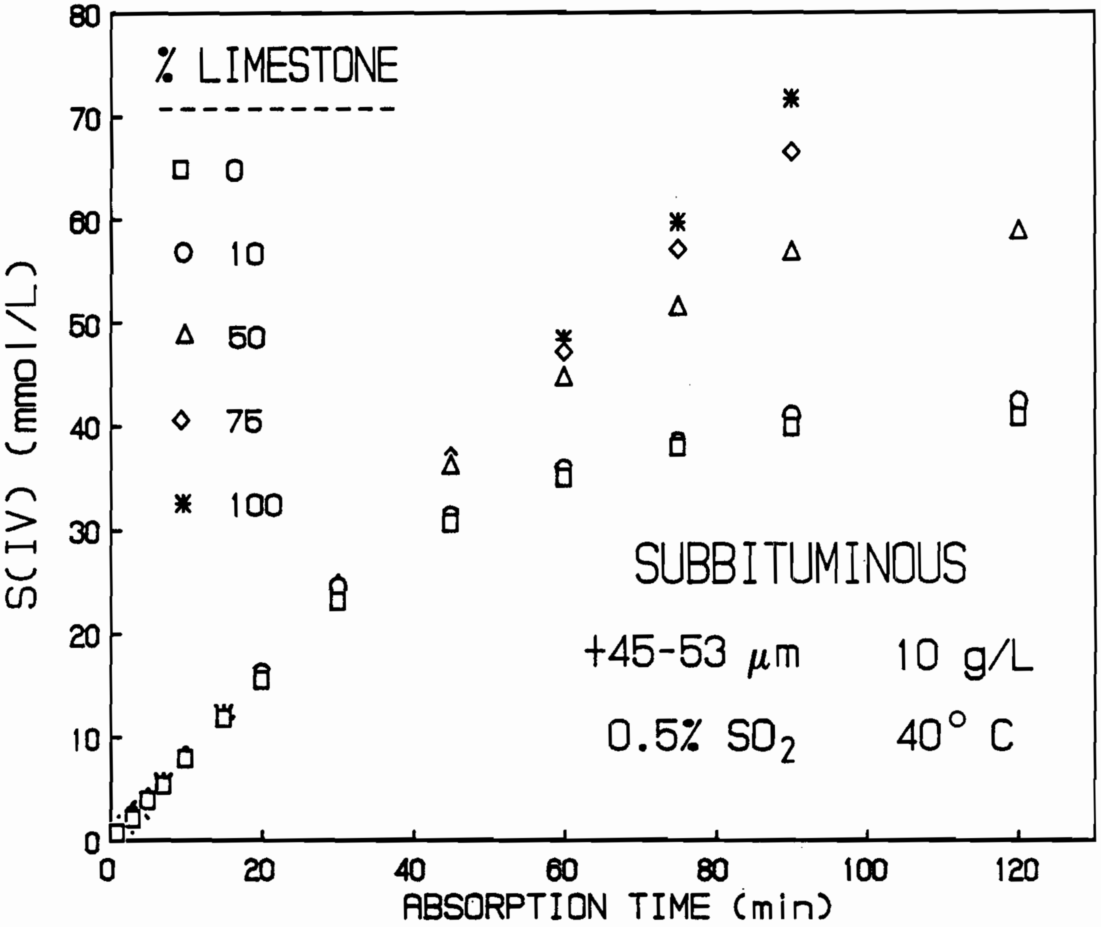

Figure 5.14 Absorption of SO_2 into slurries of SB ash and limestone mixtures

75% limestone resulted in a higher concentration consistent with this ratio. The mixture containing only 10% of limestone did not significantly increase gas absorption over that of SB ash alone.

The effect of limestone addition on the percent removal of SO_2 in SB-limestone mixtures is shown in Figure 5.15. The mixtures of 10, 50, and 75% limestone removed 58, 80 and 92% of the total incoming SO_2 until 90 minutes of absorption. A slurry of SB ash alone removed 55% of the gas at the same conditions.

Tables 5.3 and 5.4 present the values of the slurry pH during absorption into slurries of mixtures of fly ash and limestone. The only difference between these data and those of pH in ash-only slurries is that the pH drop in the first stage of absorption was smaller and the level of the constant final pH was higher. This is because of the high pH associated with the dissolution of calcium carbonate from the limestone particles.

The constant slurry pH that dominated most of the absorption process increased from 3.0 in lignite-alone or 2.7 in SB-alone slurries to 4.1 in the pure limestone slurry. Mixtures of solids resulted in intermediate pH levels of their slurries indicating the acid-alkali reaction of the process.

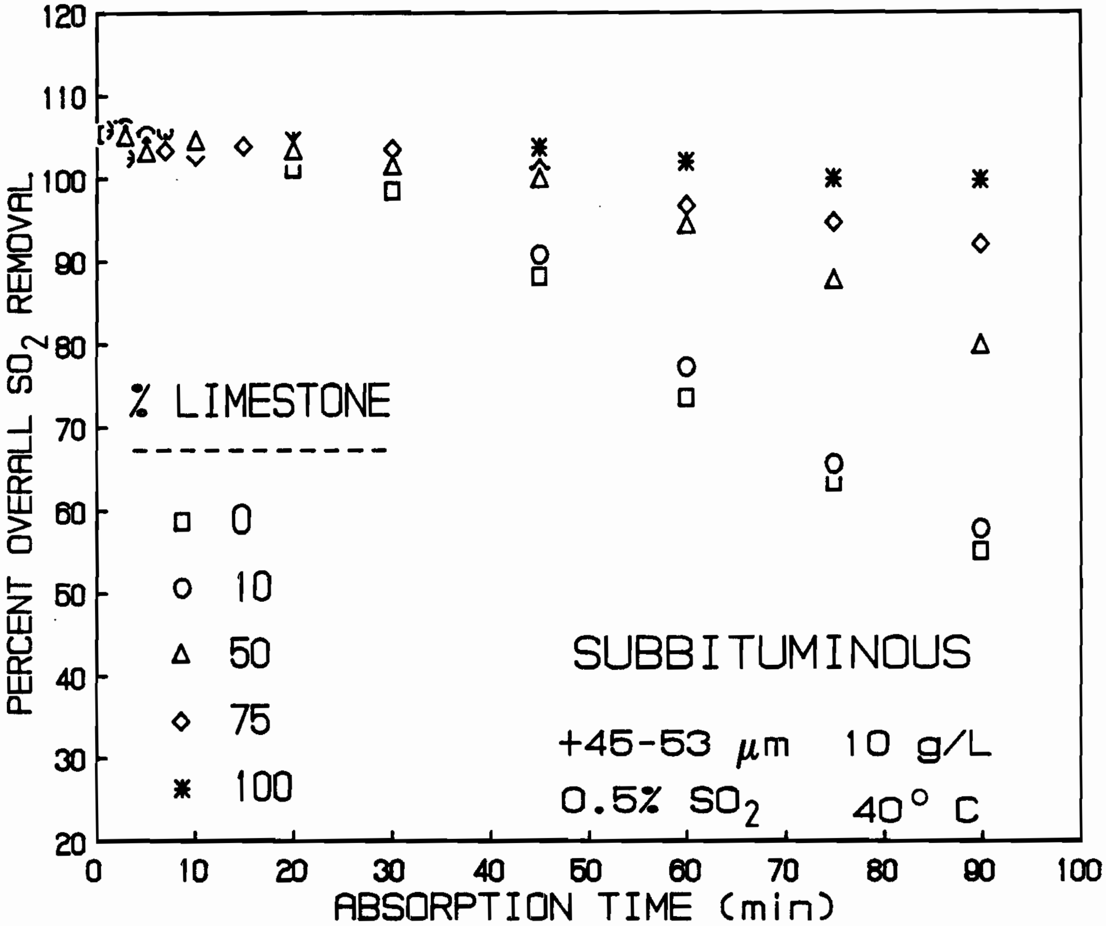

Figure 5.15 Percent overall removal of SO_2 by slurries of SB ash and limestone mixtures

Table 5.3

Variation of the Slurry pH During Absorption into Mixtures of Lignite Ash and Limestone (L.S.)

Time (min)	33% L.S.	66% L.S.	100% L.S.
0	9.6	9.5	7.7
1	-	5.3	6.0
3	5.6	4.25	4.9
5	4.7	3.9	4.75
10	3.75	-	4.5
15	-	3.8	-
20	3.65	3.8	4.35
30	3.6	3.9	4.2
45	3.6	3.85	4.1
60	3.55	3.8	4.2
75	3.5	3.7	4.2
90	3.6	3.8	4.1

Table 5.4

Variation of the Slurry pH During Absorption into Mixtures of SB Ash and Limestone (L.S.)

Time (min)	10% L.S.	50% L.S.	75% L.S.
0	7.2	7.45	7.6
1	-	5.7	-
3	3.4	3.95	4.5
5	3.2	3.7	4.25
10	3.1	-	4.1
15	3.0	3.75	-
20	2.95	-	4.0
30	2.9	3.6	3.9
45	2.8	3.6	3.8
60	2.9	3.5	3.85
75	2.9	3.45	3.75
90	2.85	3.4	3.7

5.5 Solid Dissolution During Absorption

The concentrations of calcium and magnesium dissolved from fly ash particles during sulphur dioxide absorption were determined for experiments performed at different conditions. The importance of these data in gas absorption originates from the fact that the dissolution of the alkaline metal compounds is responsible for providing the soluble alkalinity that will react with the aqueous sulphur species thus enhancing the absorption process. This was previously demonstrated in Figure 4.25.

The concentrations of calcium and magnesium dissolved during SO_2 absorption into slurries of lignite ash at 5, 10 and 20 g/L are shown in Figure 5.16. A comparison of this Figure with Figure 4.4, which showed the concentrations of the same metals dissolved from lignite ash in the absence of absorbed SO_2 indicates that the concentrations of calcium and magnesium dissolved during absorption were respectively twice and 3-4 times as much as that in the absence of SO_2. In terms of the percent metal oxides dissolved, the ratio ranged from 40-65% CaO and 2-4% MgO with absorption (depending on the slurry density) while for leaching in the absence of SO_2, the ratios were 20-46% CaO and 0.5-1.4% MgO. These comparisons are based on values obtained near the end of the experiments when the concentrations levelled-off. Also, the dissolution in the

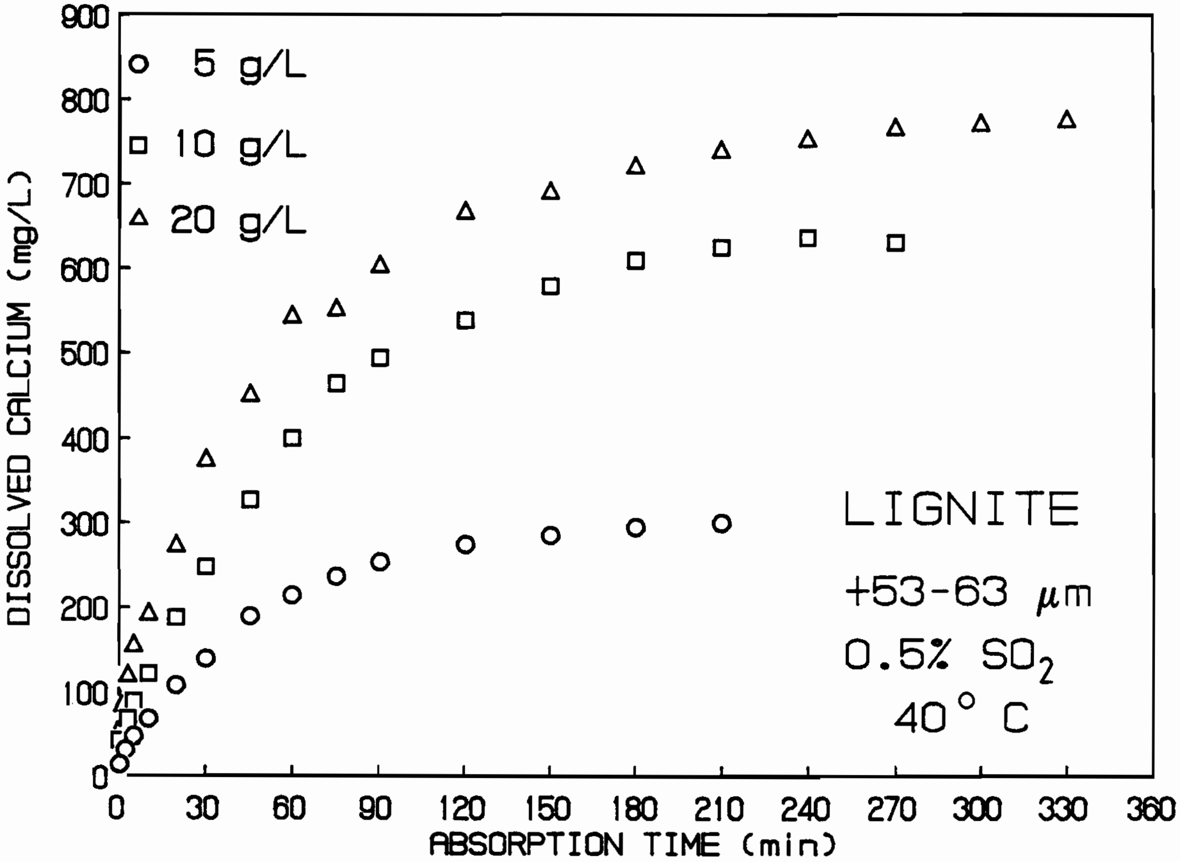

Figure 5.16 (A) Concentration of calcium dissolved during absorption into slurries of lignite ash

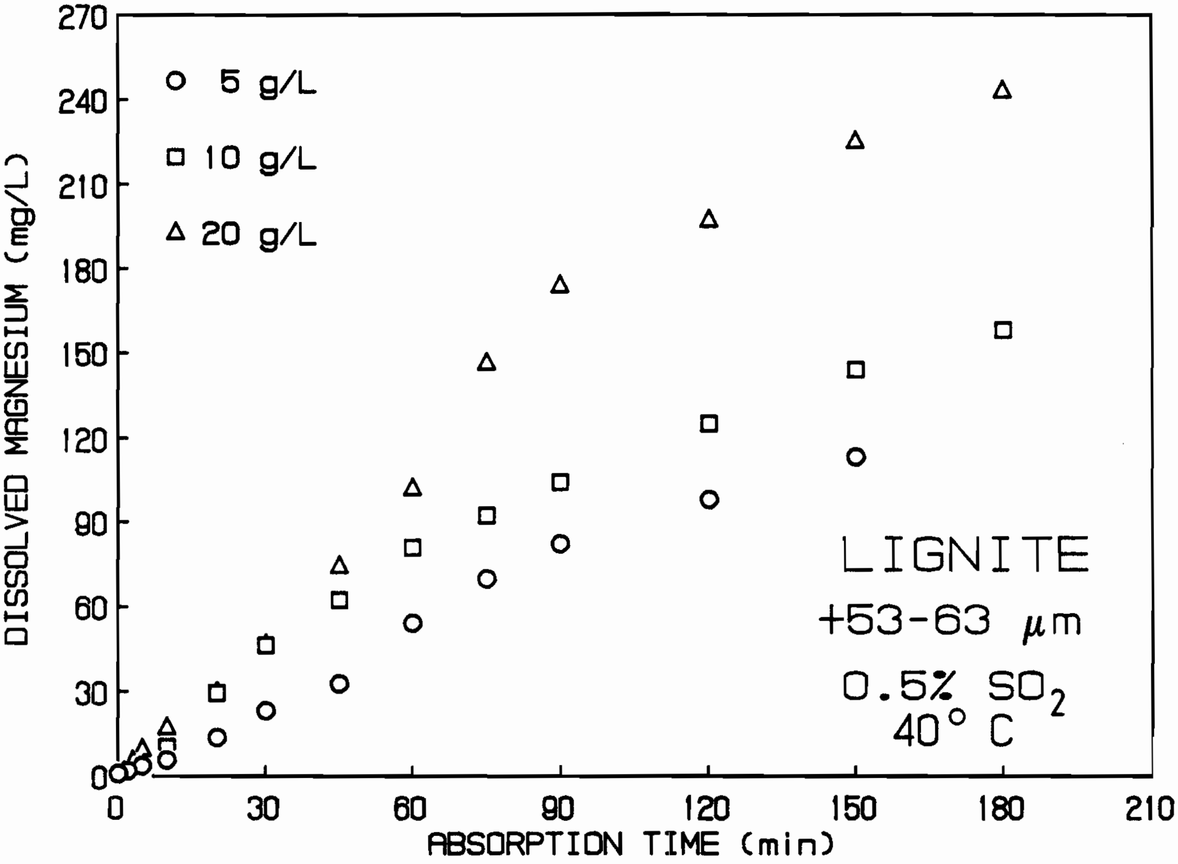

Figure 5.16 (B) Concentration of magnesium dissolved during absorption into slurries of lignite ash

presence of absorbed SO_2 continued for much longer time before the concentrations reached a constant value.

The large increase in dissolved metal concentrations can be explained by chemical reactions between the acidic species produced by the hydrolysis of sulphur dioxide with the alkaline components in the fly ash solids. A constant supply of hydrogen ions are provided by the hydrolysis of SO_2 thus maintaining a low pH throughout the absorption process. These ions react with CaO and other alkaline metal compounds in fly ash causing a large enhancement of dissolution. The difference in the prevailing slurry pH between the absence and presence of absorbed SO_2 can not be the main factor responsible for the increase in the dissolved metal concentrations during SO_2 absorption. As shown previously in Figure 4.21, the pH during leaching in the absence of SO_2 was in the range of 2-4 for a slurry density of 5 g/L, which is not much different than the pH prevailing during the corresponding absorption experiment (pH 3.0). This difference may be attributed to reactions between the dissolved S(IV) species and fly ash. Figure 5.17 shows that the particle size has a negligible effect on dissolved metal concentrations.

Similar observations can be made for SB ash as shown in Figure 5.18. For the two slurry densities of 5 and 10 g/L, the dissolved CaO was 76-84% compared to 22-40% in the absence

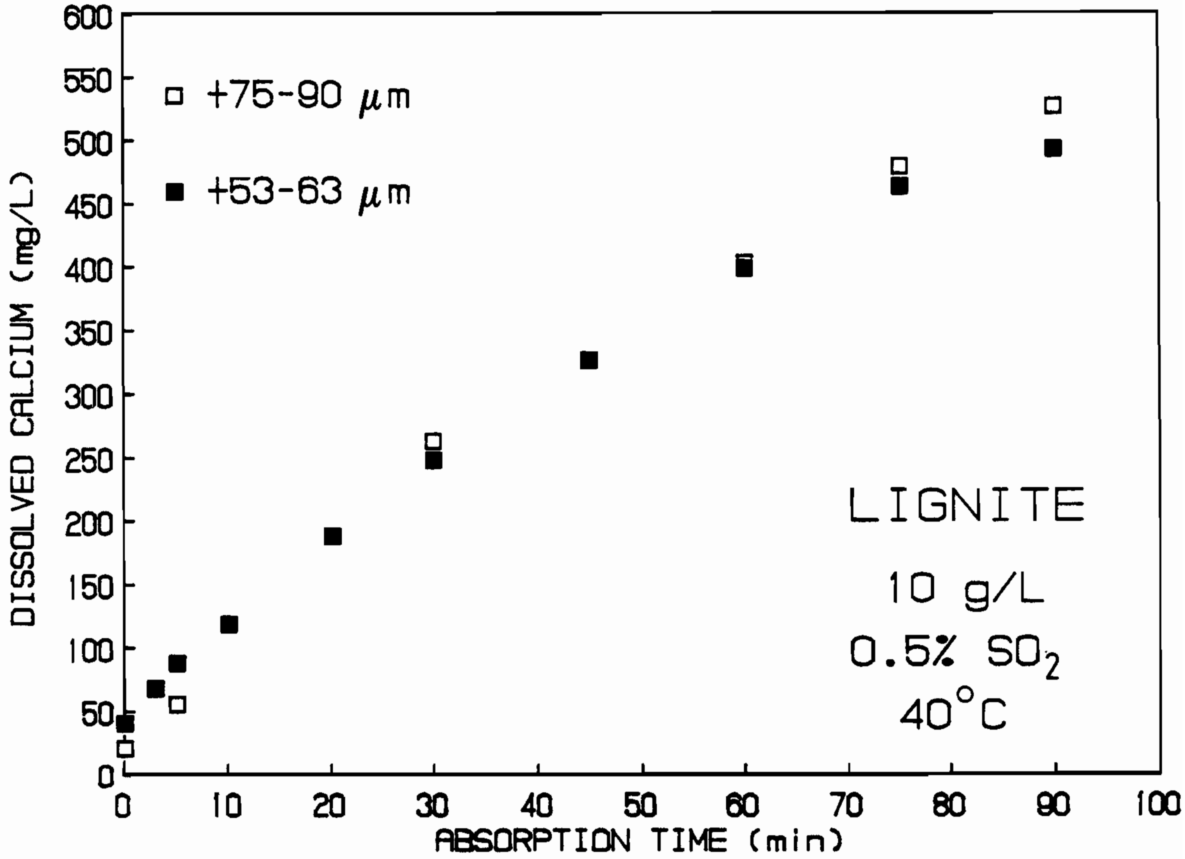

Figure 5.17 (A) Effect of particle size on the concentration of calcium dissolved during SO_2 absorption

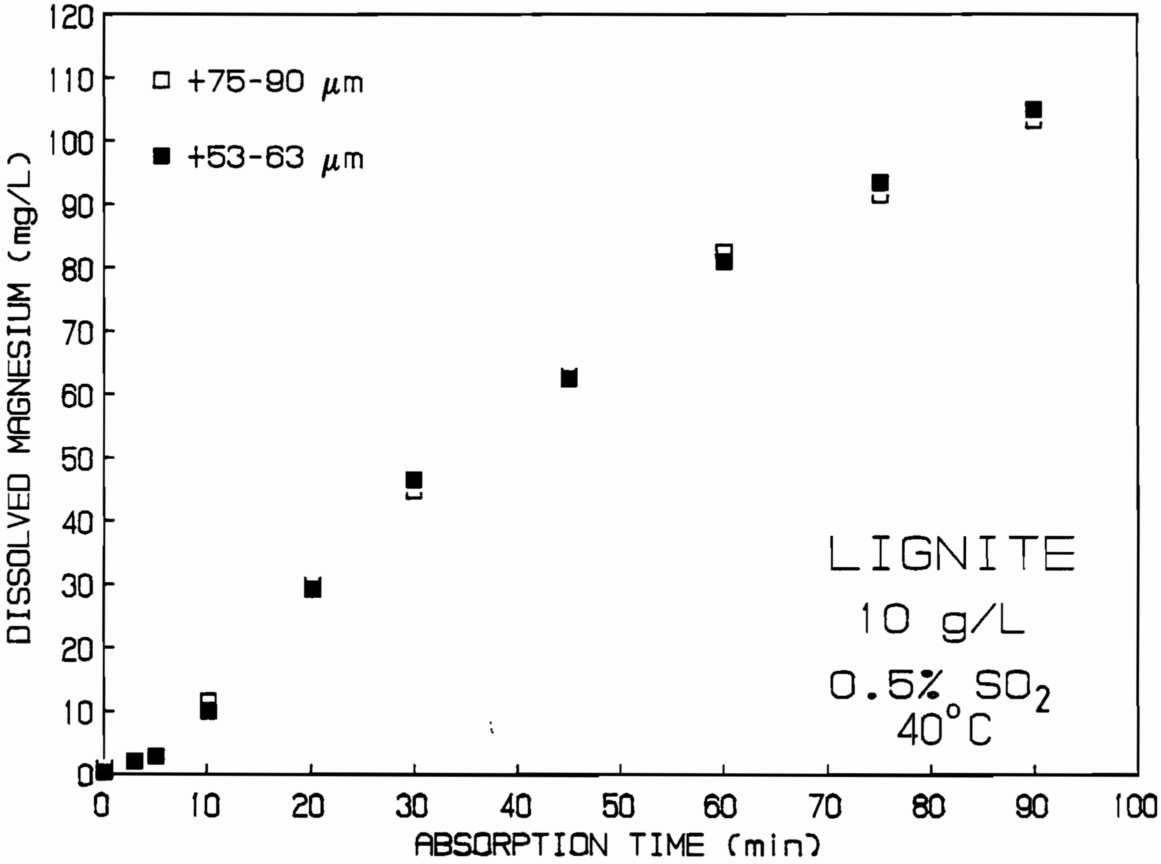

Figure 5.17 (B) Effect of particle size on the concentration of magnesium dissolved during SO_2

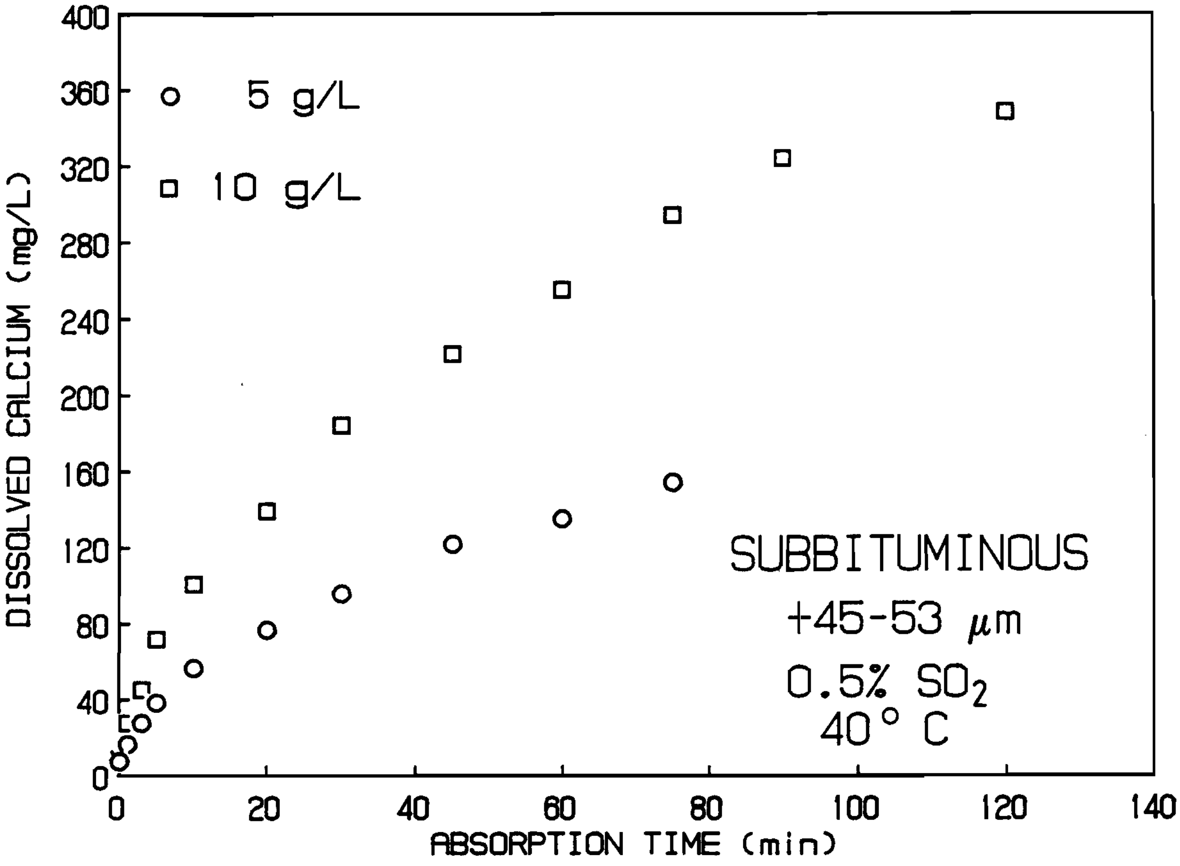

Figure 5.18 (A) Concentration of calcium dissolved during absorption into slurries of SB ash

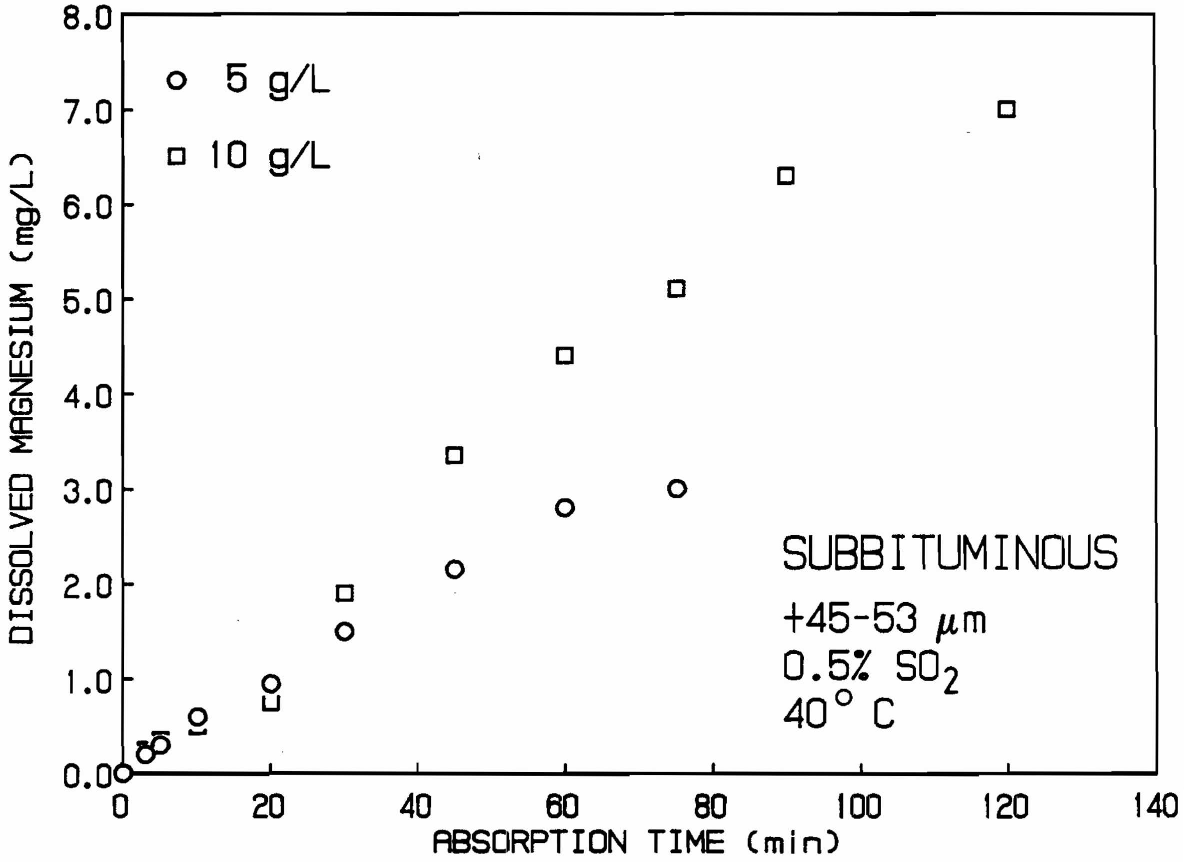

Figure 5.18 (B) Concentration of magnesium dissolved during absorption into slurries of SB ash

of absorption. No significant difference in the concentration of magnesium was observed.

5.6 Theoretical Analysis

5.6.1 Chemical Equilibria

The results described earlier in this Chapter have demonstrated that after the initial drop from highly alkaline to acidic levels, the pH was never greater than 4.5 in any of the absorption experiments performed in this study. In this pH range, the predominance diagram of sulphur species (Figure 1.1) shows that the only important species in the liquid phase are the aqueous molecular SO_2 and the bisulphite ion. Based on this, the following set of equations represent the reactions taking place in the scrubbing solution based on fly ash as a source of alkalinity:

Absorption: $SO_{2(g)} === SO_{2(aq)}$ (1.1)

Hydrolysis: $SO_{2(aq)} + H_2O === HSO_3^- + H^+$ (1.2)

Dissolution: $1/2z\ M_yO_{z(s)} + 1/2\ H_2O === y/2z\ M^{2+} + OH^-$ (5.2)

Neutralization: $OH^- + H^+ === H_2O$ (5.3) where the formula M_yO_z represents an alkaline metal oxide.

The solubility of sulphur dioxide in a solution (equation 1.1), which is often expressed in terms of Henry's law constant, H, decreases with ionic strength of that solution (4). In the liquid systems examined in this study, however, the ionic strength was not sufficiently high to significantly influence the solubility of sulphur dioxide and therefore, the latter was considered equal to the solubility of SO_2 in water. Henry's law constant for water is 763 mmol/L.atm as calculated from equation 5.4 (30) at 40° C:

$$H = \exp\,(2851.1/T - 9.3795) \qquad (5.4)$$

The maximum value for the ionic strength in fly ash solutions investigated in this study (obtained with a lignite ash slurry of 20 g/L after 300 minutes) resulted in a value of 768 mmol/L for Henry's law constant. Equations used to estimate the effect of the ionic strength on the solubility of sulphur dioxide are presented in Appendix C.

The total concentration of sulphur compounds in solution at constant pH is the sum of the concentrations of molecular SO_2 and the bisulphite ion. The sulphite ion does not exist in the solution during this period. Most of the sulphur in the liquid phase exists as bisulphite ion.

Molecular SO_2 was only 5-20% of the total dissolved sulphur in fly ash-based systems. In the case of pure water as absorbent, however, molecular SO_2 comprised 35% of the total dissolved sulphur at a pH of 2.4. Hence

$$C_T = C_A + C_B \tag{5.5}$$

where C_T = concentration of total sulphur (IV) in the bulk liquid, mmol/L.

C_A = concentration of aqueous molecular sulphur dioxide, mmol/L, and

C_B = concentration of bisulphite ion, mmol/L

Since the hydrolysis reaction is essentially instantaneous, C_A and C_B are related through the equilibrium constant of this reaction:

$$K_a = a_B . a_H / a_A \tag{5.6}$$

where a_B, a_H and a_A are the activities of bisulphite ion, hydrogen ion and molecular SO_2 in solution. K_a is a function of temperature, and it was estimated from the relationship (30):

$$K_a = \exp (1972.5/T - 10.9760) \tag{5.7}$$

The activity of each component is given by:

$$a_j = y_j . C_j \tag{5.8}$$

where y_j is the activity coefficient of the j^{th} component. Then, the equilibrium constant is given by:

$$K_a = K_y . K_c \tag{5.9}$$

where $$K_y = y_B . y_H / y_A \tag{5.10}$$

and $$K_c = C_B . C_H / C_A \tag{5.11}$$

Rearranging equation 5.11 and substituting for C_B in equation 5.5:

$$C_A = X\ C_T \tag{5.12}$$

where $$X = 1/(1 + K_c/C_H) \tag{5.13}$$

The coefficient X is a function of temperature, pH and the ionic strength of the solution which affect the activity coefficients of the individual components. Activity coefficients can be calculated from a modified Debye-Huckel law which relates y_j to the ionic strength (14).

5.6.2 Stoichiometric Relations

The constant pH after 10-15 minutes of absorption implies that the hydrogen ion concentration is also constant. For example, when the slurry density was 10 g/L (lignite ash) the pH after 10 minutes was 3.35 (Table 5.1), which corresponds to 0.47 mmol/L of hydrogen ions. After 90 minutes, the pH was 3.25 and the corresponding H^+ concentration was 0.56 mmol/L. To satisfy the dissociation equilibrium constant of water (equation 5.3), the concentration of the hydroxide ion should also be constant. Therefore, the rate of generation of hydroxide ions by the dissolution of metal compounds from fly ash is equal to the rate of generation of hydrogen ions by the hydrolysis of the dissolved SO_2. The latter rate is also equal to the rate of generation of bisulphite ions from the same reaction. The above-mentioned stoichiometric considerations indicates that

$$dC_m/dt = (y/2z)\ dC_B/dt \tag{5.14}$$

where C_m is the concentration of the alkaline metal dissolved from fly ash.

Stoichiometric relations also indicate that the rate of SO_2 absorption from the gas phase by the liquid should be equal to the rate of increase in the total concentration of S(IV) in solution, C_T, and it is given by:

$$dC_T/dt = dC_A/dt + dC_B/dt \tag{5.15}$$

or

$$dC_T/dt = (1/X)\ dC_A/dt \tag{5.16}$$

Finally, by combining equations 5.14, 5.15 and 5.16, the rate of dissolution is related to the rate of absorption by the following equation:

$$dC_T/dt = [2z/y(1-X)]\ dC_m/dt \tag{5.17}$$

To determine the rate-limiting step for the global rate of absorption, the knowledge of the concentration of gaseous SO_2 prevailing in the reactor is necessary. In order to obtain the average concentrations in the gas and in the liquid phases, appropriate models for the reactor that describe the mixing characteristics of both the liquid and the gas are required.

5.6.3 The Reactor Model

The absorption experiments were carried out in a semi-batch stirred tank reactor with continuous gas feed. The liquid phase is assumed to be well-mixed because of the very high rate of agitation. Based on this assumption, a mass balance for total S(IV) species present over the entire volume of liquid in the reactor at any time, t, is:

$$r\ V_L = d(C_T\ V_L)/dt \tag{5.18}$$

where r is the absorption rate per unit volume of the liquid. Assuming that V_L remains constant during gas absorption, the absorption rate into the liquid phase is given by:

$$r = dC_T/dt \tag{5.19}$$

The rate of absorption can be calculated from the experimental results by fitting the data on C_T as a function of time to a power correlation of the type:

$$C_T = a\ t^b \tag{5.20}$$

where a and b are constants.

Mixing in the gas phase is more complicated. Hanhart et al. (12) and Mehta and Sharma (22) have shown that the gas phase in agitated gas-liquid dispersions is almost completely mixed when the speed of agitation is high. However, in the presence of fine solid particles, the coalescence in the gas bubbles can be substantially different. This may change the mixing characteristics in the gas phase. Juvekar and Sharma (20) have found that their results on the absorption of CO_2 into a suspension of lime were more consistent when the plug flow model for the gas phase was assumed than the case when the well-mixed model was assumed. In the present work, however, both models are considered.

Based on the assumption of a well-mixed gas phase, a mass balance for SO_2 over the entire gas volume in the reactor, V_g, at any time, t, gives:

$$Q\,C_{gf} - Q\,C_g - r\,V_L = V_g\,dC_g/dt \tag{5.21}$$

where Q = volumetric flow rate of the gas, L/min

C_{gf} = feed concentration of $SO_{2(g)}$, mmol/L, and

C_g = exit concentration of $SO_{2(g)}$, mmol/L

The accumulation term is negligible because of the small values of both the gas volume, V_g, and the rate of change in the gas concentration with time. The gas volume (or holdup) in the reactor was estimated to be about 100 cm^3 which is only 5% of the liquid volume. Also, the variation of C_g with time is not high especially at later stages of absorption. Therefore

$$C_{gf} - C_g = r\,V_L/Q \tag{5.22}$$

combining equation 5.22 with equation 5.19 and rearranging gives:

$$C_g = C_{gf} - (V_L/Q)\, dC_T/dt \qquad (5.23)$$

The exit concentration is related to the exit partial pressure (p_g) by:

$$p_g = C_g R T \qquad (5.24)$$

To calculate the average concentration of SO_2 in the gas phase, C_g, during absorption based on the plug flow model, the logarithmic mean for the partial pressures of the gas at the inlet (p_f) and at the exit (p_g) was used as suggested by Juvekar and Sharma (20):

$$p_{lm} = (p_f - p_g)/\ln (p_f/p_g) \qquad (5.25)$$

The exit concentration and partial pressure of SO_2 can be calculated from the experimental data by considering the percent instantaneous SO_2 absorbed, R, which is defined by:

$$R = \frac{\text{rate of } SO_2 \text{ absorption}}{\text{rate of } SO_2 \text{ feed}} \times 100 \qquad (5.26)$$

R was calculated from the experimental data using the following equation:

$$R = (r\ V_L/Q\ C_{gf}) \times 100 \tag{5.27}$$

The values of R calculated from the data of the slurry density experiments are plotted in Figures 5.19 and 5.20 for lignite and SB ash, respectively. Very high values (90-100%) were obtained initially at the three tested levels of 5, 10 and 20 g/L. Although the percent instantaneous SO_2 absorbed decreased with time at all levels of slurry density, it remained relatively high (over 75%) at the higher level of 20 g/L compared to the slurries with less solids.

The exit concentration and partial pressure were finally calculated as follows:

$$C_g = C_{gf}\ (1 - R/100) \tag{5.28}$$

and

$$p_g = p_f\ (1 - R/100) \tag{5.29}$$

The equations derived in this Section will be used in the following two Sections to explain the experimental results.

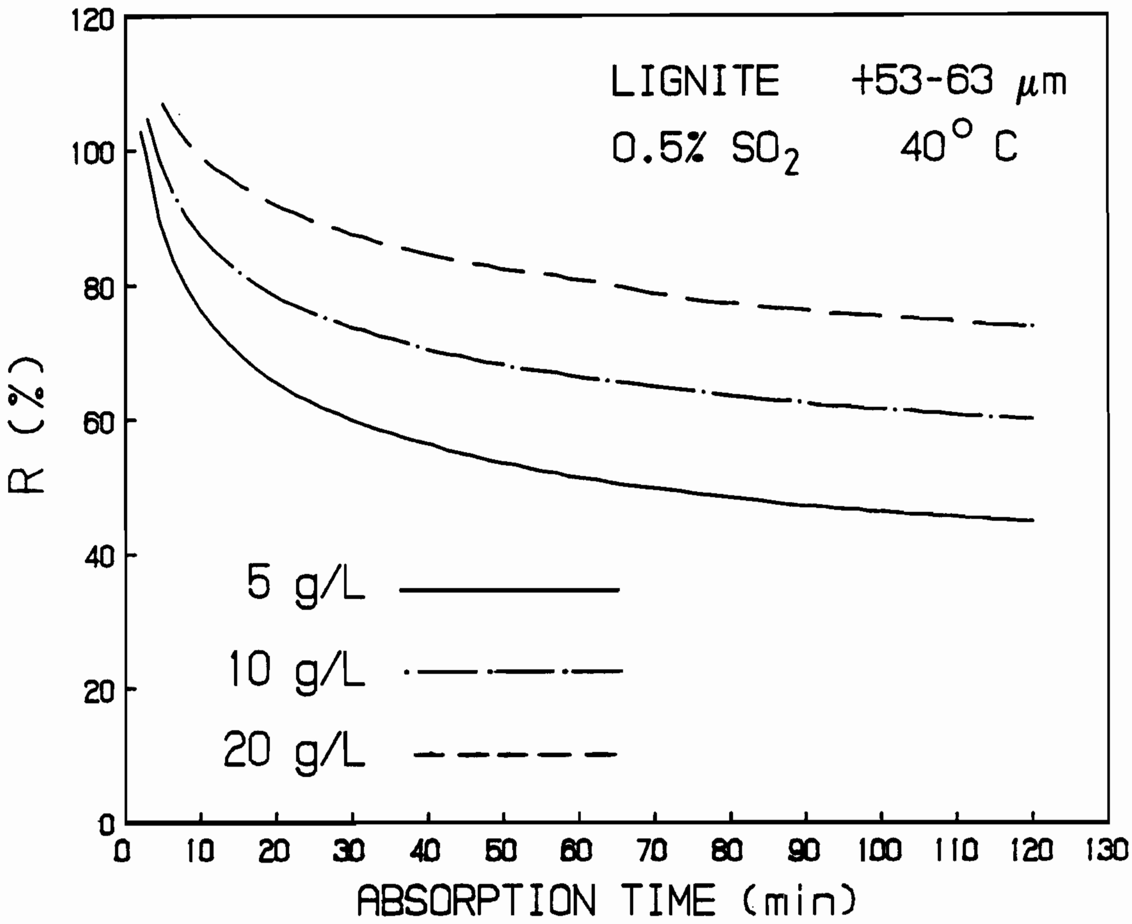

Figure 5.19 Percent instantaneous removal of SO_2 by lignite slurries

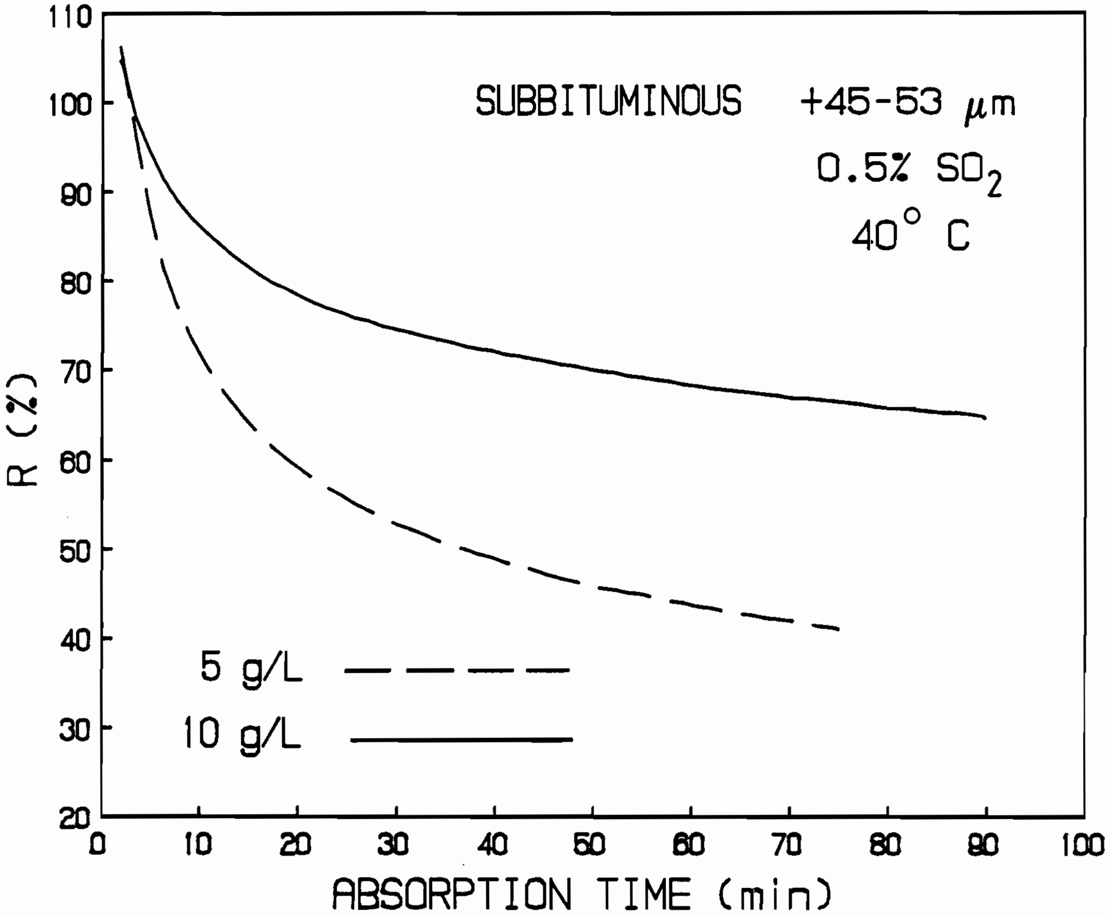

Figure 5.20 Percent instantaneous removal of SO_2 by SB slurries

5.6.4 Initial Absorption

When the SO_2 removal is close to 100 %, the exit concentration of SO_2 is very small compared to the inlet concentration; therefore, C_g can be neglected. In general, close to 100% SO_2 removals were obtained during the initial stage of absorption when the liquid phase contained abundant alkalinity. Assuming that the gas is well-mixed, the absorption rate from equation 5.23 is given by:

$$dC_T/dt = Q\ C_{gf}/V_L \qquad (5.30)$$

This equation suggests that if the volume of the liquid and the volumetric flow rate are fixed, the rate of absorption depends only on the concentration of SO_2 in the feed. Figure 5.21 shows the data for the first 15 minutes of absorption for three different inlet concentrations of SO_2 . The slopes of these lines, representing the rates of absorption, are plotted against the inlet SO_2 concentrations as shown in Figure 5.22. The slope of the resulting line is 3.1 min^{-1}. According to equation 5.30, this slope should be equal to the ratio Q/V_L. The three experiments from which data Figure 5.22 was obtained, were carried out at a flow rate of 6.5 L/min and a liquid volume of 2 L, that is, a ratio of 3.25 min^{-1}. This value is very close to that obtained from the experimental data.

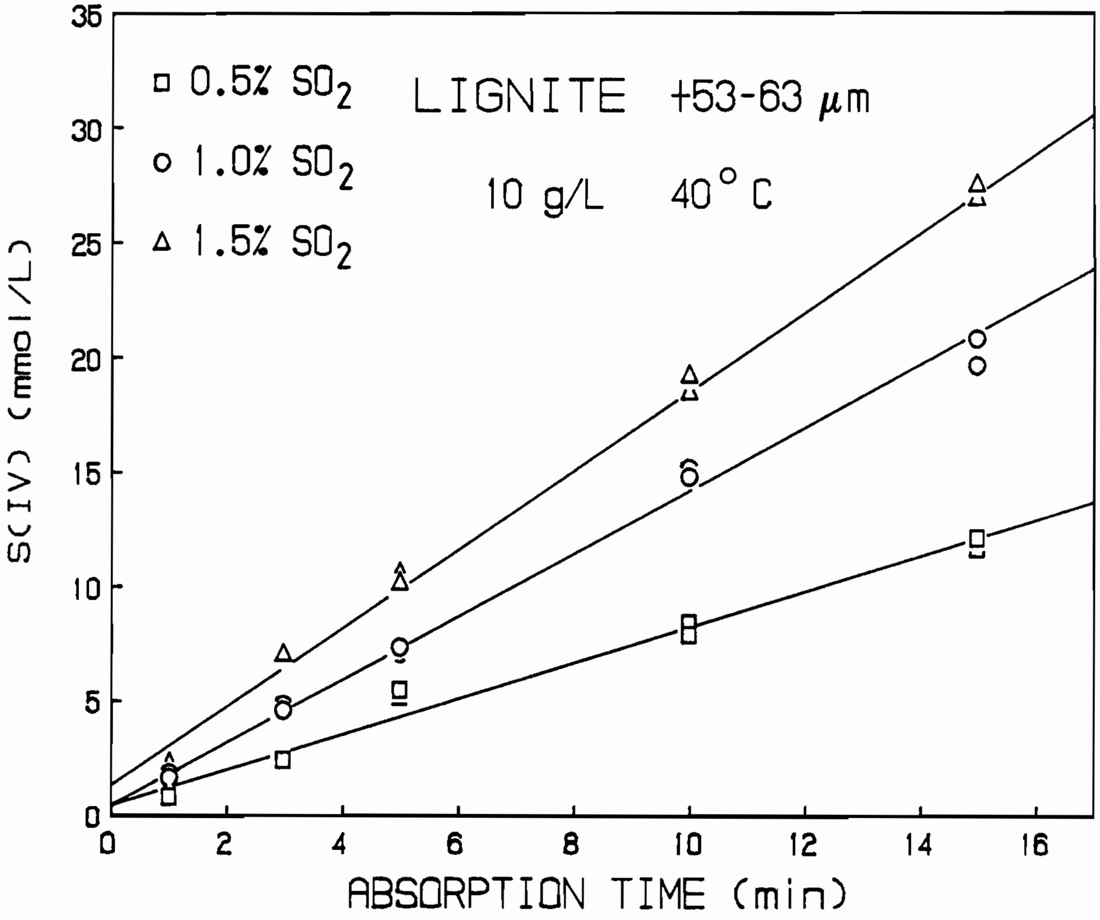

Figure 5.21 S(IV) concentration-time curves for initial absorption

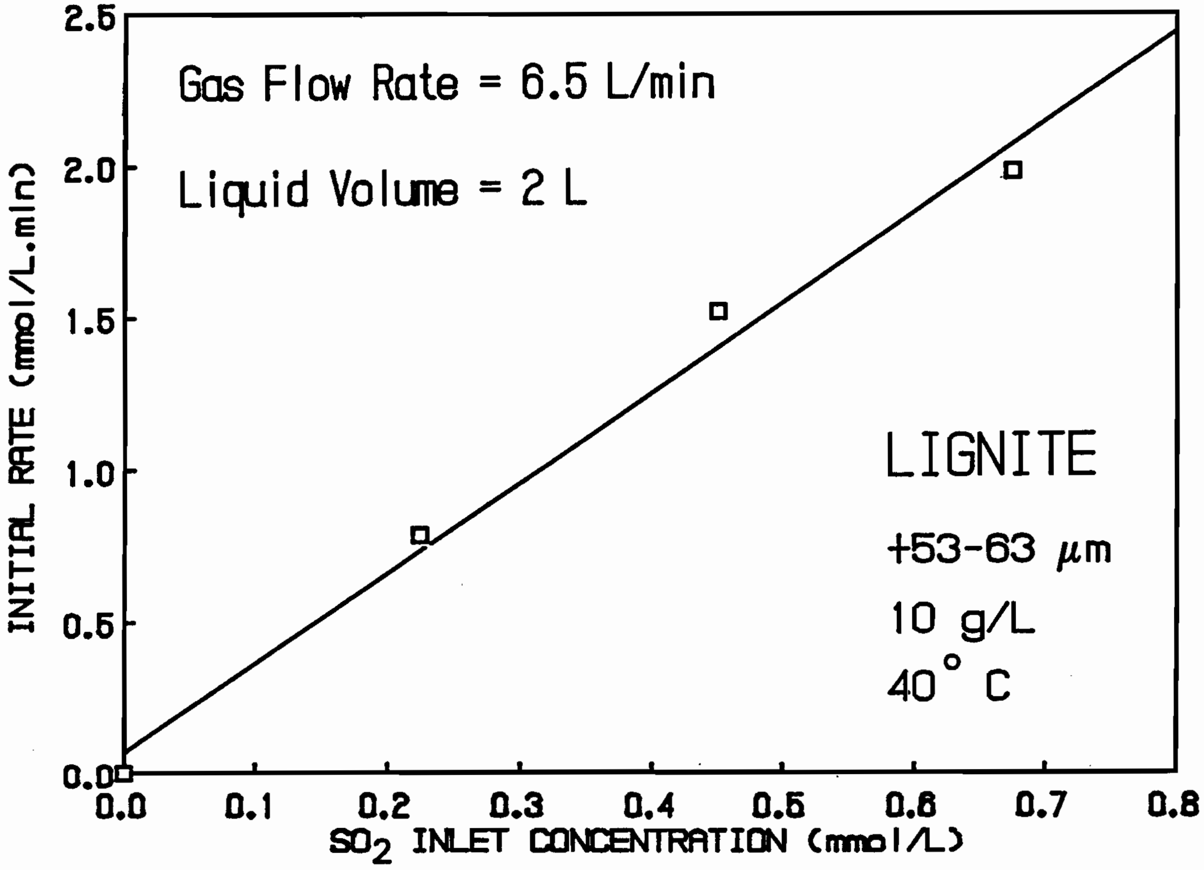

Figure 5.22 Relationship between the initial absorption rate and the SO_2 inlet concentration

Furthermore, equation 5.30 suggests that as long as the SO_2 removal is close to 100%, the rate of absorption does not depend on the absorption medium. This conclusion is essentially confirmed by the values of the initial rates obtained from a number of representative experiments. These rates are presented in Table 5.5. It is important to note that these initial rates were obtained at high levels of solution pH which prevailed at the beginning of the experiments.

5.6.5 The Constant-pH Period

Once the alkalinity which is initially present is depleted and a low constant pH is reached, the mass transfer process can be controlled by one or more of the following steps:

(1) gas-side diffusion
(2) liquid-side mass transfer
(3) solid dissolution.

Although there is no experimental proof, the gas-side diffusion is not likely to be the rate-limiting step. This is due to the high concentration of SO_2 (25) in the gas phase as well as the high rate of agitation.

If the absorption rate is controlled by liquid-side mass transfer, the rate is given by:

Table 5.5

Initial Rates of Absorption for Representative Data

Inlet SO_2 Concn.	Medium	Rate (mmol/L.min)
0.5%	Water	0.76
	Clear solution	0.81
	Lignite: 10 g/L slurry	0.79
	20 g/L slurry	0.80
	33% limestone	0.80
	66% limestone	0.79
	SB Ash: 10 g/L slurry	0.80
	50% limestone	0.79
	Limestone: 10 g/L slurry	0.77
1.0%	Lignite: 10 g/L slurry	1.52
1.5%	Lignite: 10 g/L slurry	2.00

$$r_A = k_La \ (C_{Ai} - C_A) \qquad (5.31)$$

where r_A = rate of transfer of molecular SO_2 from the gas-liquid interface to the bulk liquid

k_La = volumetric mass transfer coefficient

and C_{Ai} = interfacial concentration of molecular SO_2.

The interfacial concentration, C_{Ai}, corresponding to the partial pressure of SO_2 in the gas phase is determined from Henry's law (equation 1.1a). The partial pressure of the gas prevailing in the reactor is obtained from the reactor model (either equation 5.24 or 5.25).

Figure 5.1 has shown that the absorption of sulphur dioxide (expressed in terms of S(IV) concentration) is not sensitive to the stirring speed in the range of 800-1200 rpm at which all the absorption experiments were carried out. At such a high speed, the volumetric mass transfer coefficient for the transport of aqueous sulphur species from the gas-liquid interface to the bulk liquid is expected to be very high and the liquid-side mass transfer is not expected to be the controlling step.

Further evidence that the liquid-side mass transfer is not limiting can be obtained by considering the driving force (C_{Ai} - C_A). Combining equations 5.19 and 5.31:

$$dC_T/dt = k_La\ (C_{Ai} - C_A) \qquad (5.32)$$

In order to convert the concentration of molecular SO_2, C_A, to the experimentally measured total S(IV) concentration, C_T, the relationship in Equation 5.12 is used. To simplify the model, C_{Ai} can also be related to the total interfacial concentration of sulphur species (that is, $SO_{2(aq)}$ and bisulphite) in a similar way:

$$C_{Ti} = C_{Ai}/X \qquad (5.33)$$

In this equation, the coefficient X is assumed to be the same at the gas-liquid interface and in the bulk liquid. Since X is a function of pH and ionic strength, this assumption implies that the concentration gradients of hydrogen, bisuphite or dissolved metal ions are negligible. This is particularly true for hydrogen ion due to its high mobility (2). Therefore

$$r_A = dC_T/dt = (k_La/X)\ (C_{Ti} - C_T) \qquad (5.34)$$

This model was applied to the experimental data obtained at different slurry densities. The calculated values of $(C_{Ti} - C_T)$ were found to be very small and even became negative at later times of the experiments assuming both a well-mixed and plug flow models for the gas phase. This indicates that liquid-side mass transfer is not likely to be the limiting step.

As equation 5.17 indicates, the rate of SO_2 absorption is proportional to the rate of dissolution of alkaline metal compounds from fly ash solids. A plot of the rate of absorption against the rate of solid dissolution using different slurry densities of both lignite and SB fly ash is shown in Figure 5.23. Both rates were determined by fitting the experimental data for the total S(IV) or dissolved metal (sum of calcium and magnesium) concentrations obtained from the same experiment to a power correlation as in equation 5.20.

Figure 5.23 indicates that high absorption rates are associated with high dissolution rates. However, the dependence of the absorption rate on the rate of dissolution was rather weak when a slurry of 20 g/L of lignite was used because of the abundant amount of alkalinity provided at this high slurry density. The dependence became stronger when the slurry density was reduced to 10 g/L and a linear relationship was obtained between the two rates at the lower slurry density of 5 g/L. For the slurries of SB ash (which provided less dissolved metals and hence less soluble alkalinity), direct relationships between the two rates were valid for both 5 and

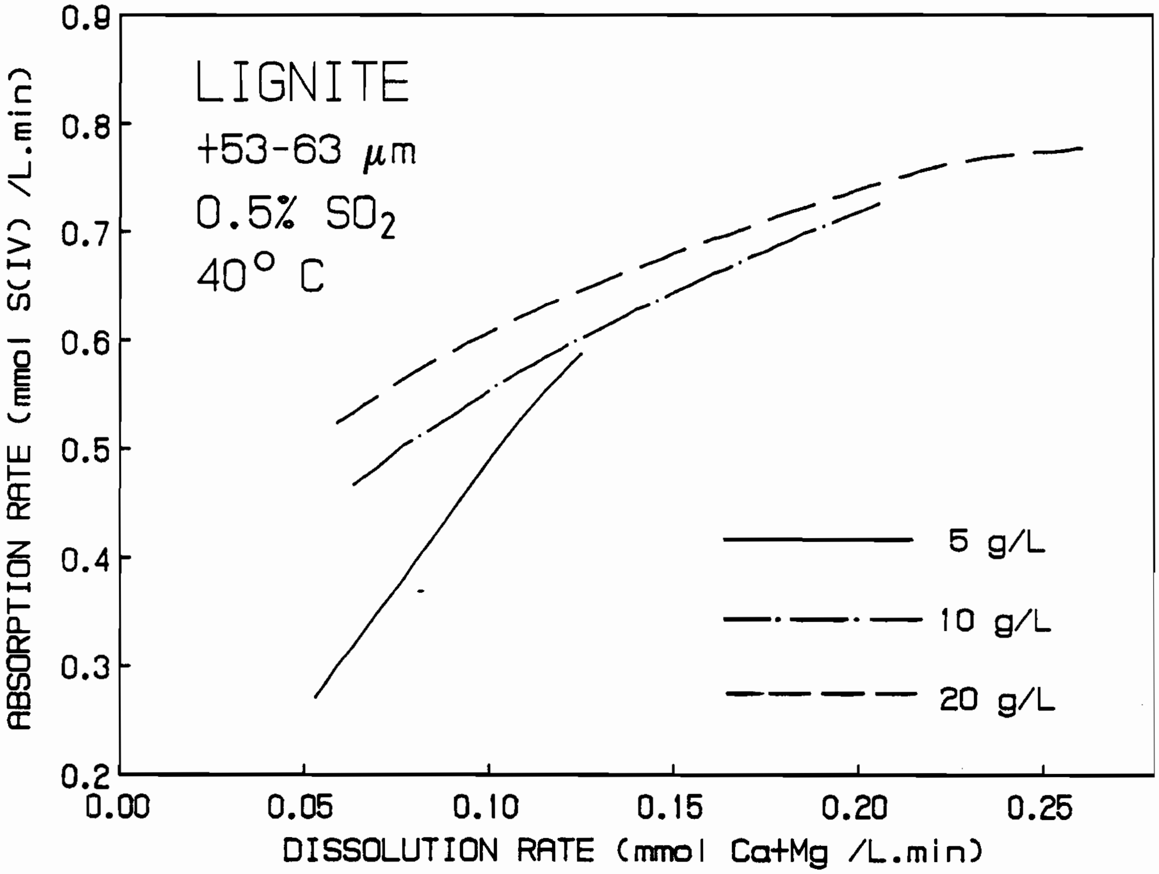

Figure 5.23 (A) Effect of solid dissolution on the rate of absorption into slurries of lignite ash

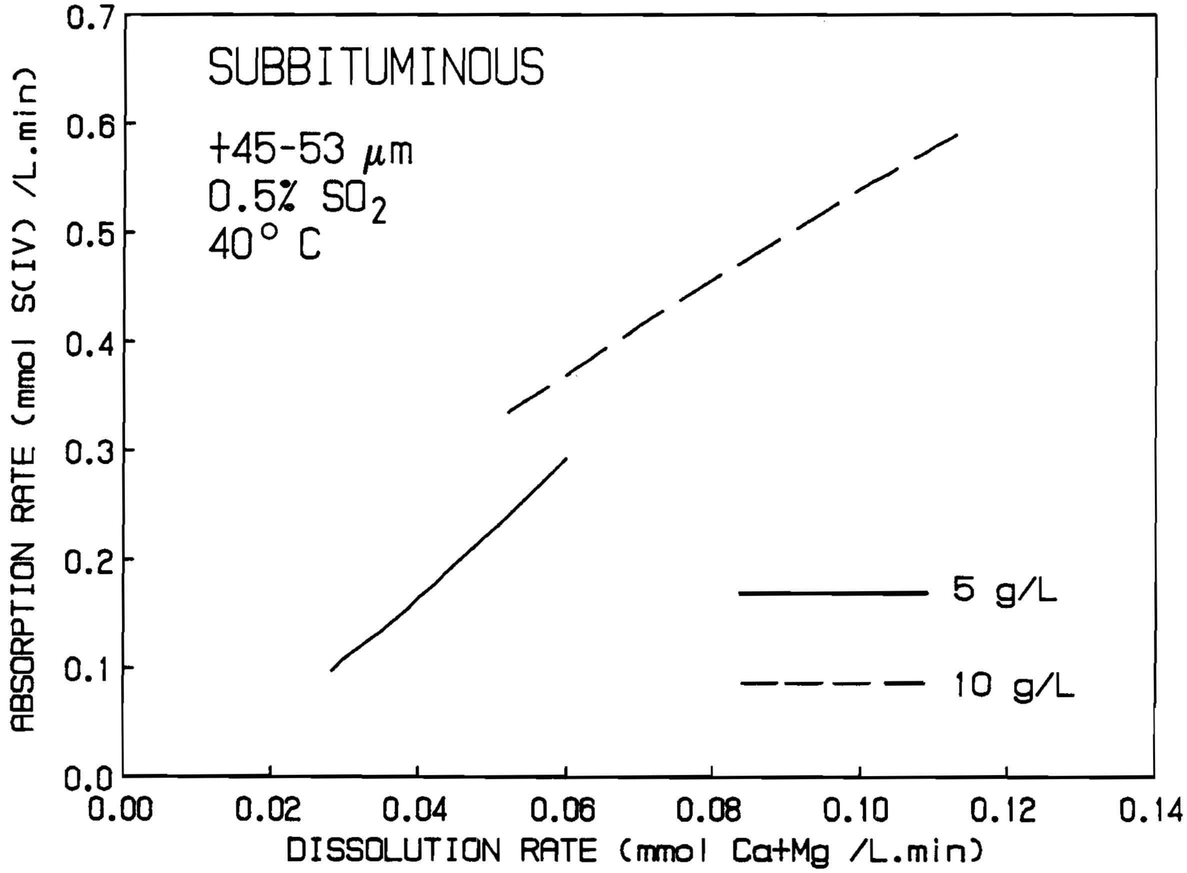

Figure 5.23 (B) Effect of solid dissolution on the rate of absorption into slurries of SB ash

10 g/L. These results suggest that the rate of absorption of sulphur dioxide, after the initial period of 15 minutes, depends on the rate of dissolution of metal compounds from fly ash when there is a limited amount of alkalinity in the liquid phase. However, this dependence becomes weaker as the amount of alkalinity available in the liquid increases.

5.7 Summary and Conclusions

The absorption of sulphur dioxide at low partial pressures into slurries of fly ash as a single source of alkalinity or augmented by the addition of lime was investigated using a stirred tank reactor. The total concentrations of aqueous sulphur species resulting from the absorption of SO_2 gas were measured as a function of time under various conditions. The slurry pH and the concentrations of dissolved metals in the presence of sulphur dioxide were also presented and discussed.

It was found that in the initial stage of absorption (about 10-15 minutes), absorption is independent of the liquid medium. After that, absorption depends on the soluble alkalinity provided by the dissolution of alkaline components in the solids. The provision of this alkalinity depends, in turn, on factors in the solid, liquid and gas phases that determine the extent of solid dissolution and the subsequent gas absorption. The alkalinity increases by increasing the slurry density (or the concentration of fly ash) and the percent of added limestone.

The use of a slurry (rather than a clear solution of an extract) of fly ash is necessary to provide the maximum amount of alkalinity for SO_2 removal from flue gas. Therefore, maintaining a low pH is important for high alkali availability. On the other hand, when the pH is low the absorption capacity declines. Simultaneous solid dissolution and gas absorption results in a constant pH that is maintained over most of the contact time between the three phases. The value of this pH, however, depends on the conditions prevailing in the reactor.

CHAPTER 6

CONCLUSIONS, ORIGINAL CONTRIBUTIONS AND RECOMMENDATIONS

6.1 Conclusions from the Dissolution Study

The main conclusions that can be drawn from the dissolution study are outlined below:

(1) Among the four alkaline metals tested in fly ash leachates, only calcium and magnesium were important in providing the soluble alkalinity intended to be used in flue gas desulphurization. This is valid for both subbituminous and lignite ashes.

(2) Lignite ash provided approximately twice as much concentrations of dissolved metals and hence total alkalinity as subbituminous ash.

(3) The initial concentrations of both dissolved metals from either type of fly ash were proprtional to the total surface area of the particles in the reactor (determined by the slurry density and the particle diameter). The final concentrations

of the dissolved metals were also dependent of the slurry density and the particle size.

(4) High concentrations of dissolved alkaline metals were obtained when the pH was maintained below 4.0 during leaching because of the increased solubility of the dissolving compounds. It was possible to maintain such a pH level when the initial pH was below 2.7 without the addition of buffers.

(5) The effect of temperature on dissolution is small and the enhancements in dissolved metal concentrations as well as in the rates of dissolution reflect an increase in the solubilities and the diffusion coefficients of the dissolving components with temperature increase.

(6) Initial rates of dissolution were high due to the high driving force for the transport of the component from the solid surface to the bulk of the liquid. The rates then declined due to the decrease in the interfacial concentration of the dissolving element caused by the depletion of the element from the particle surface.

6.2 Conclusions from the Absorption Study

The main conclusions that can be drawn from the absorption study are outlined below:

(1) The concentrations of total aqueous sulphur species, or S(IV), and the absorptive capacity of fly ash slurries (percent overall removal) increased significantly with increasing the inlet concentration of SO_2 and the slurry density.

(2) The concentration of S(IV) in solution was not influenced by the slurry temperature or the particle size within the tested period of contact time of 90 minutes.

(3) The slurry pH remained constant throughout the absorption process except for a few minutes during which the pH dropped sharply immediately after the introduction of the gas. The value of this pH is dictated by the type of absorbent used and the prevailing experimental conditions. It ranged from 2.6-2.9 in slurries of SB ash to 4.1 when limestone was used. Lignite slurries produced a slurry pH of 3.0-3.4. In large-scale industrial processes, the operational pH should be optimized with respect of both SO_2 absorption and fly ash dissolution.

(4) Lignite ash has twice the absorption capacity of subbituminous ash at the same slurry density (10 g/L). Addition of limestone may not be necessary for lignite when the inlet SO_2 concentration is low (0.5% or lower). Only 20%

less SO_2 were absorbed in lignite ash compared to limestone. For subbituminous ash, the addition of limestone doubled the absorption capacity after 90 minutes of contact with the SO_2.

(5) Initial absorption of SO_2 into slurries of fly ash or slurries of mixtures of fly ash and limestone was found to depend only on the concentration of SO_2 in the feed gas. In the later stages, absorption was limited by the dissolution of the alkaline metal compounds from fly ash. This dependence on dissolution was particularly important when the amount of available alkalinity was limited by the type of fly ash or the slurry density.

6.3 Original Contributions

6.3.1 In the Characterization of Fly Ash Dissolution

The dissolution of alkaline metal compounds from fly ash for the purpose of using the resulting soluble alkalinity in flue gas desulphurization was previously investigated in a stirred tank reactor. However, the published work was far from complete.

The contributions of the present study include generating a body of new data on the concentrations of dissolved calcium and magnesium (shown to be the only metals to leach in significant amounts accompanied by high soluble alkalinity) under a variety of experimental conditions which include different slurry densities, particle sizes, initial pH levels and temperatures. These data were obtained using fly ash samples from two Canadian coals, namely, subbituminous and lignite.

Other information claimed to be new findings are:

1. The total surface area of the particles, which combines the effects of slurry density and particle size, was found to determine the initial concentrations of dissolved metals.

2. The total soluble alkalinity extracted from fly ash and determined by acid titration was directly proportional to the combined concentration of dissolved calcium and magnesium.

6.2.2 In the Absorption of SO_2 by Fly Ash Slurries

As far as the author knows, this is the first study on the absorption of SO_2 into fly ash slurries which is carried out using a laboratory stirred tank reactor. As mentioned earlier in the Literature Survey, most of the work in this field has been done at the pilot plant and the large-scale commercial levels dealing with the operational problems. This study offers a substantial amount of new data that is obtained from bench-scale experiments on the characterization of the sulphur dioxide scrubbing media based on fly ash alkalinity.

The data include the quantification of the concentration of total aqueous sulphur species, the percent removal of SO_2 (which expresses the absorption capacity) and the change in the slurry pH during absorption into fly ash-based media under a variety of experimental conditions. For selected experiments, the concentrations of dissolved calcium and magnesium (which increased the ionic strength of the scrubbing solution) were also determined. Lignite fly ash was the main source of alkalinity used, but subbituminous fly ash and limestone were also investigated.

The following results are claimed to be new findings:

1. The slurry temperature in the range 20-55° C has no effect on the absorption of SO_2 into fly ash slurries.

2. A slurry of lignite ash used in this study has twice the absorption capacity of that of subbituminous ash at the same slurry density.

3. The slurry pH stabilizes during the absorption of SO_2 into fly ash slurries shortly after the start of absorption. The value of this pH is dictated by the particular conditions prevailing in the reactor and it is lower than that of limestone.

4. The same absorption capacity can be obtained with or without the addition of limestone to lignite ash in the first 60 minutes. In the case of subbituminous, this period lasts for 45 minutes.

5. The overall rate of absorption of SO_2 into fly ash slurries depends on the rate of dissolution of alkaline metal compounds after the initial stage of absorbent-independent stage. This dependence is strong when the fly ash solids cannot provide high soluble alkalinity (in the case of low alkaline metal content or low slurry densities) and it is weak when the solids provide abundant soluble alkalinity (in the case of high alkaline metal content or high slurry densities).

6.4 Recommendations for Further Research

It is suggested that future work in this subject considers the following recommendations in order to increase the current knowledge on the behaviour of fly ash as a source of alkalinity in flue gas desulphurization processes:

1. Using fly ash as recieved for both dissolution and absorption experiments. This is expected to provide more alkalinity and hence more absorption capacity as well as faster rates of absorption due to the higher surface area of the very fine particles (less than 45 μm). In general, the effect of particle size of fly ash on the absorption of SO_2 needs further investigation.

2. The chemical reactions taking place during absorption of SO_2 into fly ash slurries are not exactly known. In particular, a study of the possible reactions between the dissolved sulphur species and fly ash particles enhancing the dissolution of alkaline metal compounds will be of interest.

3. Performing some of the absorption experiments using laboratory reactors of designs similar to the industrial scrubbers. Experimental conditions can be limited to those encountered in practice including the presence of oxygen. A continuous operation with respect to the gas and the liquid phases will be useful.

REFERENCES

1. Atkins, R.S. Commercialization of lime-limestone flue gas scrubbing technology. ACS Sympo. Series No. 139, American Chemical Society, Washington, D.C., pp. 120-129 (1974).
2. Chang, C.S. and G.T. Rochelle. SO2 absorption into aqueous solutions. AIChE Journal 27 (2), 292-298 (1981).
3. Chue, T.T.; R.J. Ruane and P.A. Krenkel. Characterization and reuse of ash pond effluents in coal-fired power plants. J. Water Pollut. Cont. Fed. (11), 2494-2508 (1978).
4. Danckwerts, P.V. Gas-liquid reactions. McGraw Hill, New York (1970).
5. Davidson, R.L.; D.F.S. Natusch; J.R. Wallace and C.A. Evans. Trace elements in fly ash: Dependence of concentration on particle size. Environ. Sci. Technol. 8 (12), 1107-1113 (1974).
6. Davis, W.T. and G.D. Reed. Reactivity of fly ashes in a spray dryer FGD process. U.S. Dept. of Energy, Report No. DE 83 017534, Washington (1983).

7. Dudas, M.J. Long-term leachability of selected elements from fly ash. Environ. Sci. Technol. 15 (7), 840-843 (1981).

8. Elliott, T.C. and R.G. Schwieger (Eds.). The acid rain source-book. McGraw-Hill, Inc., New York (1984).

9. Elseewi, A.A.; A.L. Page and S.R. Grimm. Chemical characterization of fly ash aqueous systems. J. Environ. Qual. 9 (3), 424-428 (1980).

10. Environment Canada. Environmental codes of practice for steam electric power generation. Report No. EPS 1/PG/1A, Ottawa, Canada (1986).

11. Furuya, K.; Y. Miyajima, T. Chiba and T. Kikuchi. Elemental characterization of particle size-density separated coal fly ash. Environ. Sci. Technol. 21 (9), 898-903 (1987).

12. Hanhart, J.; H. Kramer and K.R. Westerterp. The residence time distribution of the gas in an agitated gas-liquid contactor. Chem. Eng. Sci. 18, 503-509 (1963).

13. Hansen, L.D. and G.L. Fisher. Elemental distribution in coal fly ash particles. Environ. Sci. Technol. 14 (9), 1111-1117 (1980).

14. Harned, H.S. and B.B. Owen. The physical chemistry of electrolytic solutions. Third Edition, Reinhold, New York (1958).

15. Henry, W.M. and K.T. Knapp. Compound forms of fossil fuel fly ash emissions. Environ. Sci. Technol. 14 (4), 450-456 (1980).

16. Hikita, H.; S. Asai and H. Nose. Absorption of sulphur dioxide into water. A.I.Ch.E. Journal 24(1), 147-149 (1978).

17. Hulett, L.D. and A.J. Weinberger. Some etching studies of the microstructure and composition of large aluminosilicate particles in fly ash from coal-burning power plants. Environ. Sci. Technol. 14 (8), 965-970 (1980).

18. Johnson, C. Fly ash removes SO2 effectively from boiler flue gases. Power Eng. pp. 61-63, June 1979.

19. Johnson, C. Minnesota Power's operating experience with integrated particulate and SO2 scrubbing. J. Air Pollut. Cont. Assoc. 31 (6), 701-705 (1981).

20. Juvekar, V.A. and M.M. Sharma. Absorption of CO_2 in a suspension of lime. Chem. Eng. Sci. 28, 825-837 (1973).

21. Kyte, W.S. Some chemical and chemical engineering aspects of flue gas desulphurization. Trans IChem E 59, 219-228 (1981).

22. Mehta, V.D. and M.M. Sharma. Mass transfer in mechanically agitated gas-liquid contactors. Chem. Eng. Sci. 26, 461-479 (1971).

23. Meyer, B. Sulphur, energy and the environment, Elsevier Sci., Amsterdam (1977).

24. Murarka, I.P.(Ed.). Solid waste disposal and reuse in the United States, Vol. 1. CRC Press, Boca Raton, Florida (1987).

25. Nannen, L.W.; R.E. West and F. Kreith. Removal of SO_2 from low sulphur coal combustion gases by limestone scrubbing. J. Air Pollut. Cont. Assoc. 24 (1), 29-39 (1974).

26. Natusch, D.F.S.; C.F. Bauer and others. Characterization of trace elements in fly ash. Institute of Environ. Studies, Univ. of Illinois. Report No. IES-3 (1977).

27. Ness, H.M.; P. Richmond; G. Eurick and R. Kruger. power plant flue gas desulphurization using alkaline fly ash from Western coals. Proc., Sympo. on FGD, Las Vegas, Nevada (1977). U.S. Environ. Protec. Agency, Report No. EPA-600/7-79-176 B.

28. Ness, H.M.; E.A. Sondreal; F.Y. Murad and K.S. Vig. Flue gas desulphurization using fly ash derived from Western Coals. Technical Report No. EPA-600/7-77-075 (1977).

29. Ness, H.M.; E.A. Sondreal and P.H. Tufte. Status of flue gas desulphurization using alkaline fly ash from Western coals. Proc., Sympo. on FGD, New Orleans, LA (1976). Report No. EPA-660/2-76-136 A.

30. Rabe, A.E. and J.F. Harris. Vapour liquid equilibrium data for the binary system, sulphur dioxide and water. J. Chem. Eng. Data 8 (3), 333 (1963).

31. Ramachandran, P.A. and M.M. Sharma. Absorption with fast reaction in a slurry containing sparingly soluble fine particles. Chem. Eng. Sci. 24, 1681-1686 (1969).

32. Ray, S.S. and F.G. Parker. Characterization of ash from coal-fired power plants. U.S. Environ. Protection Agency, Technical Report No. EPA-600/7-77-010, Washington, D.C. (1977).

33. Record, F.A.; D.V. Bubenick and R.J. Kindya. Acid rain information book. Noyes Data Corp., Park Ridge, New Jersey (1982).

34. Reed, G.D.; D.t. Mitchell and D.G. Parker. Water quality effects of aqueous fly ash disposal. Proceedings, 31st Industrial Waste Conference, Purdue Univ., Lafayette, Indiana, pp. 337-343 (1976).

35. Reynolds, S.D. Oxidation of calcium-sulphite slurries in a continuous reactor. Ph.D. Thesis, Univ. of Virginia (1984).

36. Rochelle, G.T. Flue gas desulphurization. In "Coal processing and pollution control" by T.F. Edgar. Gulf Publications, Houston, Texas, pp. 337-372 (1983).

37. Rochelle, G.T. and C.J. King. The effect of additives in mass transfer in CaCO3 or CaO slurry scrubbing of SO2 from waste gases. Ind. Eng. Chem. Fundam. 16 (1), 67-75 (1977).

38. Rowland, C.H.; A.H. Abdulsattar and D.A. Burbank. Effects of aqueous chemical equilibria on wet scrubbing of

sulphur dioxide with magnesia-enhanced limestone. In "Thermodynamics of aqueous systems with industrial applications". ACS Sympo. Series No. 133, Amer. Chem. Soc., Washington, D.C., pp. 247-267 (1980).

39. Roy, W.R.; R.G. Theiry; R.M. Schuller and J.J. Suloway. Coal fly ash: A review of the literature. Illinois State Geol. Survey, Environ. Geology Notes No. 96, pp. 69 (1981).

40. Sada, E.; H. Kumazawa and M.A. Butt. Single gas absorption with reaction in a slurry containing fine particles. Chem. Eng. Sci. 32, 1165 (1977).

41. Sada, E.; H. Kumazawa, M.A. Butt and T. Sumi. Removal of dilute sulphur dioxide by aqueous slurries of magnesium hydroxide particles. Chem. Eng. Sci. 32, 972-974 (1977).

42. Sada, E.; H. Kumazawa; I. Hashizume and M. Kamishima. Desulphurization by limestone slurry with added magnesium sulphate. Chem. Eng. J. 22, 133-141 (1981).

43. Sada, E.; H. Kumazawa and C.H. Lee. Chemical absorption into concentrated slurry. Chem. Eng. Sci. 39 (1), 117-120 (1984).

44. Sada, E.; H. Kumazawa and H. Nishimura. Absorption of sulphur dioxide into aqueous double slurries containing limestone and magnesium hydroxide. A.I.Ch.E. Journal 29 (1), 60-65 (1983).

45. Sada, E.; H. Kumazawa; Y. Sawada and I. Hashizume. Kinetics of absorption of lean sulphur dioxide into

aqueous slurries of calcium carbonate and magnesium hydroxide. Chem. Eng. Sci. 36, 149-155 (1981).

46. Santhanam, C.J.; C.G. Greenwald and J.J. Stahr. Utilization of Western fly ash in wet scrubbing FGD processes. U.S. Dept. of Energy, Report No. DE 85 009373, (1985).

47. Smith, J.M. Chemical Engineering Kinetics. Mc Graw-Hill, Third Edition, New York (1981).

48. Thomas, W.J. The absorption of sulphur dioxide in water: Part 1- Theory. Trans. Instn. Chem. Engrs. Vol. 42, pp. T3-T6 (1964).

49. Thunem, C.B. Laboratory studies on the availability of Western fly ashes to wet scrubbing for sulphur dioxide removal. M.S. Thesis, Univ. of North Dakota (1975).

50. Uchida, S.; H. Moriguchi; K. Koide and S. Kageyama. Absorption of sulphur dioxide into limestone slurry in a stirred tank reactor. Can. J. Chem. Eng. 56 (12), 690-697 (1978).

51. Uchida, S. and O. Ariga. Absorption of sulphur dioxide into limestone slurry in a stirred tank. Can. J. Chem. Eng. 63 (10), 778-783 (1985).

52. Uchida, S. and C.Y. Wen. Rate of gas absorption into a slurry accompanied by instantaneous reaction. Chem. Eng. Sci. 32, 1277-1281 (1977).

53. U.N. Economic Comission for Europe. Air-borne sulphur pollution: effects and control. Air Pollution Studies No. 1, The United Nations, New York (1984).

54. Warren, C.J. and M.J. Dudas. Weathering processes in relation to leachate properties of alkaline fly ash. J. Environ. Qual. 13 (4), 530-538 (1984).

55. Zeliger, H.I. Powder from Western coal: Fly ash as a reagent for SO_2 scrubbing. Proc., 4th Joint Conf. Sens. Environ. Pollut., pp. 159-161 (1978).

APPENDIX A

Calibration of Gas Flow Meters

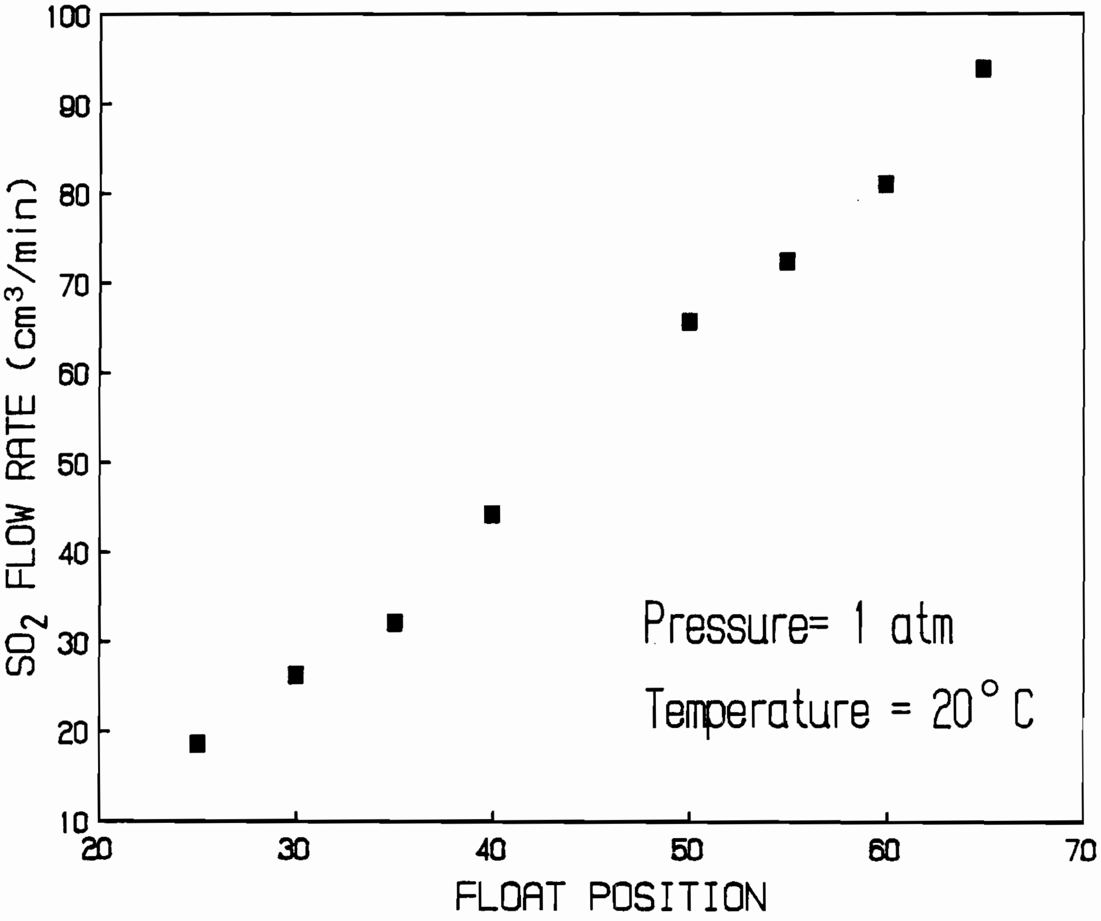

Figure A.1 Calibration of the SO_2 flow meter

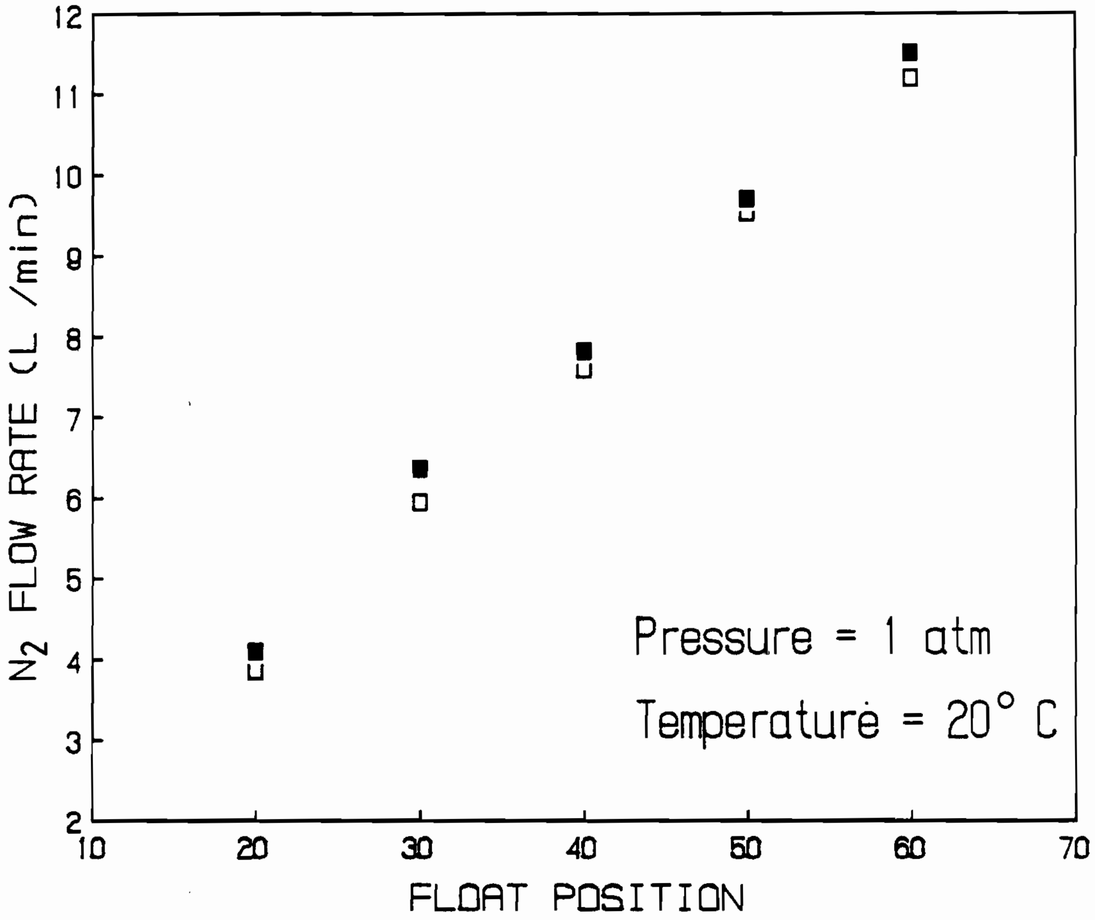

Figure A.2 Calibration of the N_2 flow meter

APPENDIX B

IODOMETRIC TITRATION

Iodometric titration was used to determine the concentration of total aqueous sulphur species, or S(IV). The procedure followed in this study is described below (Ref. 35).

One gram of sodium bicarbonate and several drops of 6 N HCl were added to a 100 cm^3 Erlenmeyer flask. A known volume of 0.1 N standard iodine solution (A & C Chemicals) was added to the flask (in excess of the S(IV) concentration) and the flask was capped and weighed. At the desired time during the absorption experiment, a sample was added to the flask directly from the reactor through the sampling pipe and the flask is reweighed. A magnetic stirring bar was added to the flask and the solution was stirred for 5 minutes (longer stirring times were found to be unnecessary).

The sample was then titrated with 0.1 N standard arsenious acid (A & C Chemicals) using a 10 cm^3 burette. As the titration proceeded, the colour of the solution changed from reddish-brown to pale-yellow at which point several drops of starch solution were added as an indicator. The end point was reached when the colour changed from violet to clear. The excees iodine from the reaction with sulphur species was consumed by arsenious acid. A balance on iodine yields:

$$N_I V_I = N_S V_S + N_A V_A \tag{B.1}$$

where N = normality, V = volume and the subscripts I, S and A denote iodine, sample and arsenious acid, respectively. Therefore,

$$N_S = (N_I V_I - N_A V_A)/V_S \tag{B.2}$$

In terms of molarity,

$$M_S = N_S/2 \tag{B.3}$$

The volume of the sample was calculated by dividing its weight over the density of the dilute aqueous solution which is the same as the water density.

APPENDIX C

Estimation of Henry's Law Constant in Ionic Solutions

Henry's law constant changes with the ionic strengh of the solution. The value of the constant in ionic solutions in relation to that in water can be estimated from the following equations (Ref. 4):

$$\log H/H_0 = - h.I \qquad (C.1)$$

where H = Henry's law constant in the solution

H_0 = Henry's law constant in pure water

h = overall salting coefficient which can be expressed as

$$h = h_- + h_+ + h_g \qquad (C.2)$$

where h_-, h_+ and h_g refer to contributions of cations, anions and gases.

and I = ionic strength of the solution which is defined by:

$$I = 1/2 \sum m_j . z_j^2 \qquad (C.3)$$

where m_j and z_j are the molar concentration and charge of species j, respectively.